

MODELLING OF SINGLE VERTICAL PILES SUBJECTED TO
MONOTONIC AND CYCLIC LATERAL LOADS AND FREE-
FIELD MOVEMENTS

by

Saman Vazinkhoo

B.A.Sc. University of British Columbia

A THESIS SUBMITTED IN PARTIAL FULFILLMENT OF
THE REQUIREMENTS FOR THE DEGREE OF
MASTER OF APPLIED SCIENCE

in

THE FACULTY OF GRADUATE STUDIES
CIVIL ENGINEERING

We accept this thesis as conforming
to the required standard

THE UNIVERSITY OF BRITISH COLUMBIA

October, 1996

© Saman Vazinkhoo, 1996

In presenting this thesis in partial fulfillment of the requirements for an advanced degree at the University of British Columbia, I agree that the Library shall make it freely available for reference and study. I further agree that permission for extensive copying of this thesis for scholarly purposes may be granted by the head of my department or by his or her representatives. It is understood that copying or publication of this thesis for financial gain shall not be allowed without my written permission.

Civil Engineering

The University of British Columbia

2324 Main Mall

Vancouver, Canada

V6T 1W5

Date:

October 22, 1996

Abstract

In the past twenty years, many researchers and practitioners have become interested in the behaviour of piles under lateral loading conditions. Although piles are generally used to carry axial loads, quite often, such as in the case of seismic loads and/or lateral loads caused by ground displacement, they are required to carry lateral loads. The ability to predict the performance of piles under lateral loading caused by earthquakes is very important and is the focus of this thesis. To date very few and limited modelling techniques have been developed based on data obtained from testing of full size piles. This is due to the high costs involved with performing comprehensive experiments on prototype piles.

The response of piles to lateral loads may be analyzed using different methods ranging from complex 3-D finite element techniques to simple closed-form solutions for an elastic beam on an elastic foundation. This thesis employs the modulus of subgrade reaction approach due to its versatility and ease of use.

In the last five years, large amount of data from pile lateral load tests have become available. In this thesis, the available methods and models for analysing laterally loaded vertical piles are first reviewed and then two new models are developed. The first is a new cyclic P-y curve model based on the Hydraulic Gradient Similitude (HGS) tests carried out by Yan (1990). Then a new numerical model is developed which incorporates the first model and other P-y curves for analysis of laterally loaded vertical piles. The new numerical model is incorporated into the computer program

CYCPILE which is calibrated and verified using the available test data. In general, excellent agreement between the model predictions and the test data is obtained.

Table of Contents

Abstract	ii
Table of Contents	iv
List of Tables	vii
List of Figures	x
Acknowledgements	xiii
Chapter 1 Introduction	1
1.1 Introduction	1
1.2 Objectives and Scope of Thesis	2
1.3 Organization of Thesis	2
Chapter 2 Review of Present Analytical Methods of Pile Response to Lateral Loads	4
2.1 Introduction	4

2.2	Analytical Studies	5
2.2.1	Static Response	5
2.2.2	Cyclic Response	19
2.3	Experimental Studies - Static and Cyclic Loading	22
2.3.1	Model Tests	22
2.3.2	Field Testing	27
2.4	Summary	41
 Chapter 3 A Cyclic P-y Curve Model		 42
3.1	Introduction	42
3.2	Experimental Setup	42
3.3	Two-way Cyclic Loading	44
3.3.1	Loading Segments	50
3.3.2	Unloading Segments	56
3.3.3	Gap Segments	59
3.3.4	Residual Soil Reaction	63
3.4	One-Way Cyclic Loading	65
3.5	Summary and Conclusions	76
 Chapter 4 Numerical Model		 78
4.1	Introduction	78
4.2	Model Principles	78

4.3	Model Formulation	81
4.4	Summary	91
Chapter 5 Model Verification		92
5.1	Introduction	92
5.2	Closed-Form Solutions	93
5.3	Finite Difference Solutions	96
5.4	Model Tests	97
5.4.1	Monotonic Loading	97
5.4.2	Cyclic Loading	104
5.5	Full Scale Tests	107
5.5.1	BC Hydro Laboratory Tests on Timber Piles	107
5.5.2	BC Hydro Full Scale Field Tests on Timber Piles	113
5.6	Summary	121
Chapter 6 Summary and Conclusions		122
Bibliography		125
Appendix I - Shape Functions Used in The Numerical Model		133
Appendix II - Computer Program CYCPILE		137

List of Tables

Table 2.1: Methods of Analysing Pile Responses Under Cyclic Lateral Loads; after Yan (1990)	
.....	21
Table 2.2: A Summary of Field Pile Load Tests in Sand. After Yan (1990).	29

List of Figures

Figure 2.1: Schematic Representation of Winkler Springs (after Fleming et al, 1985)	10
Figure 2.2: a) Factors for P_u . b) n_{hi} vs. Relative Density. After Murchison and O'Neill (1984).	14
Figure 2.3: Normalized Experimental P-y Curves at Different Depths and Hydraulic Gradient Scale factors (N). After Yan (1990).	24
Figure 2.4: Variation of Pile Head Deflection with Time under Constant Amplitude One-way Loading. After Yan (1990).	25
Figure 2.5: Normalized Pile Head Deflection with Number of Loading Cycles. After Yan (1990).	26
Figure 2.6: Applied Loading Sequence in BC Hydro's Timber Pile Laboratory Tests. After Lee et al (1992).	31
Figure 2.7: Typical Measured Load-Displacement and Calculated Moment-Curvature Relationships from BC Hydro Laboratory Tests on Timber Piles. After Madson (1992).	32
Figure 2.8: Typical Cyclic Load-Deflection Response of BC Hydro Laboratory Tests on Timber Piles. After Lee et al (1992).	33
Figure 2.9: Measured Transverse Deflections and Extrapolated Pile Cap Displacements from BC Hydro Laboratory Tests on Timber Piles. After Lee et al (1992).	34
Figure 2.10: Moment-Curvature Curves Adjusted to 270mm Pile Diameter from BC Hydro	

Laboratory Tests on Timber Piles: After Lee et al (1992).....	35
Figure 2.11: Typical Input Displacement History for BC Hydro Field Tests. After Lee et al (1992).	37
Figure 2.12: Typical Maximum Moments and Loads vs. Lateral Displacements. After Wong (1992)	38
Figure 2.13: Typical Measured Deformed Shapes as measured by electro-levels from BC Hydro Field Tests on Timber Piles. After Wong (1992).....	39
Figure 2.14: Moment vs. Curvature Adjusted to Below the Pile Cap and to 270mm Pile Diameter from BC Hydro Field Tests on Timber Piles. After Lee et al (1992).	40
Figure 3.1: Time Histories of Applied Lateral Two-way Load and Pile Head Deflection at 88mm above sand surface. After Yan (1990)	45
Figure 3.2: Normalized Pile Head Peak Deflection with Number of Loading Cycles. After Yan(1990)	46
Figure 3.3: Cyclic P-y Curves for different Loading Cycles at 1 and 2 Pile Diameter Depths. After Yan (1990).	47
Figure 3.3: Cyclic P-y Curves for different Loading Cycles at 3 and 4 Pile Diameter Depths. After Yan (1990).	48
Figure 3.3: Cyclic P-y Curves for different Loading Cycles at 5 Pile Diameter Depth. After Yan (1990).	49
Figure 3.4: Variation of E_{max} with Number of Cycles. Back-calculated from Measured Cyclic P-y Curves (Yan, 1990).	52
Figure 3.5: Curves Fitted to the Experimental Data for Variation of E_{max} with Number of Cycles.	

.....	53
Figure 3.6: Variation of F_n and F_c with Effective Vertical Stress.	55
Figure 3.7: Proposed Cyclic P-y Curves Before Adjustments At Shallow Depths.	57
Figure 3.8: Proposed Cyclic P-y Curves with Adjustment At Shallow Depths.	58
Figure 3.9: Variation of Soil-Pile Gap with Stress Level.	60
Figure 3.10: Linear Approximations of Variation of the Gap with Soil Stress Level.	61
Figure 3.11: Variation of A_n and B_n with Number of Cycles.	62
Figure 3.12: Variation of the Residual Soil Reaction with Effective Vertical Stress.	64
Figure 3.13: Variation of Pile Head Deflection with Time under Constant Amplitude One-Way Cyclic Loading. After Yan (1990).	66
Figure 3.14: Pile Head Response at Loading Point under Constant Amplitude One-way Cyclic Lateral Load. After Yan (1990).	67
Figure 3.15: Example of Soil Element Response from Drained Cyclic Triaxial Test. After Lamb and Whitman, 1975.	68
Figure 3.16: P-y Curves under One-way Pile Head Loading at Depths of 1 to 2 Pile Diameters, Fixed Head Pile, HGST Model Scale Factor $N=48$, Eccentricity $=45\text{mm}$, Load Amplitude $=40\text{ N}$. After Yan (1990).	70
Figure 3.16: P-y Curves under One-way Pile Head Loading at Depths of 3 to 4 Pile Diameters, Fixed Head Pile, HGST Model Scale Factor $N=48$, Eccentricity $=45\text{mm}$, Load Amplitude $=40\text{ N}$. After Yan (1990).	71
Figure 3.16: P-y Curves under One-way Pile Head Loading at a Depth of 5 Pile Diameters, Fixed Head Pile, HGST Model Scale Factor $N=48$, Eccentricity $=45\text{mm}$, Load Amplitude $=40\text{ N}$.	

After Yan (1990).	72
Figure 3.17: Variation with Number of Cycles of Normalized P (Normalized with P max) At Intersection Point of the Reload Portion with the Unload Portion of the P-y Curve	73
Figure 3.18: Variation of A_p and B_p with the Effective Vertical Stress.	75
Figure 4.1: General Representation of Soil and Pile in Proposed Model.	80
Figure 4.2: A Pile Element Showing Variables and Sign Conventions.	82
Figure 4.3: The Beam Element with Applied Loads.	85
Figure 5.1: Comparison of CYCPILE with Closed-Form Solutions, a) Rigid Beam on a Constant Foundation, b) Rigid Beam on a Linear Foundation.	94
Figure 5.2: Comparison of Results of CYCPILE with LATPILE for Arbitrary Soil and Pile Conditions.	98
Figure 5.3: Comparison Between CYCPILE and LATPILE Under Free-Field Loading Conditions.	99
Figure 5.4: Typical Model Test Setup in Yan's (1990) HGS Tests. After Yan (1990).	101
Figure 5.5: a) Prediction of Pile Head Deflection (Model Test, Free Head). b) Prediction of Pile Bending Moment Distribution (Model Test, Free Head).	102
Figure 5.6: a) Prediction of Pile Head Deflection (Model Test, Fixed Head). b) Prediction of Pile Bending Moment distribution (Model Test, Fixed Head).	103
Figure 5.7: Applied Lateral Pile Head Loading and Measured Pile Head Deflections under Two-way Constant Amplitude Cyclic Loading. After Yan (1990).	105
Figure 5.8: CYCPILE Prediction of The Pile Head Response under Two-way Cyclic Loading.	106

Figure 5.9: Applied Pile Head Loading and Measured Pile Head Deflections under Constant Amplitude One-way Loading. After Yan (1990).	108
Figure 5.10: CYCPILE Prediction of The Pile Head Deflections under Constant Amplitude One-way Loading.	109
Figure 5.11: Comparison of Moment-Curvature and Load-Deflection from BC Hydro Laboratory Tests and CYCPILE.	110
Figure 5.12: Comparison of Moment-Curvature Curves Adjusted to 270mm Pile Diameter from BC Hydro Laboratory Tests on Timber Piles and CYCPILE's Predictions.	112
Figure 5.13: Typical Test Setup, BC Hydro Field Tests. After Wong (1992).	114
Figure 5.14: Applied Loading Sequence For The BC Hydro Field Tests. After Wong (1992).	115
Figure 5.15: Comparison of Predicted versus Measured Load-Deflection Curves at Pile Cap for the BC Hydro Field Tests on Timber Piles. a) Test Pile 1; b) Test Pile 2; c) Test Pile 3.	116
Figure 5.16: Predicted and Measured Deformations Along the Length of The Test Piles (BC Hydro's Field Tests on Timber Piles, 1992). a) Test Pile 1; b) Test Pile 2; c) Test Pile 3.	118
Figure 5.17: Moment vs. Curvature Adjusted to 270mm Pile diameter. After Lee et al (1992).	119
Figure 5.18: Moment vs. Curvature Curves Further Adjusted for Rigid Body Motions Caused by Rotation of Pile Caps.	120

Acknowledgements

I would like to hereby gratefully acknowledge the continued guidance and support of professor Peter Byrne at the University of British Columbia, and Dr. Michael Lee of BC Hydro. I would like to also acknowledge the financial assistance of BC Hydro without which this research would not have been possible. Continued dedication of BC Hydro to research on this topic has been key to its success.

Special thanks to my wife, Diana, my family and my friends for their unparalleled patience and support during the past four years.

Chapter 1 Introduction

1.1 Introduction

Historically, piles have been mostly designed to carry vertical loads. In seismically active areas, it is important to consider lateral loads and horizontal ground movements in the design and analysis of new and existing structures supported on piles. To date, numerous models have been developed to capture the behaviour of laterally loaded piles (Poulos, 1987; Yan, 1990) by various researchers. Unfortunately, very little test data have been available to calibrate and verify these models under field loading conditions until recently. Fundamental aspects of soil-pile interaction are still poorly understood. Soil parameters required for most of these models have not been fully calibrated in a fundamental manner. Observation of performance of laterally loaded piles in recent earthquakes have indicated that in reality, piles generally perform much better than current models suggest (Lee et al, 1992, Naesgaard, 1992).

A number of model tests at field stress levels (Yan, 1990) and full-scale field tests have been carried out in recent years (Yan, 1990; Yan and Byrne, 1992; Lee et al, 1992; Naesgaard, 1992). Results confirm that current methods of analysis for laterally loaded piles are very conservative and inconsistent with actual observations. The test data now allow us to develop, calibrate and verify a new model to capture the behaviour of piles under such loading conditions. In this thesis, the

development of the new empirical model, which uses basic material properties as input, is presented and then the model is calibrated and verified using the model and field test results.

1.2 Objectives and Scope of Thesis

The main objectives of this thesis are as follows:

1. to review and examine the available information and current methodologies regarding the response of laterally loaded vertical piles,
2. to develop a new model to capture the observed response of laterally loaded vertical piles to both monotonic and cyclic lateral loadings, and
3. to calibrate and verify the model using recent Hydraulic Gradient Similitude model and full-scale test results.

The scope of this thesis is limited to the study of laterally loaded single piles embedded vertically in soil. The study includes cyclic loading effects but does not include any dynamic effects. The effects of dynamic forces and movements on the lateral response of single piles is presently under development at UBC.

1.3 Organization of Thesis

The thesis is comprised of 6 chapters presenting a review of present methodologies and then developing, calibrating and verifying a new model to capture the behaviour of laterally loaded single piles.

Chapter 1 introduces the background information and scope of this research work. Chapter 2 provides a review of current literature with emphasis on laterally loaded vertical piles in granular materials, realizing that a wealth of information already exists for fine-grained soils. Further, more recent developments and testing is presented and discussed.

A cyclic P-y curve model is developed in chapter 3 using the test data reviewed in Chapter 2 in order to be able to accurately capture the behaviour of piles under cyclic lateral loading conditions.

In chapter 4, a new numerical model is derived for analyzing lateral loading of single vertical piles. The model is based on an advanced structural model to represent the pile. The soil is modelled using P-y curves based on the conclusions of the preceding chapters.

Calibration and verification of the proposed model is presented in Chapter 4. The proposed model is validated by comparison with closed-form solutions and with the finite difference LATPILE solution. It is then verified by comparing with Hydraulic Gradient Similitude (HGS) tests (Yan, 1990; Yan and Byrne, 1992) and BC Hydro's laboratory tests on timber piles (Lee et al, 1992). Furthermore, the model is used to predict and compare the results of a set of full-scale experiments (Lee et al, 1992).

Finally, in Chapter 6, a summary and conclusions of the present research are made. The applicability of the proposed model to a more general problem is discussed. Some recommendations on future research for further calibration and extension of the proposed model and analysis of pile groups are also presented.

Chapter 2 Review of Present Analytical Methods of Pile Response to Lateral Loads

2.1 Introduction

Piles have been used to increase the vertical load carrying capacity of foundations for many decades. For the most part, design of pile foundations has been based on empirical formulations and procedures. To date, there has been much research effort focussed on the design and behaviour of pile foundations to meet increasing needs for efficient and cost effective construction in more and more unfavourable grounds. Many analytical models which are based on sound engineering principles have been developed in the last two decades. These models generally represent the soil as an elastic medium (Poulos & Davis, 1970) or replace the soil with uncoupled, Winkler springs, termed P-y curves. The P-y curve methods have proved to be very versatile and useful as they can be non-linear and have different shapes and form which better represent the soil behaviour. Unfortunately, due to the high cost of full scale experiments on piles, soil parameters required for the various models have not been fully calibrated, nor have the models been fully verified yet. Fundamental aspects of soil-pile interaction are still poorly understood. Therefore, engineers are still not able to design pile foundations confidently and in a cost effective manner.

Yan (1990) critically reviewed currently available analytical methods and experimental work with emphasis on advantages and limitations of each. His review was limited to laterally loaded

vertical piles in granular materials. Subsequently, he presented his own experimental work and findings in terms of non-linear P-y curves (Yan, 1990, 1992). British Columbia Hydro and Power Authority in conjunction with the University of British Columbia performed a series of full scale lateral loading tests on single timber piles. The findings of this research work is presented in Lee et al (1992, 1994) and will be briefly discussed in this thesis.

In this chapter, a summary of Yan's review along with more recent experimental work is presented and critically analyzed. Some attention is also given to response of laterally loaded piles in fine-grained, cohesive soils.

2.2 Analytical Studies

2.2.1 Static Response

Early research efforts were mainly focussed on finding an acceptable design method for determining the lateral load carrying capacity of piles. The design methods for lateral loads are similar those for vertical loads. The critical factor for the structural design of laterally loaded piles is usually the modulus of rupture (MOR) which reflects the maximum deflection under design conditions. The ultimate lateral load carrying capacity of a pile or pile group is generally only reached after unacceptably large deflections. For stiff piles, the ultimate lateral capacity is reached when plastic failure of soil occurs along the full length of the pile. For flexible piles, the ultimate lateral capacity is governed by the formation of plastic hinges at the locations of maximum bending moment (Broms, 1964; Poulos and Davis, 1980). Furthermore, the concept of the ultimate lateral capacity

assumes perfectly plastic response after yielding occurs in the soil and/or pile. Such a condition does not normally exist for cohesionless soils (Yan, 1986, 1990).

Today, lateral pile response may be analyzed using sophisticated 3D analysis with non-linear stress-strain relations for the soil and with special interface elements to represent the soil-pile interaction. However, this method is very costly and time consuming and is not feasible for most projects. For practical applications, simplified soil behaviour is used in analyses.

Presently available methods of static analysis can be classified into three categories according to the degree of simplification of soil-pile interaction behaviour (Yan, 1990):

4. the elastic boundary element approach,
5. the finite element approach, and,
6. the modulus of subgrade reaction approach.

The first and last categories differ only in the way the soil is modelled and both are independent of the way the pile may be modelled.

Elastic Boundary Element Approach

The elastic boundary element approach (sometimes referred to as the Elastic Continuum Approach) was first developed by Poulos (1971). This was the first systematic analytical study of static lateral load-displacement behaviour of piles. This method assumes that the soil is a linear-elastic half-space and uses Mindlin's solutions for soil displacements due to a point load within a homogeneous medium. The pile is modelled as a vertical strip with a rigidity value, EI , (the modulus of elasticity, E , times the moment of inertia, I , in the direction of bending) equivalent to that of the pile. The

main input parameters for the soil are the Young's modulus of elasticity, E , and Poisson's ratio, ν . Various solutions using this methodology are available and have been summarized by Poulos and Davis (1980). These solutions have been presented in the form of design charts and tables which have been used by many researchers and practitioners to date. The model has also been extended to include an elastic-perfectly-plastic continuum.

The main limitation of this method is that it is only applicable to small soil strains and to soils that have a constant elastic modulus with depth. The latter may only be true for some cohesive soils such as stiff clay. Various correction factors have been developed to account for soil non-homogeneity, finite depth of soil layer and pile length.

For most practical problems, it is very difficult to determine the appropriate elastic modulus and Poisson's ratio of the soil because they both depend on the loading intensity and soil type. Furthermore, both parameters vary with depth and are affected by local soil yielding near the surface. Another limitation of this method is that it does not account for soil-pile slippage and/or separation.

The advantages of the elastic continuum approach are its ease of use due to availability of design charts and that the model can be easily extended to pile groups because of the assumption of linear elasticity for the soil-pile system (Poulos 1974, 1980, 1987).

Finite Element Approach

The finite element method (FEM) is a powerful tool in handling soil-pile interaction in a rigorous manner. Various formulations are presently available to model the actual behaviour of the soil-pile

system, ranging from true non-linear 3D analysis (Faruque and Desai, 1982) to elastic, quasi-3D analysis (Desai, 1977; Kuhlemeyer, 1979; Baguelin et al, 1979; Randolph, 1981). The quasi-3D finite element formulations take advantage of the symmetry of the problem and expand the displacement field in terms of a Fourier series. The latter solution procedure is therefore more economical.

During the solution process, the soil-pile system is broken up into elements of finite size. Each element can be assigned unique properties so that non-homogeneous and non-linear soil behaviour can be included. Sophisticated stress-strain and strength models can be used to model the soil-pile interface. Structural elements are used to model the pile.

Although, recent advances in computer technology make it possible to perform non-linear 3D finite element analysis, much of the current practise is still focussed on elastic finite element analysis. This is due to both the high cost of non-linear analysis and the difficulties in selecting appropriate non-linear parameters for the soil and soil-pile interface.

Randolph (1981) presented results of his parametric studies using elastic, quasi-3D finite element modelling in the form of algebraic equations fitted to the solutions. Comparison with solutions from the elastic continuum approach showed good agreements. This is not surprising as both methods model the soil as an elastic material (Poulos and Randolph, 1982; Poulos, 1982). The advantage of the elastic finite element method is that soil non-homogeneity and variation of soil parameters with depth can be taken into account.

The elastic finite element method suffers from the same major limitations as other elastic continuum approaches. The elastic parameters needed for the analysis depend on the load level and pile deflection and are therefore difficult to determine.

Modulus of Subgrade Reaction Approach

The modulus of subgrade reaction approach may be one of the oldest, yet most versatile, methods for analyzing response of piles to lateral loads. In this method, the soil is modeled as a series of uncoupled Winkler springs. The uncoupled Winkler springs (see Figure 2.1) are used to model the reaction load of the soil on the pile due to the deflection of the pile into the soil material. Non-linear load-displacement relationships can be used in these springs to better model the non-linear stress-strain relationship of the soil. This model is unaffected by how the pile is represented, however, the pile is usually assumed to be a linear-elastic beam in a number of present implementations (Reese et al, 1977).

The governing equation for this type of soil-pile system is derived from the classical Hetenyi's solution for a beam-column on an elastic foundation (Hetenyi, 1946). Here, soil reaction is taken as a linearly distributed load on the pile. The governing equation is in the form:

$$EI \frac{d^4 y}{dz^4} + P_z \frac{d^2 y}{dz^2} - P = 0 \quad (2.1)$$

where P_z = axial load on the pile, y = lateral deflection of the pile at a point, z , along the pile length, P = soil reaction force per unit length, and EI is the flexural rigidity of the pile. The Winkler springs define P in the above model in terms of P-y curves specified at points along the pile length. The advantage of this method is that soil non-homogeneity and non-linearity can be modelled by using

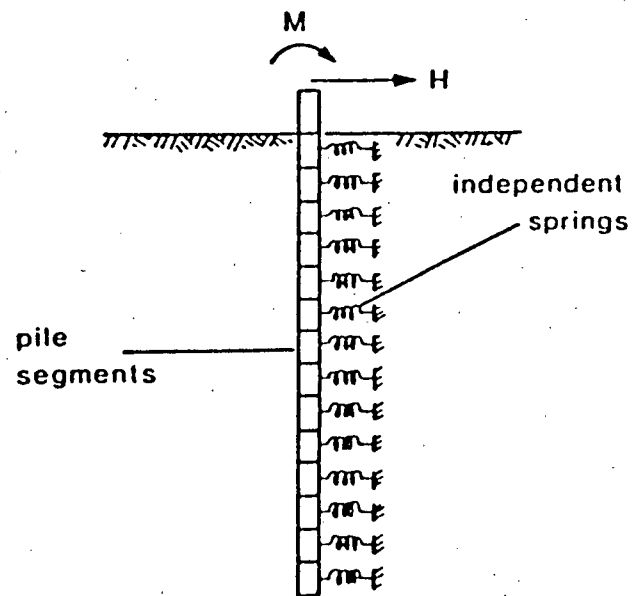


Figure 2.1: Schematic Representation of Winkler Springs (after Fleming et al, 1985)

different nonlinear P-y curves at different depths. The method is limited by the fact that it ignores soil continuity by assuming that the soil reaction, P , at any point, z , is unaffected by the soil displacements at locations other than at the point z . Extension to pile group analysis may not be readily achievable.

In early applications of P-y curves, a linear relationship was assumed such that:

$$P = K_h y \quad (2.2)$$

where K_h is called the coefficient of horizontal subgrade reaction modulus. Terzaghi (1955) introduced the coefficient of horizontal subgrade reaction k_h in terms of soil pressure p such that

$$p = k_h y \quad (2.3)$$

where k_h is related to K_h through the pile diameter, D , as shown in Equation (2.4).

$$k_h = \frac{K_h}{D} \quad (2.4)$$

Terzaghi (1955) defined k_h as:

$$k_h = n_h \frac{z}{D} \quad (2.5)$$

which implies that k_h varies linearly with depth. n_h is defined as constant of subgrade reaction modulus and is a function of soil density. Values of n_h for various soil densities were suggested by Terzaghi (1955).

Closed form solutions to Equation (2.1) are available for constant and linear variations of n_h (Scott, 1981; Poulos, 1982). The availability of such solutions has resulted in great effort being spent on back calculating n_h values from different case histories (Habibagahi and Langer, 1984; Robinson, 1979). Unfortunately, the linear assumptions made in this case lead to the same limitations as the boundary element approach (Poulos, 1987).

In reality, the lateral load-deflection behaviour, or P-y relationship, is non-linear. The variation of the P-y relationship with depth may also be non-linear (Yan, 1990; Yan and Byrne, 1992). The non-linear P-y curve approach has been widely used in the offshore industry for many years. The key element in this approach is being able to construct the nonlinear P-y curves based on basic soil parameters (Yan, 1990).

The concept of P-y curves was first proposed by McClelland and Focht (1958). To date, P-y curves for granular materials have been generally constructed based on the following methods,

- ◆ semi-empirical method,
- ◆ insitu testing method, and,
- ◆ finite element method.

Semi-empirical Method

Among all semi-empirical methods, the procedure proposed by Reese et al (1974) has been most widely used, and was incorporated into the American Petroleum Institute (API) design code in 1976. This procedure was initially based on back-analysis of one full scale instrumented pile load test in sand at Mustang Island, Texas (Cox et al, 1974). The basic components of the Reese et al P-y

curves are that there is an initial "elastic" portion, and a final horizontal portion representing an "ultimate" soil resistance. The other portions of the curves were empirically fitted to the shape of the experimental curves.

The original Reese et al P-y curves have been further simplified and modified as more experimental information has become available (Bogard and Matlock, 1980; Murchison and O'Neill, 1984), but the basic concepts have more or less remained the same. Bogard and Matlock (1980) proposed the following equations for the ultimate soil resistance, P_u , in sand:

$$P_u = (C_1 + C_2 D) \gamma z \quad (2.6)$$

$$P_u = C_3 D \gamma z \quad (2.7)$$

where C_1 , C_2 , and C_3 are given in Figure 2.2a.

To avoid having different equations for each part of the P-y curves, Murchison and O'Neill (1984) proposed a single analytical function to describe the Reese et al P-y curves,

$$P = \eta A P_u \tanh\left(\frac{n_{hi} z}{A \eta P_u}\right) \quad (2.8)$$

In the above equation, P_u is taken as the lesser of Equations (2.6) and (2.7). n_{hi} is given in Figure 2.2b, the empirical adjustment factor, A , is:

$$A = 0.9 \quad \text{for cyclic loading,} \quad (2.9)$$

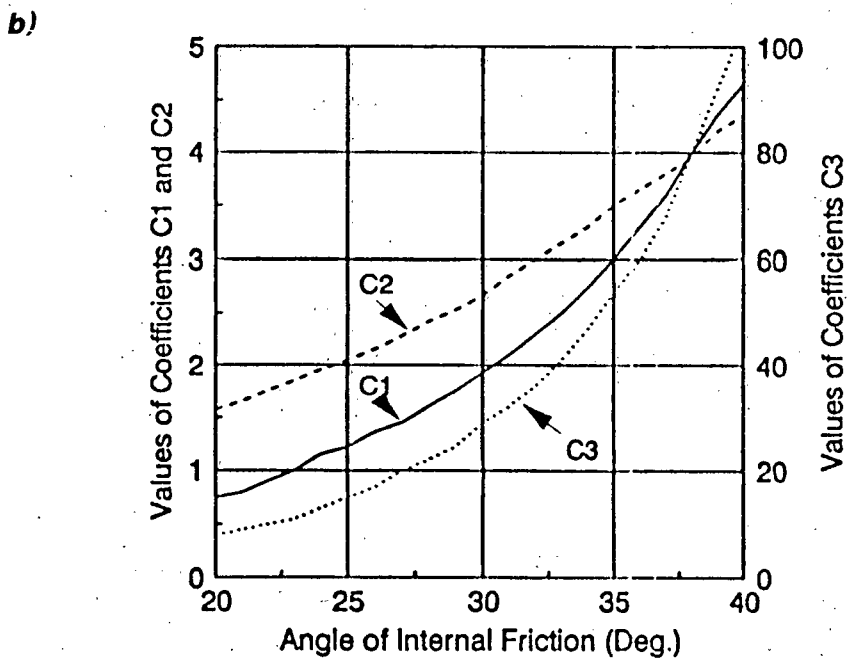
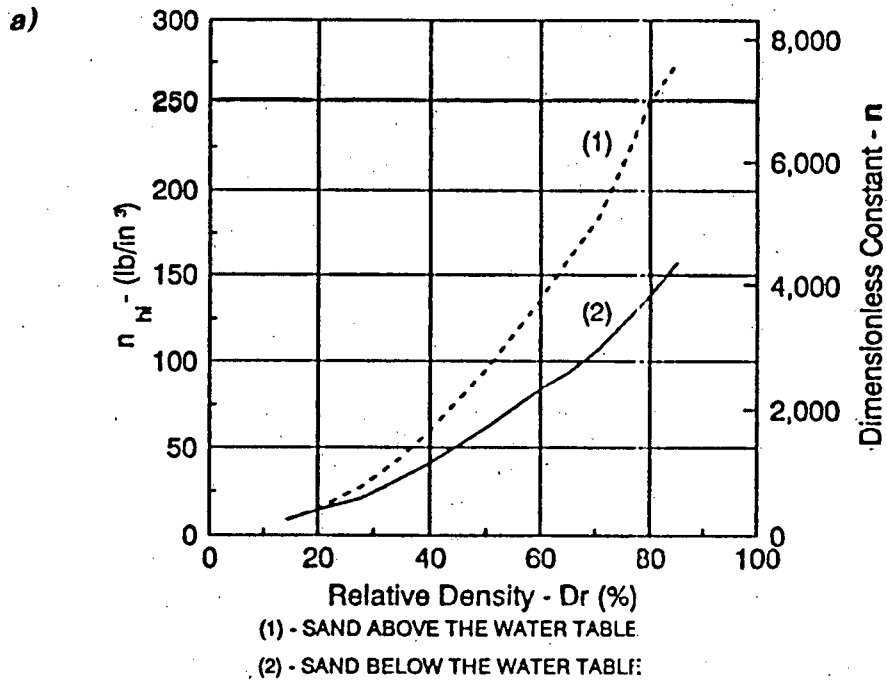


Figure 2.2: a) Factors for P_u . b) n_H vs. Relative Density. After Murchison and O'Neill (1984).

$$A = 3 - 0.8 \frac{z}{D} \geq 0.9 \quad \text{for static loading} \quad (2.10)$$

and η is a factor used to describe the pile shape effects. The recent version of API code (1987) has adopted this equation to describe P-y curves in sand. Note that this method does not include an initial "elastic" portion to represent the initial elastic behaviour of soil.

The limitation of the above method of P-y construction, other than ignoring the initial elastic behaviour of soil, is that P_u is not well defined (Kubo, 1966; Yoshida and Yoshinaka, 1972; Scott, 1981; Ting et al, 1987; Reese et al 1988) for cohesionless soils. Ignoring the initial elastic behaviour of soil may lead to under-estimation of pile head response at small deflections. Using a P_u that is lower than actual at large deflections may lead to over estimation of pile head response (Yan, 1990; Yan and Byrne, 1992) in these cases.

Scott (1980) proposed a simple, semi-empirical approach for constructing P-y curves based on centrifuge test results on model piles. Scott's P-y curves are bilinear with the initial segment representing the Young's modulus, E_s , of soil, and the second segment being empirically defined as having a slope equal to $E_s/4$. Thus, the "ultimate" soil resistance concept is not applied here. However, he did not specify the strain level at which the soil Young's modulus, E_s , is to be evaluated nor the method to obtain it.

Yan and Byrne (1992) have proposed a new method of P-y construction which was initially based on results of finite element studies (Yan, 1986). This method was later confirmed and modified with results of Hydraulic Gradient Similitude (HGS) model tests (Yan, 1990; Yan and Byrne, 1992). Their P-y curve consists of two segments, an initial "elastic" portion, and, a parabolic

portion fitted to the finite element and experimental results. They found that the parabolic portion of the P-y curves can be expressed in the form

$$\frac{P}{E_i D} = \alpha \left(\frac{y}{D} \right)^\beta \quad (2.11)$$

where α and β are curve fitting parameters, D is pile diameter, and E_i is the initial Young's modulus of soil which can be determined from hyperbolic stress-strain parameters (Duncan and Chang, 1970; Duncan et al, 1980; Byrne et al, 1987). The initial elastic portion is defined to have a slope equal to E_i . The intersection between the two segments is defined as the point where:

$$\frac{P}{E_i D} = \frac{y}{D} = (\alpha)^{\frac{1}{1-\beta}} \quad (2.12)$$

Since it may be difficult to determine E_i in practical applications, Yan and Byrne (1992) expressed Equation (2.11) in terms of soil's maximum Young's modulus, E_{max} ,

$$\frac{P}{E_{max} D} = \alpha \left(\frac{y}{D} \right)^\beta \quad (2.13)$$

For the equation in this form, Yan and Byrne (1992) found that β has a value of about 0.5 and α is function of relative density of the soil, such that

$$\alpha = 0.5(D)^{-0.8} \quad (2.14)$$

They found that P-y curves defined as above predict the experimental results much better than the API (1987) curves.

In situ Testing Method

In situ testing tools have been used in pile foundation design for axial loading for many years (Davis, 1987). It is generally believed that in situ testing tools provide a more direct assessment of pile performance in the field. The pressuremeter test is a tool which exerts a similar loading pattern on soil as does a laterally loaded pile.

Generally speaking, two approaches have been taken in making use of the pressuremeter test results:

- ◆ obtaining the horizontal modulus of soil reaction, K_h ,
- ◆ obtaining P-y curves from scaled pressuremeter curves.

In the first category, Menard and Gambin (Gambin, 1979) proposed a set of empirical formulae for K_h from Menard pressuremeter modulus, E_m . However, the Menard pressuremeter suffers from many operational problems and its results are largely affected by soil disturbance and stress relief.

In the second category, two approaches have been taken:

- ◆ the P-y curves are constructed by scaling the entire pressure-expansion curves with certain factors (Robertson et al, 1984; Atukorala et al, 1986; Hughes, 1994), or,

- ◆ the mechanism of soil resistance to the lateral movement of piles is separated into two components: frontal reaction and side frictional reaction (Briaud et al, 1982, 1983; Smith, 1987). The frontal reaction is obtained from the pressuremeter curve directly, but a theoretical assumption has to be made in order to interpret the side frictional reaction. Then, the P-y curve is constructed from the combined frontal and side frictional reaction curves.

Although it has been shown that both approaches are promising and of practical interest, none have properly taken account of different installation effects on the pressuremeter curve and P-y curve. Yan (1986) has shown that the two curves may be affected differently under different loading mechanisms. Thus correlations developed from one site may not be usable on another site.

Finite Element Method

Because the modulus of subgrade reaction method is based on uncoupled Winkler springs, the P-y curves may be derived from 2D finite element analyses. This allows for a much more economical analysis of laterally loaded pile compared to a true non-linear 3D finite element analysis as discussed earlier.

Yegian and Wright (1973) analyzed the response of a single pile under short term static loads in soft clay using both plane stress and plane strain models, and compared results with Matlock (1970) P-y curves. Yan (1986) found many limitations in that study arising from boundary effects.

A similar study was carried out by Barton et al (1983) on piles embedded in sand using a plane strain model. They modelled the soil as an elasto-plastic material incapable of tension.

Overall, their findings did not compare well with centrifuge test data they used for their comparisons.

As mentioned earlier, Yan (1986) studied the lateral loading of a single pile in sand using a plane strain 2D finite element model. The soil was modelled using hyperbolic stress-strain parameters. The soil-pile interface behaviour (slip and gapping) was simulated by using the thin layer interface element (Desai, 1981; Desai et al, 1984; Yan, 1986). The results of his findings were discussed in an earlier section (*Semi-Empirical Method*) and were found to be in good agreement with experimental test results.

2.2.2 Cyclic Response

Pile response under cyclic lateral loading can be differentiated into two categories: 1) one-way cyclic loading, and 2) two-way cyclic loading. Under the one-way cyclic loading, the pile is subjected to loading in one direction only and the applied lateral load never becomes less than zero. Under the two-way cyclic loading, the applied lateral load reverses direction and becomes negative.

Research on pile response to lateral cyclic loading has been mainly focussed on piles embedded in clays. General observations are that pile head deflection under the same load increases with number of loading cycles and is more severe under two-way cyclic loading than under one-way cyclic loading (Reese et al, 1988). The difference in deflections can be attributed to the degradation of the pile-soil system. Theoretically, the difference may take two forms (Swane and Poulos, 1982):

- ◆ material degradation,
- ◆ mechanical degradation.

Material degradation in soil would be indicated by increased pore pressures, changes in soil density, and rotation of principal stress directions. The effect of development of gaps, residual pressures and stresses along the pile length would be defined as mechanical degradation. Such degradations would lead to increased pile deflections and bending moments along the pile length. If the degradation stabilizes, the pile is said to "shake down" to a state of permanent strains and residual stresses. No further increase in deflections and stresses will take place in subsequent loading cycles. Otherwise, the pile will collapse (Yan, 1990). There are a number of methods for modelling structural shake down (Pande et al, 1980; Aboustit and Reddy, 1980; Swane and Poulos, 1982). A summary of currently available analytical methods for cyclic response of piles has been given by Poulos (1982, 1987) and is listed in Table 2.1.

As shown in the table, only the methods based on P-y curves are versatile and applicable to piles embedded in sands. Although, again, care should be taken in using these P-y curves as they are based on very limited field test data.

Until recently, only a few well instrumented pile test data has been available to understand the cyclic response of piles in sands. Yan (1990), Dou (1991) and Panwalkar (1994) have carried out many HGST tests at field stress levels on model piles (single and groups of two) embedded in sand. Further, British Columbia Hydro and Power Authority in conjunction with the University of British Columbia have performed a series of full scale tests on timber piles, alone and embedded in sand (Lee et al, 1992). The data obtained from these tests may be used to increase our understanding of pile-soil behaviour under static and cyclic lateral loadings and have suggested that many limitations exist in current methods of analysis. These tests will be discussed in greater detail next.

Table 2.1: Methods of Analysing Pile Responses Under Cyclic Lateral Loads; after Yan (1990)

Application	Method	Parameters Required	Comments	Reference
Sand	Empirical from 1g model tests	Soil Unit Weight	Deflection related to No. of cycles, and loading cond.	Gudehus & Hettler (1981)
Clay	Solution from Elast. Bound. Element Theory	E_s, p_u , critical cyclic strain vs. No. of Cycles e.g. Idriss et al (1978)	Corr. fact. for pile deflection and bending moment	Poulos (1982)
Clay Sand	P-y curves	P-y curve envelope	Derived from field data; give envelope to the response	Reese & Desai (1977)
Clay Sand	Cyclic P-y curves	Cyclic, hysteretic P-y curves	Cycle-by-cycle analysis. Allows for cyclic degradation and gapping, SPASM program	Matlock et al (1978)

2.3 Experimental Studies - Static and Cyclic Loading

2.3.1 Model Tests

Due to their low cost and relative ease in setting up, laboratory model tests, as compared to field tests, have often been used for parametric studies. Most model tests in the past were performed under 1g stress conditions because of unavailability of convenient testing devices that allow for the simulation of insitu stress conditions. Such tests have severe limitations because of their inability to simulate stress-level effects in soils. Since stress-strain behaviour of soil is highly stress-level dependent, large inaccuracies will develop when extrapolating the results of such tests to field conditions where the magnitudes of stress levels are much different.

Yan (1990) summarized some of the model tests that have been documented to date. The main focus of the 1g model studies have been to better understand the factors affecting the subgrade reaction modulus, K_b .

The centrifuge technique has been used over the past twenty years to increase the stress levels. These tests have generally been aimed at simulating previous field tests, namely, the Mustang Island full scale pile test. However, these tests have been limited in many ways and could not provide or support an analytical method that includes all the factors that significantly affect the soil-pile behaviour.

In his review, Yan (1990) concluded that despite its shortcomings, the nonlinear subgrade reaction method based on nonlinear P-y curves appears to be the most simple and versatile method of modelling the soil. However, prior to his studies (Yan, 1990, 1992), no comprehensive study had

been done which could be used to develop a rational expression for obtaining P-y curves from fundamental soil parameters. To overcome this, he performed a series of well instrumented model pile tests using the Hydraulic Gradient Similitude Technique (Yan, 1990) to increase the soil stress levels to field scales. The advantage of the HGS Technique is lower costs as compared to the centrifuge technique. Also, the test set up is a lot simpler.

The primary conclusion of his experiments confirmed his findings from earlier finite element parametric studies of P-y curve relationships for granular soils (Yan, 1986, 1990).

Yan (1990) studied monotonic, one way and two way cyclic lateral loading on the model piles. From the monotonic tests, he concluded that the non-linear P-y curves could be represented by a two-segment, linear-parabolic curve as discussed in an earlier section. However, the behaviour of the soil-pile interaction may be different under small stress levels as indicated by his test results at a depth of one pile diameter, or, at very small HGS scale factors. As can be seen from Figure 2.3, the normalized P-y curves all collapse into a very narrow band except for those at depth of 1D and HGS scale factor, N, of 1 (i.e. 1g model test). Therefore a different failure mechanism governs the shape of the P-y curve at low stress levels and may prevail at very shallow depths.

The results of the one-way cyclic tests show that displacements tend to increase with the number of loading cycles. This is perhaps mainly due to mechanical degradation where residual, locked stresses tend to develop around the pile. The measured displacements generally consisted of a "plastic" part and an "elastic" portion as shown on Figure 2.4. The development of permanent, plastic strains confirm the existence of residual stresses after loading has been removed.

The two-way cyclic tests showed that the amplitude of deflections initially decreased with number of loading cycles and then increased (Figure 2.5). The initial decrease in deflections is due

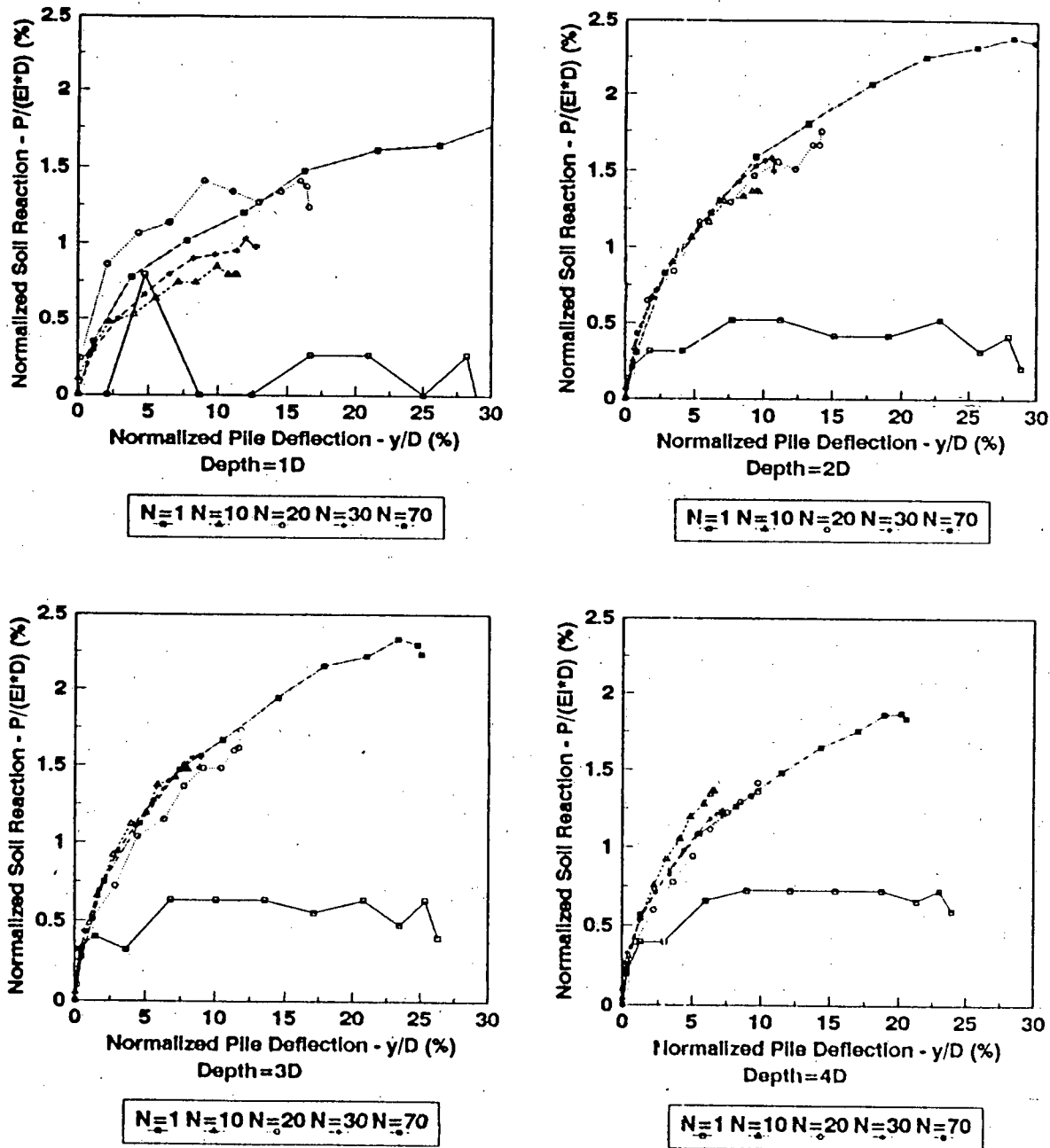


Figure 2.3: Normalized Experimental P-y Curves at Different Depths and Hydraulic Gradient Scale factors (N). After Yan (1990).

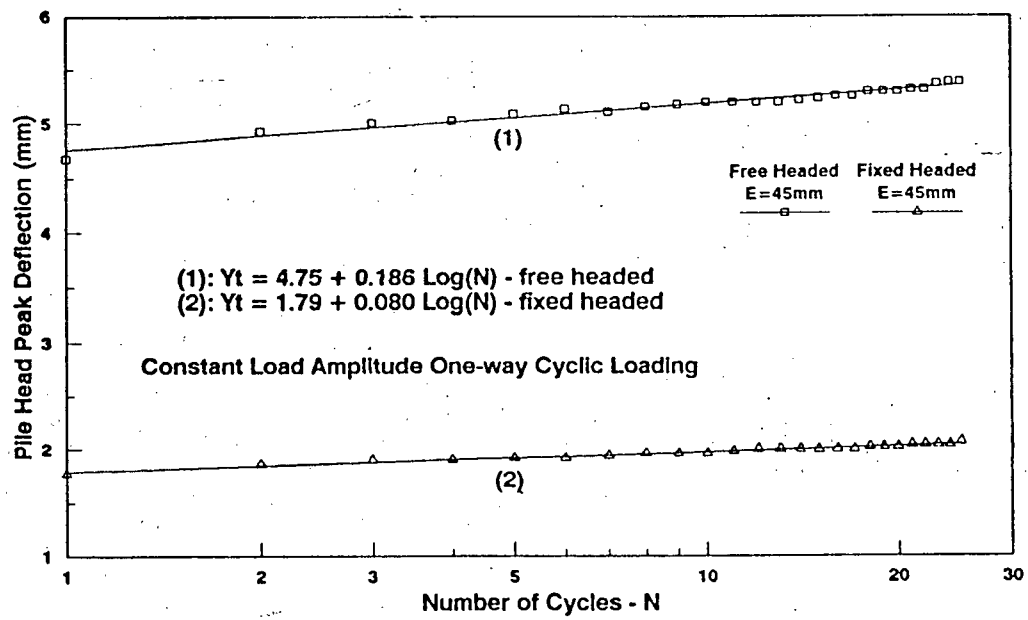


Figure 2.4: Variation of Pile Head Deflection with Time under Constant Amplitude One-way Loading. After Yan (1990).

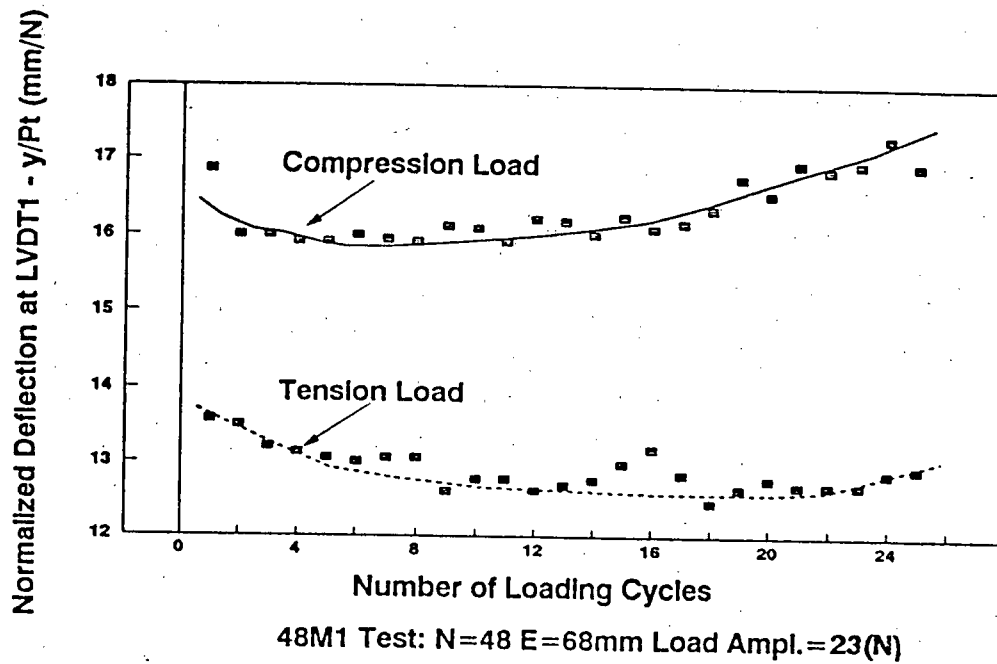


Figure 2.5: Normalized Pile Head Deflection with Number of Loading Cycles. After Yan (1990).

to soil densification around the pile from the applied cyclic shearing action (Oh-oka, 1976; Shaw and Brown, 1986; Leshchinsky and Rawlings, 1988). The deflection increases seem to be more towards the direction of first time loading. Similar to the one-way cyclic loading, this is perhaps due to mechanical degradation and formation of gaps between the pile and the soil (Yan, 1990).

2.3.2 Field Testing

Most field lateral loading tests on piles are project oriented in practice. Due to high costs, only a few full scale pile load tests have been performed on fully instrumented piles from which soil-pile interaction behaviour along the pile has been evaluated. In most other cases, only pile response at pile head has been measured. A parametric study on full scale pile load tests would be prohibitively expensive.

The classic early field work on fully instrumented piles was the lateral load tests on steel H-piles in medium dense sand during the Arkansas River Project (Alizadeh and Davisson, 1970) in which static and one-way cyclic loading was performed. Lateral loads were applied to a free-head connection at the ground line. It was found that when the observed pile head response was modelled elastically using the Matlock and Reese (1960) method, the parameter n_h depended heavily on the load level. The pile head deflection was found to increase significantly with the number of loading cycles under the one-way loading. Soil-pile interaction in terms of non-linear P-y curves was not evaluated in that study.

Cox et al (1974) reported results of lateral monotonic and cyclic loading tests on a single instrumented pile embedded in sand. This was the basis for the early P-y curve construction method proposed by Reese et al (1974).

More recently, single pile tests under displacement controlled two-way cyclic loading were conducted at the University of Houston by Brown et al (1987) for piles embedded about 10 pile diameters deep in sand overlying a stiff clay deposit. From this study, it was found that, unlike in the case of stiff clay, piles in sand were not affected significantly by the number of two-way loading cycles. In addition, Reese et al (1974) P-y curve procedure was found to under estimate the field measurements. P_u values were then increased by a factor of 1.55 to match the field data (Reese et al, 1988).

Some full scale tests on piles in sand under cyclic loading are summarized in Table 2.2. It can be seen that these studies are not comprehensive and do not allow for a fundamental study. This table does not include the recent tests performed by BC Hydro (Lee et al, 1992) and Naesgaard (1992). These tests will be discussed in some detail next.

As mentioned earlier, BC Hydro performed laboratory and field lateral loading tests on full size timber piles (Lee et al, 1992). Attempts were made to carry out the tests to failure which was defined as the point where axial load can no longer be sustained by the pile.

The laboratory testing program consisted of three-point-bending tests on 27 size 300 Douglas fir timber piles under different pile conditions. The purpose of these tests was to assess the moment-curvature and bending failure mechanism under simple boundary fixities and a range of moisture content and treatment conditions. One test was also carried out to assess the fixity provided by setting the timber pile in a concrete pile cap.

Reference	Loading Cond.	Soil & Pile Cond.	Comments
Alizadeh (1969)	free head, one-way cyclic	natural soil, timber unistr'ed pil	
Gleser (1953)	similar to above fixed and free	steel pipe pile unistr'ed	
Wagner (1953)	static and free head at G.L.	uninstr'ed timber pile in clay, silt, till	
Alizadeh & Davisson (1970)	free head, stat. & one-way cyclic at G.L.	natural fine silty sand, instr'ed piles	Matlock and Reese (1956) method
Cox et al (1974)	free head, two-way cyclic, at 1ft above G.L.	backfilled med to dense sand instr'ed pile	developed Reese et al P-y curves
Brown et al (1987)	same as above	same as above instr'ed pile	examined Reese et al P-y curves
Robinson (1979)	free headed one-way cyclic at G.L.	natural soil, timber pile, uninstr'ed pile	Reese & Matlock (1956), n_h , k_h values
Davis (1987)	same as above	uninstr'ed pipe pile, backfill	DMT P-y curve Robertson et al (1986)

Table 2.2: A Summary of Field Pile Load Tests in Sand. After Yan (1990).

The loading was applied in a displacement controlled manner simulating a two-way cyclic, followed by a one-way cyclic, and then monotonic loading to failure. Figure 2.6 shows a typical loading sequence for the laboratory tests. The measured data included the axial load, lateral load, and lateral displacements at different locations along the pile length. From these measurements, moments and curvatures were calculated. Typical reported load-displacement and moment curvature relationships are shown on Figure 2.7 (monotonic portion, Madson, 1992). A typical plot of cyclic load-displacement measurements is shown on Figure 2.8. As can be inferred from both figures, the timber piles undergo material degradation beyond a displacement of about 140 mm. The modulus of elasticity decreases with the level of maximum previous loading but is not affected much by the number of loading cycles when the displacement amplitude is less than about 140 mm. The results of these tests showed considerable scatter consistent with behaviour of timber materials and cumulative frequency plots such as those shown on Figure 2.9 are used. Moment-curvature plots normalized to a constant pile diameter of 270mm and ranked according to their frequency of occurrence (Figure 2.10) were also reported.

These results indicate that the conventional methodology for calculating the maximum moments and forces in piles is perhaps overly conservative and that (at least) timber piles are capable of undergoing much larger displacements and still carry the vertical load (Lee et al, 1992).

The BC Hydro field tests were performed on three size 350 Douglas fir timber piles. The purpose of the field tests was to investigate the effects of actual field conditions on the response behaviour of the timber piles to large horizontal displacements of about 1 m. The piles were driven through a soft silt (approximately 4m thick) into a loose to compact sand to silty sand, a total of 9m. The soft silt surrounding the pile was subsequently excavated to about 4 m deep to represent a

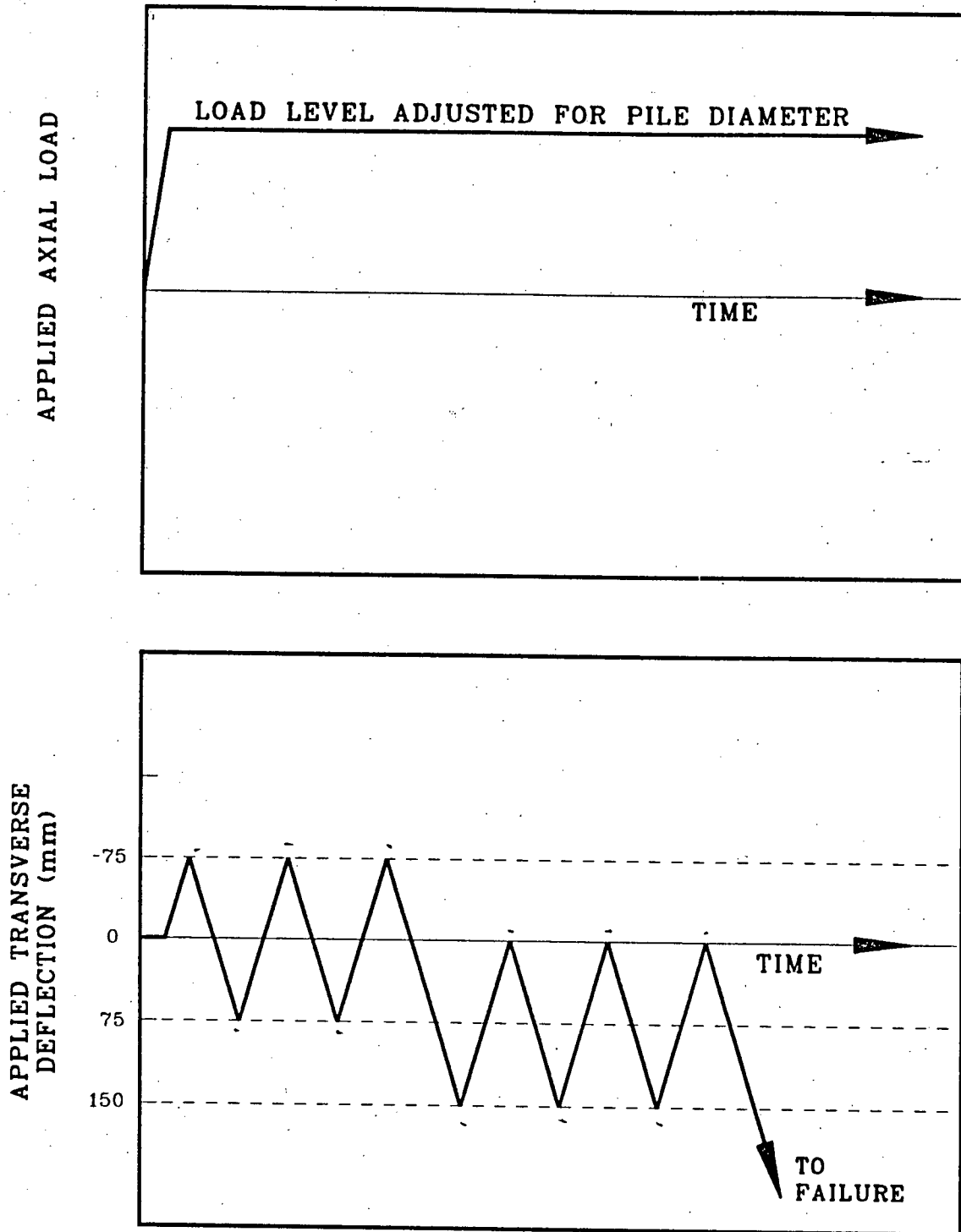


Figure 2.6: Applied Loading Sequence in BC Hydro's Timber Pile Laboratory Tests. After Lee et al (1992).

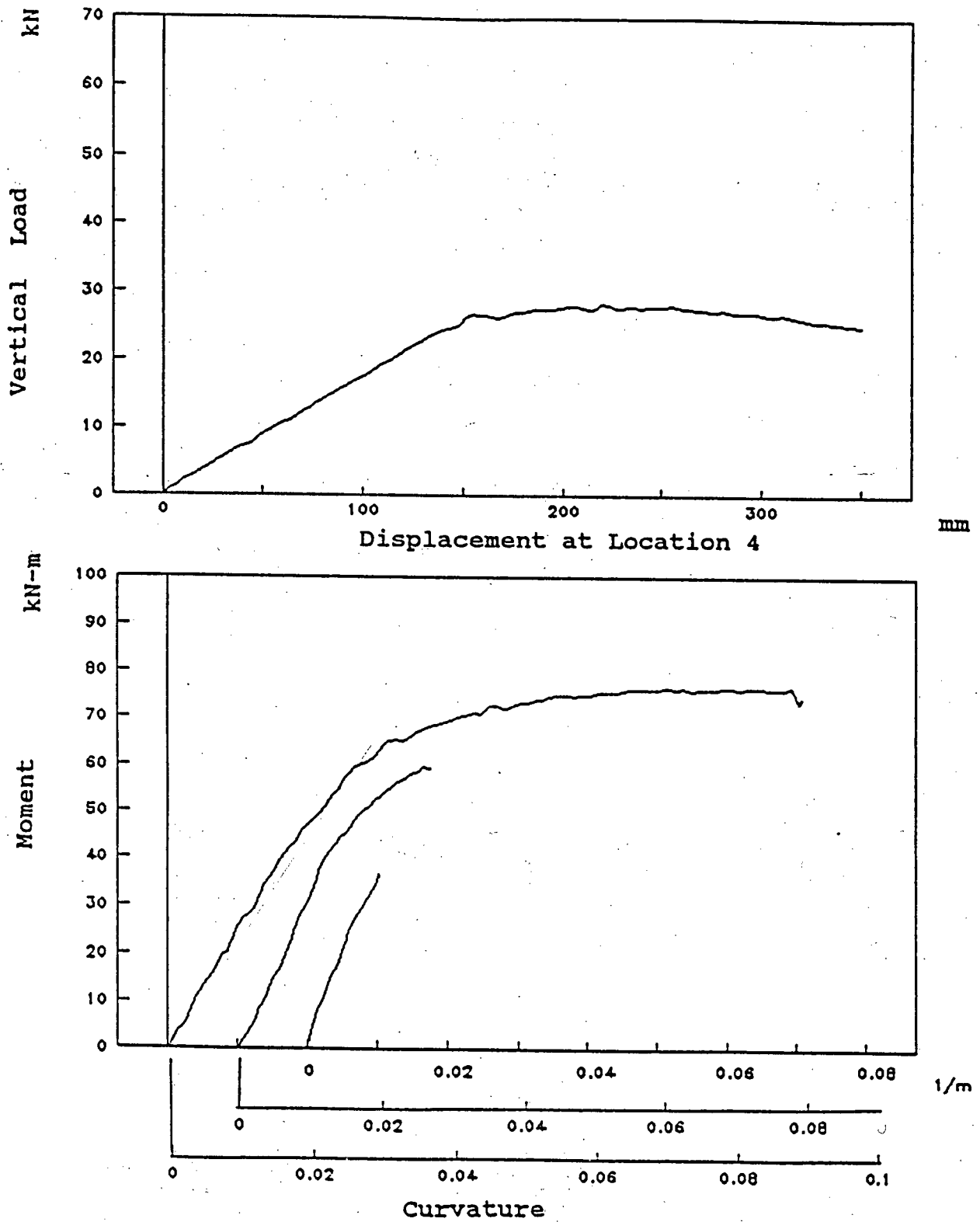


Figure 2.7: Typical Measured Load-Displacement and Calculated Moment-Curvature Relationships from BC Hydro Laboratory Tests on Timber Piles. After Madson (1992).

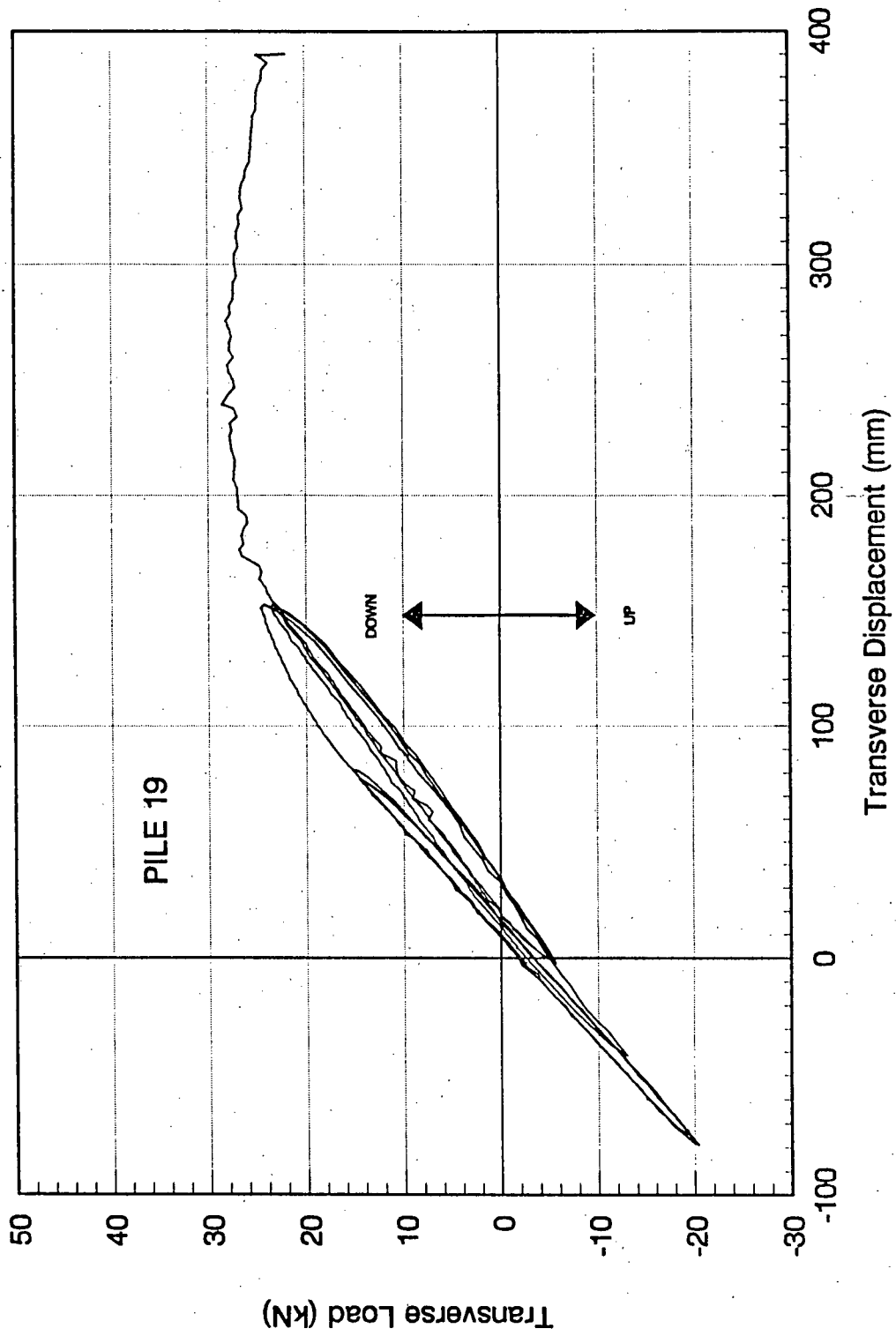


Figure 2.8: Typical Cyclic Load-Deflection Response of BC Hydro Laboratory Tests on Timber Piles. After Lee et al (1992).

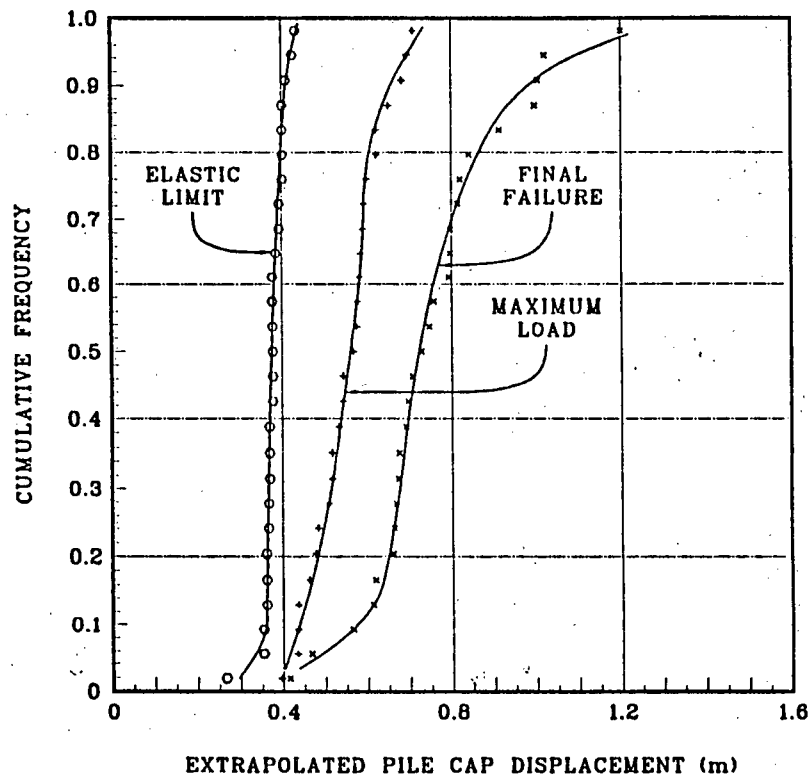
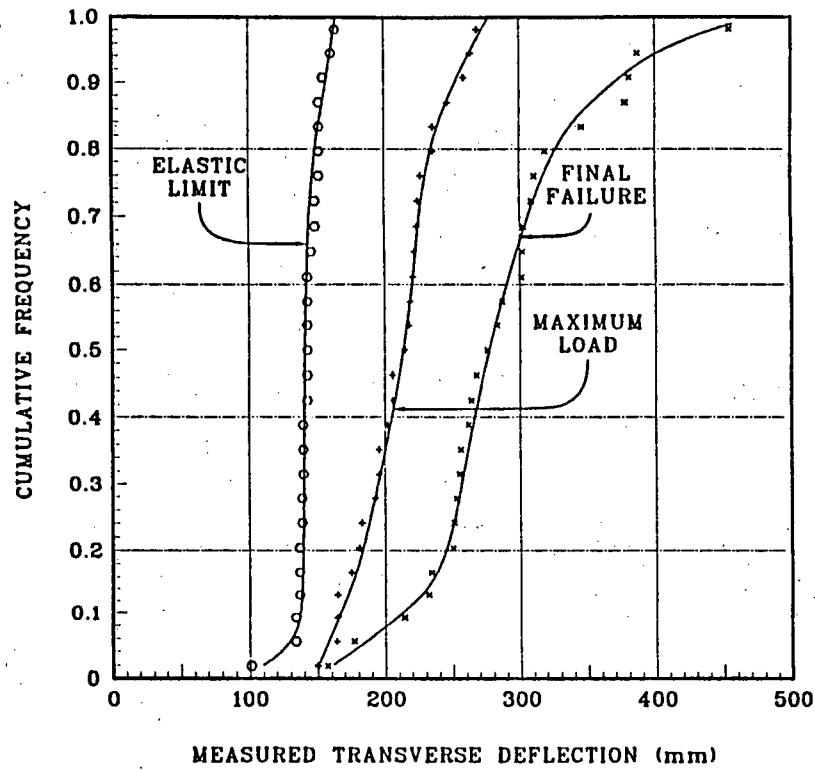


Figure 2.9: Measured Transverse Deflections and Extrapolated Pile Cap Displacements from BC Hydro Laboratory Tests on Timber Piles. After Lee et al (1992).

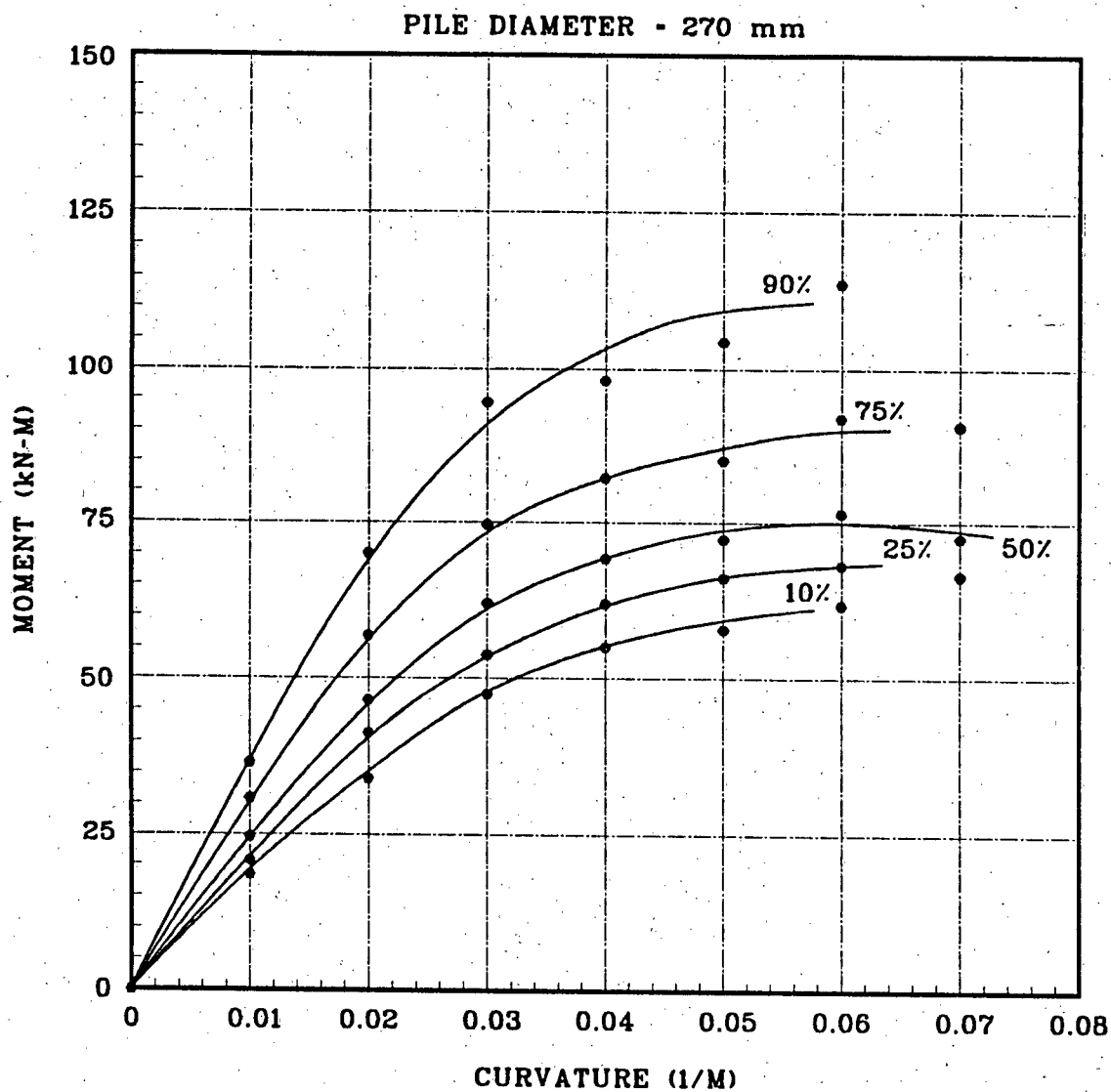


Figure 2.10: Moment-Curvature Curves Adjusted to 270mm Pile Diameter from BC Hydro Laboratory Tests on Timber Piles. After Lee et al (1992).

liquefied layer. The piles were then loaded in a fixed-head, displacement-controlled condition to failure, under an increasing one-way cyclic loading. A typical input displacement history is shown on Figure 2.11.

The following parameters were measured during the tests:

- ◆ lateral displacement of the pile cap,
- ◆ vertical displacement of the pile cap,
- ◆ deflected shape of the timber pile using electro-level gauges,
- ◆ strains in the timber pile using strain gauges,
- ◆ applied moment at the pile cap using a specially made moment cell,
- ◆ lateral load.

Comparison of measured vertical displacements of the pile cap with theoretical rigid body movements indicated that no pile cap settlements occurred other than those associated with rigid body motions. Typical measured lateral loads and moments versus displacements at pile cap are shown on Figure 2.12. Typical deformed shapes of the piles is shown on Figure 2.13. Figure 2.14 shows the measured moments (corrected to below the pile cap) versus curvature for all the three piles adjusted to a pile diameter of 270mm. Out of 3 piles tested to maximum displacement of the pile cap of 1 m. all piles were able to support the design vertical load of about 10 tons when the rotational constraint was maintained; however, only 2 of 3 piles were able to support the vertical load when the rotational constraint was removed.

In short, these results confirm that piles may be capable of carrying their vertical load after

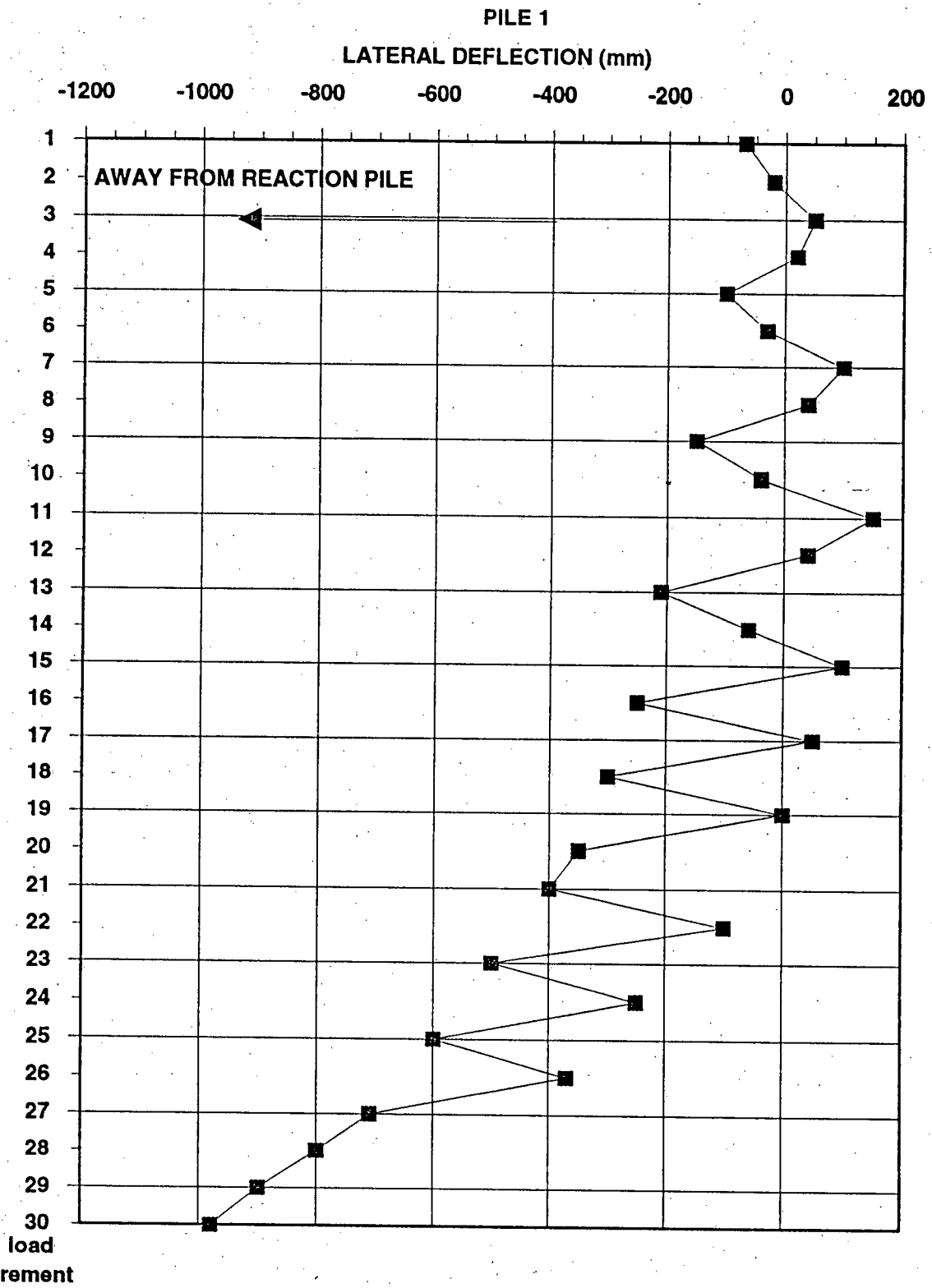


Figure 2.11: Typical Input Displacement History for BC Hydro Field Tests. After Lee et al (1992).

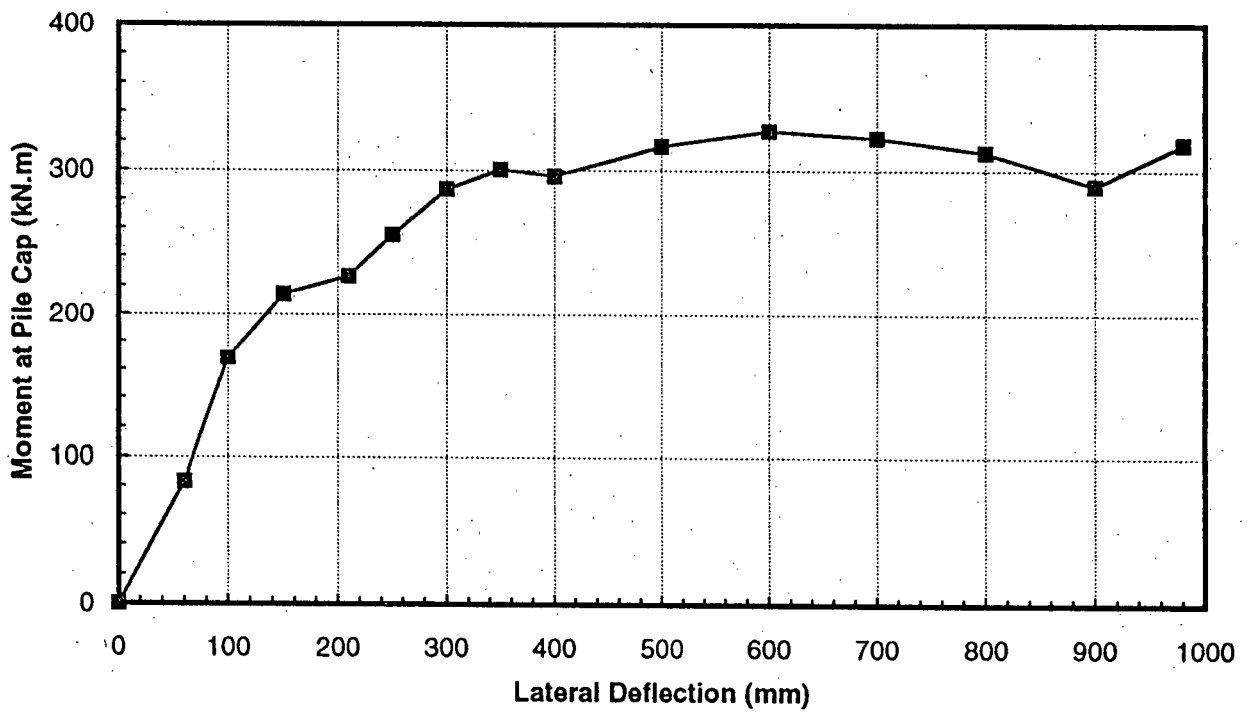
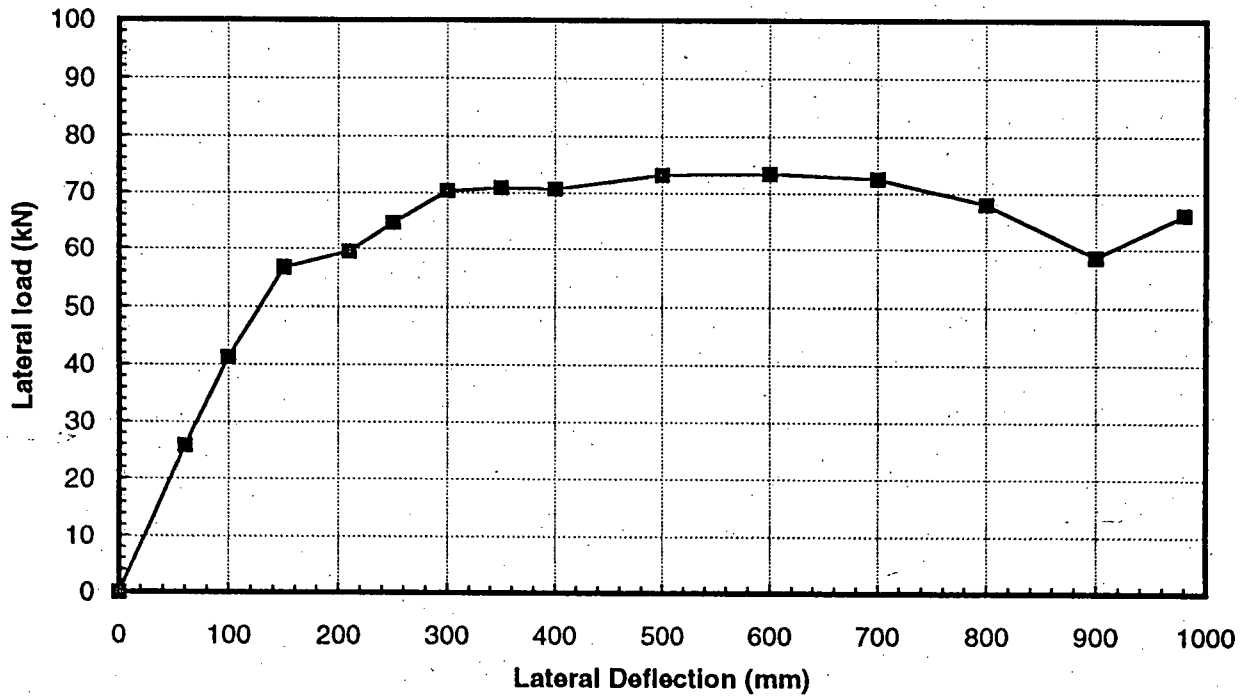


Figure 2.12: Typical Maximum Moments and Loads vs. Lateral Displacements. After Wong (1992)

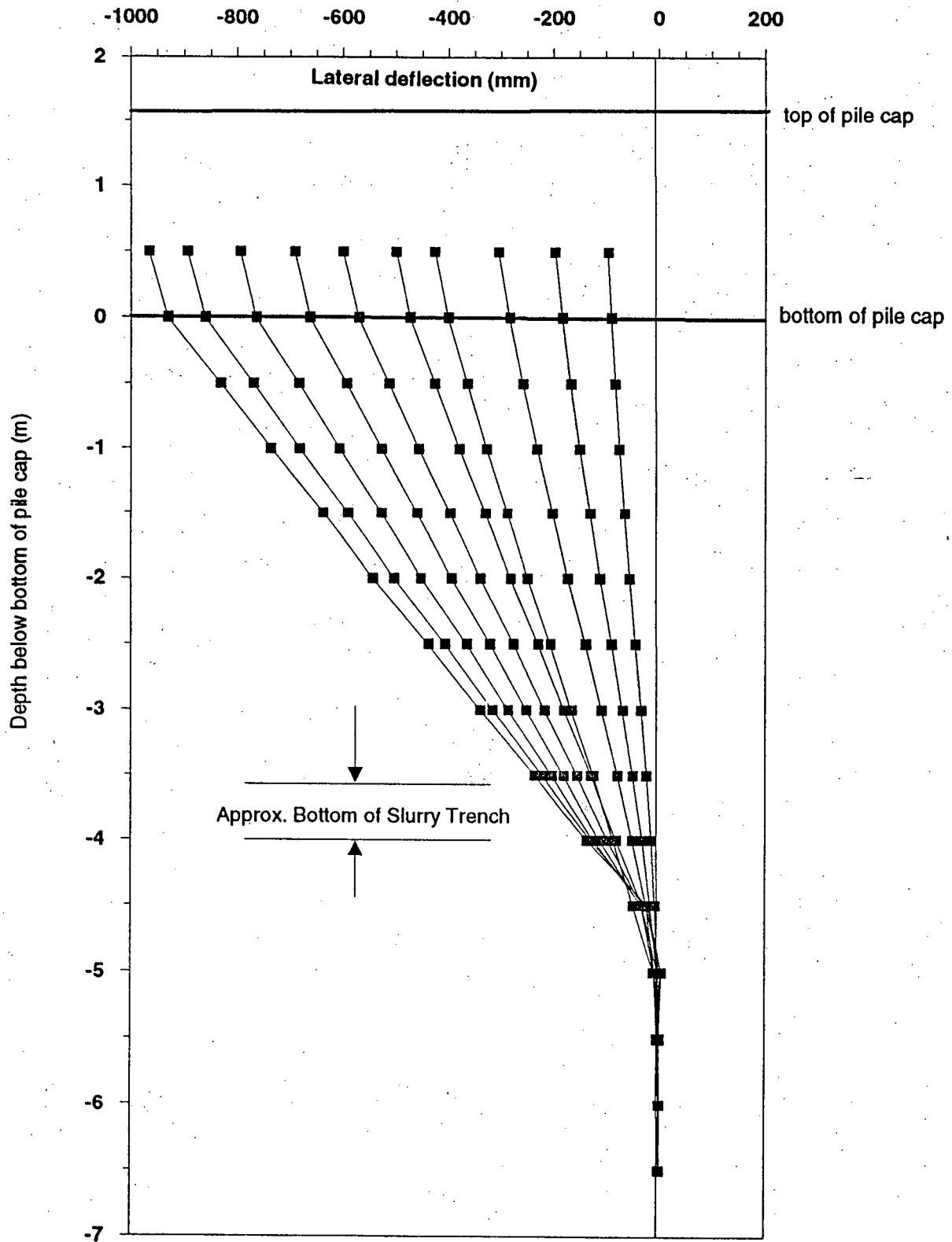


Figure 2.13: Typical Measured Deformed Shapes as measured by electro-levels from BC Hydro Field Tests on Timber Piles. After Wong (1992).

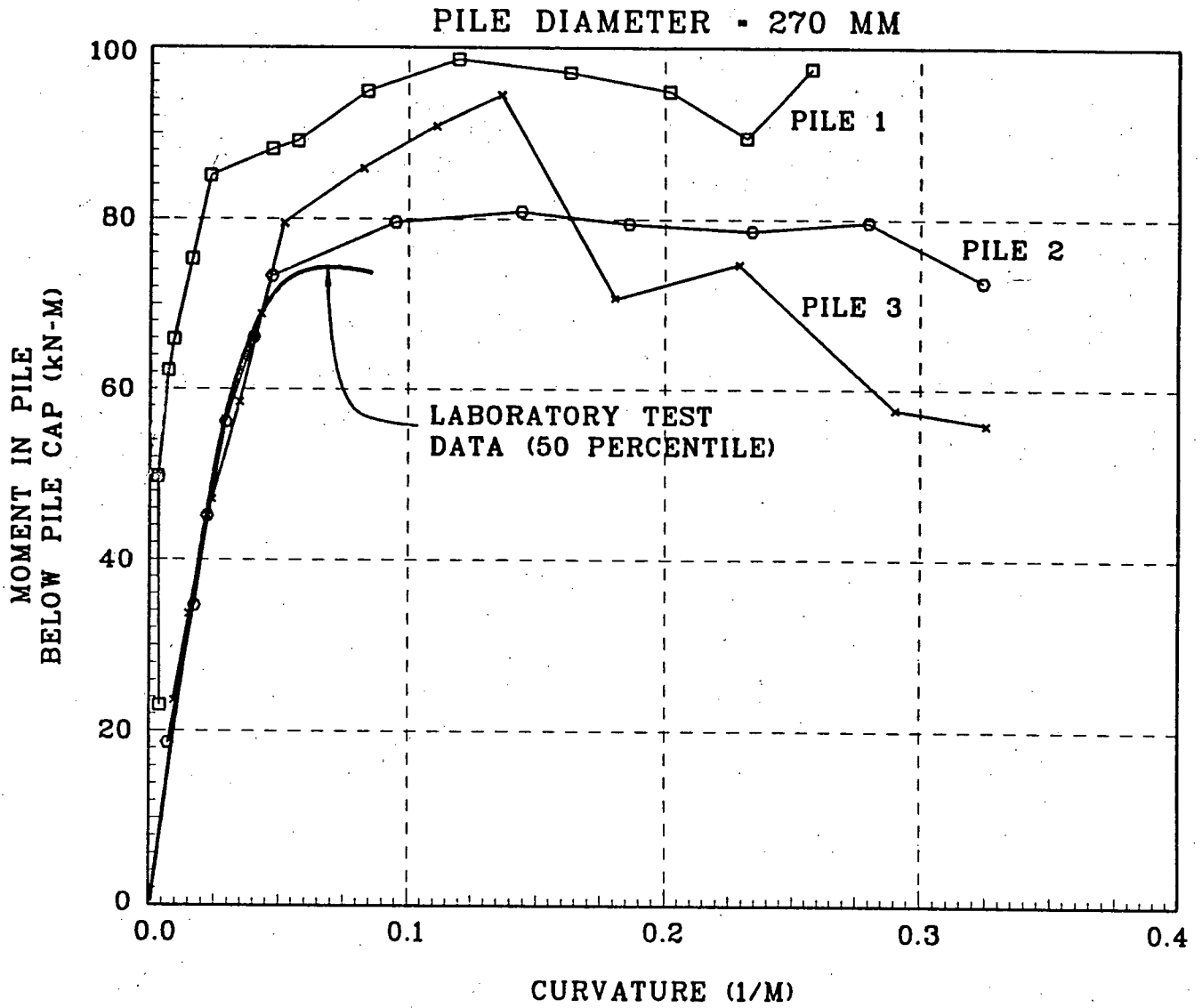


Figure 2.14: Moment vs. Curvature Adjusted to Below the Pile Cap and to 270mm Pile Diameter from BC Hydro Field Tests on Timber Piles. After Lee et al (1992).

undergoing large lateral displacements. This generally confirms the results of the BC Hydro (Lee et al, 1992) laboratory tests.

2.4 Summary

Based on the above review, it is observed that soil-pile interaction behaviour is highly non-linear and should be taken into account in any practical analysis of laterally loaded pile foundation. It seems that at present, 1996, the non-linear P-y curve approach is the most versatile method for modelling this behaviour. A wealth of information already exists for constructing P-y curves for fine-grained soils. Yan's (1986, 1990, 1992) research and experimental work has provided us with a robust method of obtaining P-y curves in granular soils.

Existing models for assessing pile response under lateral loading are limited in many ways. A new model is required which would be capable of analyzing a non-linear soil, a yielding pile, and cyclic applied loads. The full scale tests by BC Hydro have provided the opportunity to formulate and verify a new model which uses Yan's P-y curves. However, at present, there are no methods available for constructing cyclic P-y curves based on fundamental soil properties to properly represent measured test data (Yan, 1990). In the following chapter, a simple cyclic P-y curve model is developed using the test data presented by Yan (1990).

In the following chapters a comprehensive numerical model is developed based on a finite element formulation for the pile and P-y curves for the soil. This combination provides a versatile, yet efficient, model for analyzing laterally loaded piles. The model is then verified and used to predict the full scale test results.

Chapter 3 A Cyclic P-y Curve Model

3.1 Introduction

In this chapter, the experimental data presented by Yan (1990) is evaluated and reduced in an attempt to develop a simple, empirical cyclic P-y curve model. The significant features of the experimental P-y curves are determined and an attempt is made to develop empirical relationships for the modelling of the cyclic P-y curves. The objective of this study is to enable the practising engineer to extrapolate the results of the present and other experimental studies to actual field and design conditions using a relatively simple and general model.

As mentioned in Chapter 2, the cyclic P-y curves will be presented under two separate categories: 1) two-way cyclic P-y curves, and 2) one-way cyclic P-y curves. In the following chapter a numerical model will be developed based on the empirical relationships presented in this chapter. This model will be incorporated into a computer program and will be verified with field measurements and laboratory test results.

3.2 Experimental Setup

As mentioned earlier, few comprehensive cyclic lateral load tests have been performed on piles. In the present study, only the experimental data presented in Yan (1990) will be used because this is

the only study where accurate measurements of the pile deflections under cyclic loading have been made and reported for the derivation of soil-pile interaction P-y curves.

The Hydraulic Gradient Similitude test procedures are explained in detail in Yan (1990). The testing process consisted of both one-way and two-way cyclic loading of an instrumented 6.35 mm diameter aluminum pipe pile embedded in uniform sand. The lateral load was applied at a period of 40 seconds per cycle. It is assumed that at such a slow loading rate, dynamic effects may be ignored. It is also assumed that drained conditions prevail in the sand at such a slow loading rate.

It should be mentioned that the amount of experimental data is not as plentiful as one likes to have and the P-y curve formulation which will be presented here will also be of limited accuracy. It is hoped that this model will be updated and verified as more experimental information becomes available.

Since monotonic loading is really a subset of cyclic loading, the various factors that affect the response of a pile to static loading also affect the response in cyclic loading. However, two additional factors will influence the pile response under cyclic loading. These are:

- ◆ the nature of applied load; ie whether the applied loading is one-way cyclic or two-way cyclic;
- ◆ the number of loading cycles; and,
- ◆ the magnitude of applied load.

The effect of the number of loading cycles will be presented as the effect on each of the two types of applied loading.

3.3 Two-way Cyclic Loading

Figure 3.1 shows the time histories of applied lateral load and pile head deflection for a free head model pile under the two-way cyclic loading condition. It can be seen that the pile head deflections are biased in the first-time loading direction. It is also observed that there is some change in the pile head displacements with the number of loading cycles, however, the magnitude of the change is small relative to the maximum pile displacements. Figure 3.2 shows the pile head peak deflections with the number of loading cycles. The pile head deflections in this figure have been normalized to the maximum lateral load applied to the pile. It may be seen from the figures that the pile head deflection under a constant two-way cyclic loading decreases initially then increases with the number of loading cycles in both compression and tension directions.

The above observations will be investigated by analyzing the measured cyclic P-y response along the pile.

The experimental cyclic P-y curves at different depths for the above-mentioned pile are shown on Figure 3.3. It is seen that the general shape of the cyclic P-y curves is nonlinear and hysteretic. The curves are very soft near the surface and become stiffer with depth as the soil confining stress increases. The cyclic P-y curves also appear to be non-symmetrical about the zero pile deflection axis with a bias in the first-time loading direction. The formation of gaps on both sides of the pile is evident on most of the experimental P-y curves. There also seems to be some residual soil reaction against the pile within the "gap" zone. This soil reaction is perhaps due to the skin friction along the sides of the pile as it moves through the gap zone. The magnitude of the gap is generally affected by the pile deflection and the number of loading cycles. The cyclic P-y curves

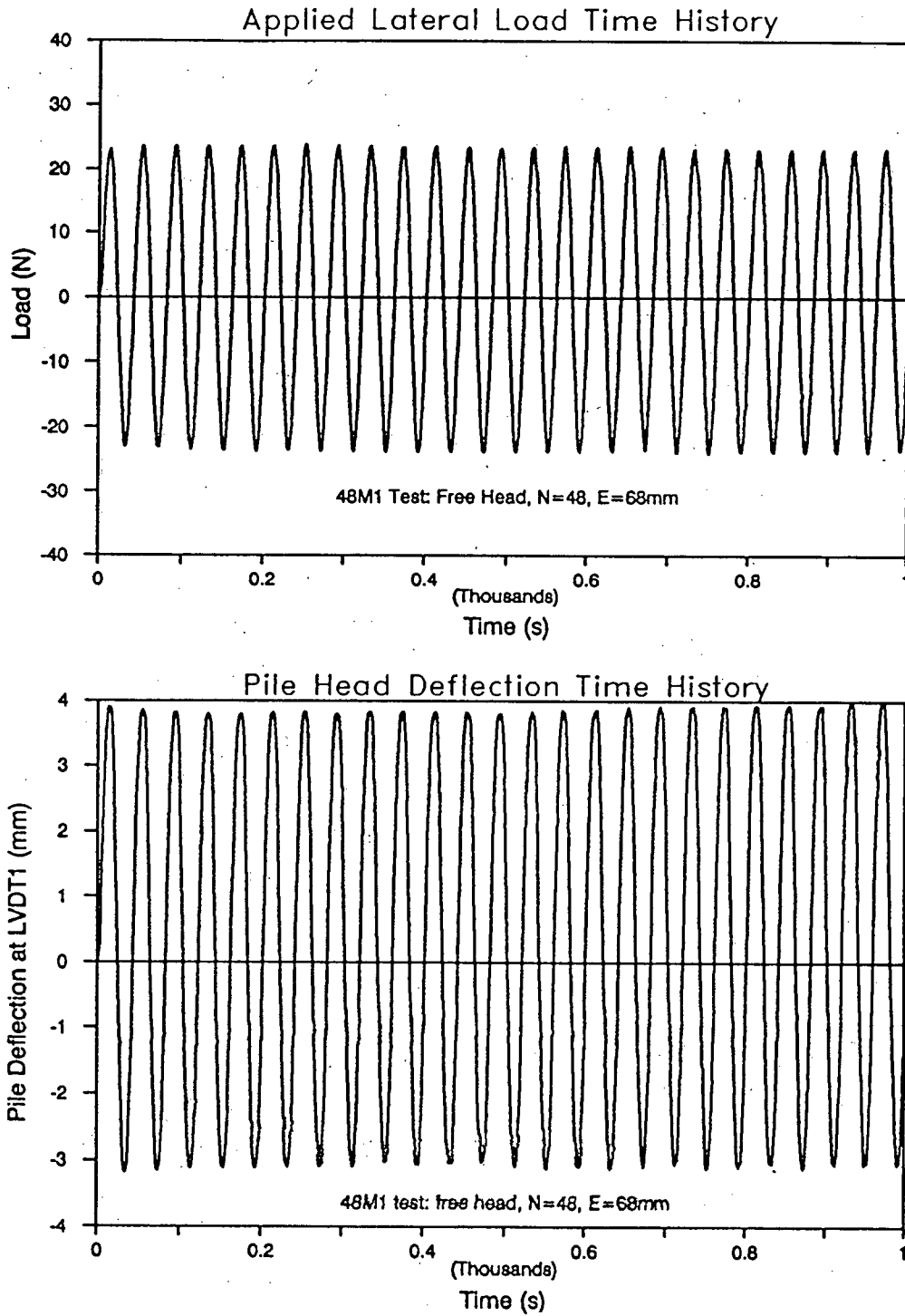


Figure 3.1: Time Histories of Applied Lateral Two-way Load and Pile Head Deflection at 88mm above sand surface. After Yan (1990)

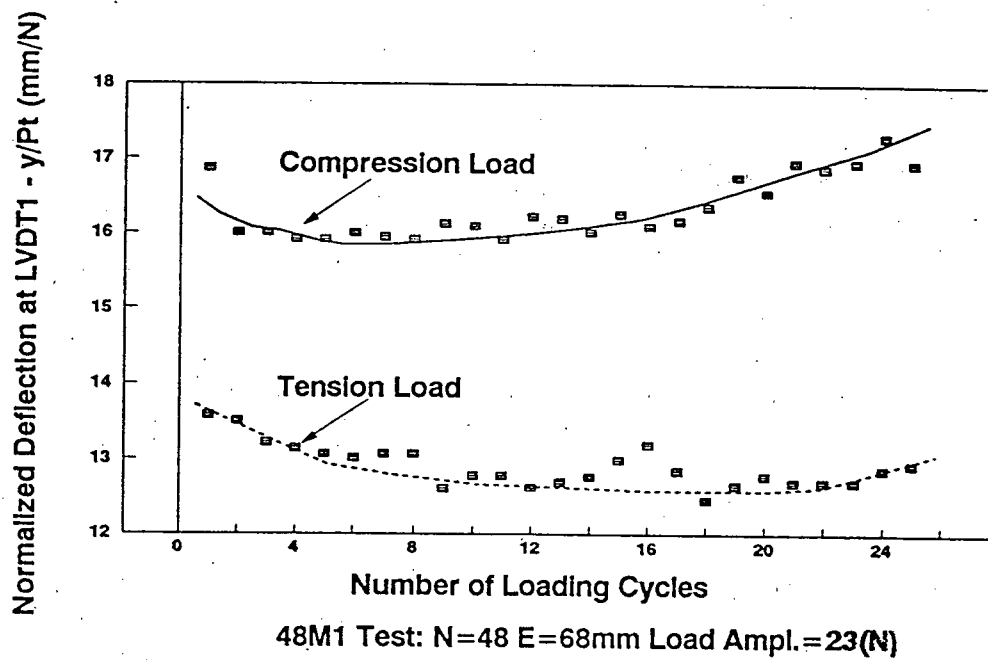


Figure 3.2: Normalized Pile Head Peak Deflection with Number of Loading Cycles. After Yan(1990)

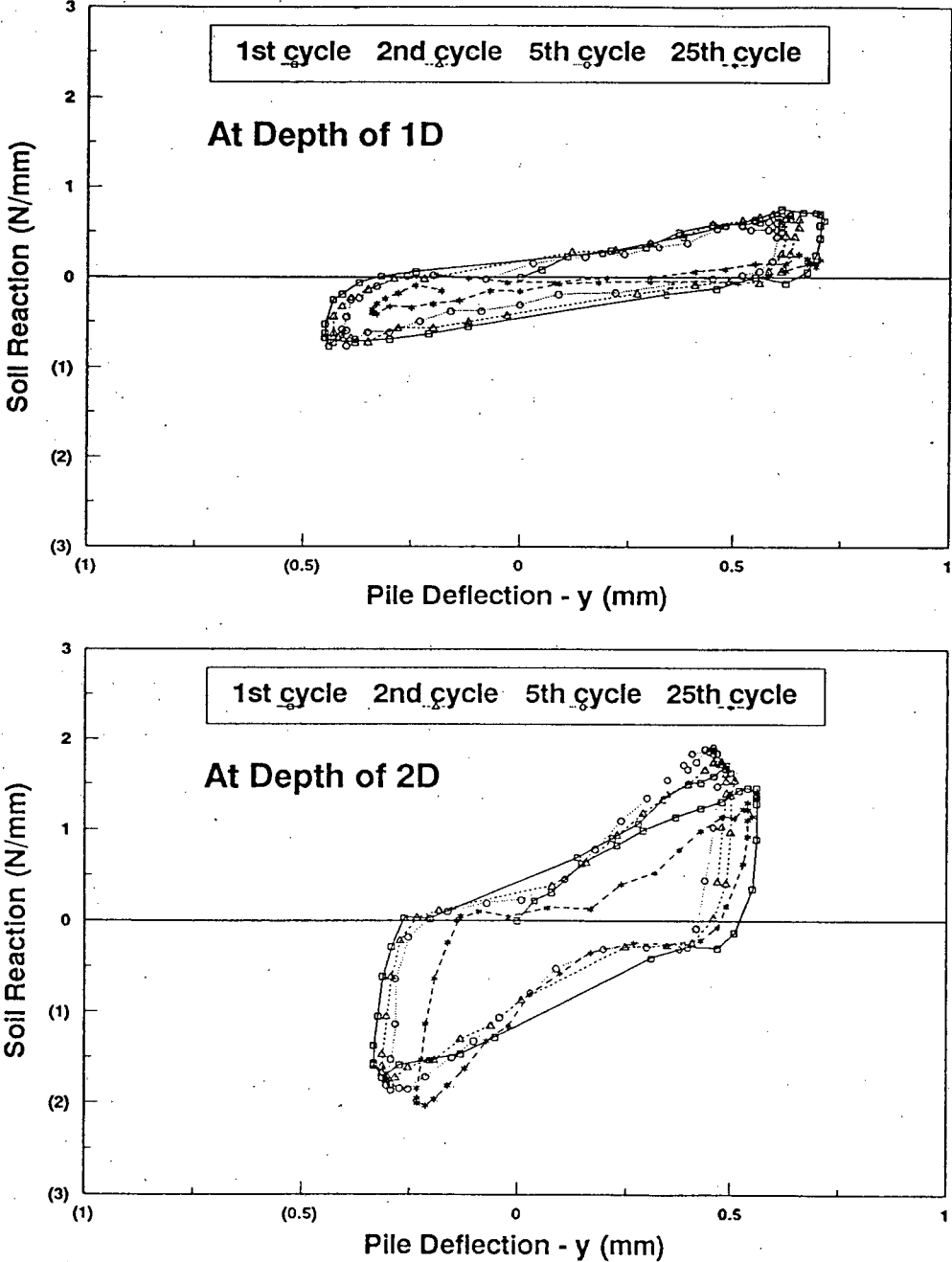


Figure 3.3: Cyclic P-y Curves for different Loading Cycles at 1 and 2 Pile Diameter Depths. After Yan (1990).

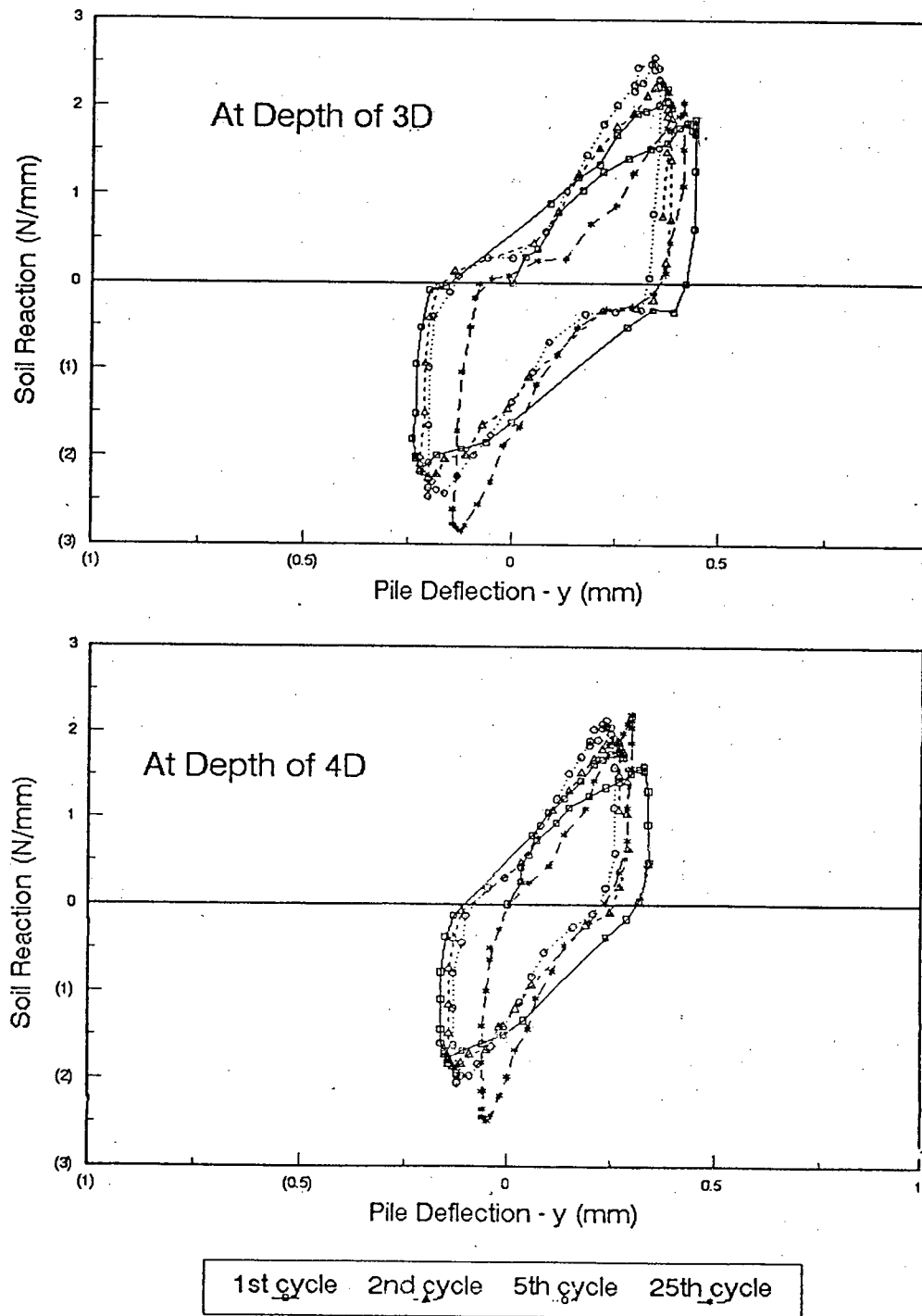


Figure 3.3: Cyclic P-y Curves for different Loading Cycles at 3 and 4 Pile Diameter Depths. After Yan (1990).

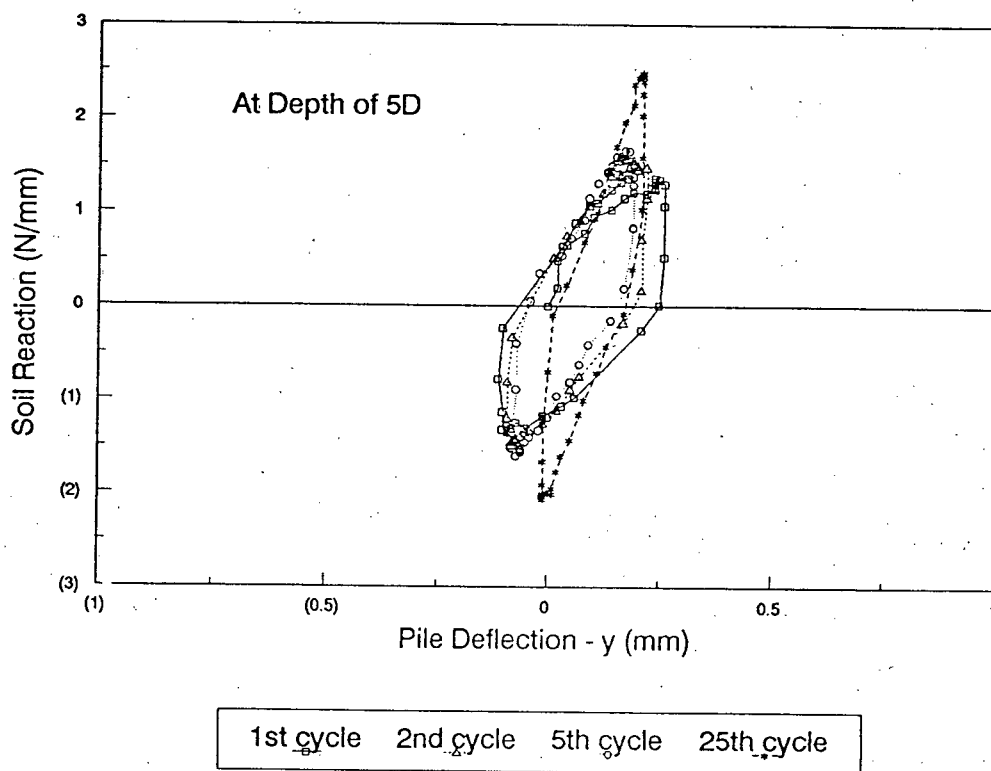


Figure 3.3: Cyclic P-y Curves for different Loading Cycles at 5 Pile Diameter Depth. After Yan (1990).

clearly indicate that the magnitude of the gap is much less than the total soil displacement at that point. This would suggest that as the pile deflects, the soil yields and moves around the pile to fill in some of the gap behind the pile, similar to a bearing type of failure.

The loading cycles affect the cyclic P-y curves differently with depth. The variations of the following features will be discussed next.

1. Loading segments (both in the direction of first time loading (positive) and in the opposite direction (negative));
2. unloading segments (positive and negative);
3. gap segments (positive and negative); and,
4. residual soil reaction (on both positive and negative sides).

3.3.1 Loading Segments

At shallow depths (about one pile diameter), the cyclic P-y curves become softer with the number of cycles. At depths of 2 and 3 pile diameters, the P-y curves in the positive loading direction first become stiffer and then softer with number of cycles. However, at these depths, the P-y curves in the negative loading direction continually become stiffer with the number of cycles. At 4 and 5 pile diameter depths, the cyclic P-y curves show continued stiffer response with number of loading cycles in both loading directions.

Although it is difficult to see from Figure 3.3, the shape of the loading portion of the experimental P-y curves do not appear to change very much, other than becoming stiffer or softer, with the number of loading cycles. To determine the parameters governing the shape of the P-y

curves under repeated loading, we can examine Yan's (1990, 1992) formulation for the monotonic P-y curve which was presented in Chapter 2. The only soil properties in his formulation are the maximum Young's modulus, E_{\max} , and α , which depend on the soil's relative density, D_r . Therefore, for simplicity, it can be assumed that the cyclic loading procedure simply changes the E_{\max} of the surrounding soil by either densifying or loosening the soil. The E_{\max} of the soil may be back-calculated from the experimental P-y curves using Yan's (1992) formulation,

$$\frac{P}{E_{\max} D} = \alpha \left(\frac{y}{D} \right)^\beta \quad [1]$$

where D is the pile diameter, P is the soil reaction force, y is the pile deflection, β has a value of about 0.5, and α is a function of the relative density of the soil (Yan, 1986, 1990, 1992). Figure 3.4 shows the variation of E_{\max} with number of cycles normalized to the initial value, $E_{\max, i}$, at each depth. As can be seen, during the first few cycles, the E_{\max} values all normalize very closely. However, at the 25th cycle, the normalized E_{\max} values are very different for different depths. This is consistent with the observation from the cyclic P-y curves that at shallow depths, the cyclic P-y curves initially harden and then soften with the number of cycles, while at greater depths, the P-y curves continually become stiffer with the number of cycles. The curves fitted to the experimental data are shown on Figure 3.5 and appear to have the form:

$$\frac{E_{\max}}{E_{\max, i}} = 1 + F_n (1 - e^{-F_n (1-N)}) \quad [2]$$

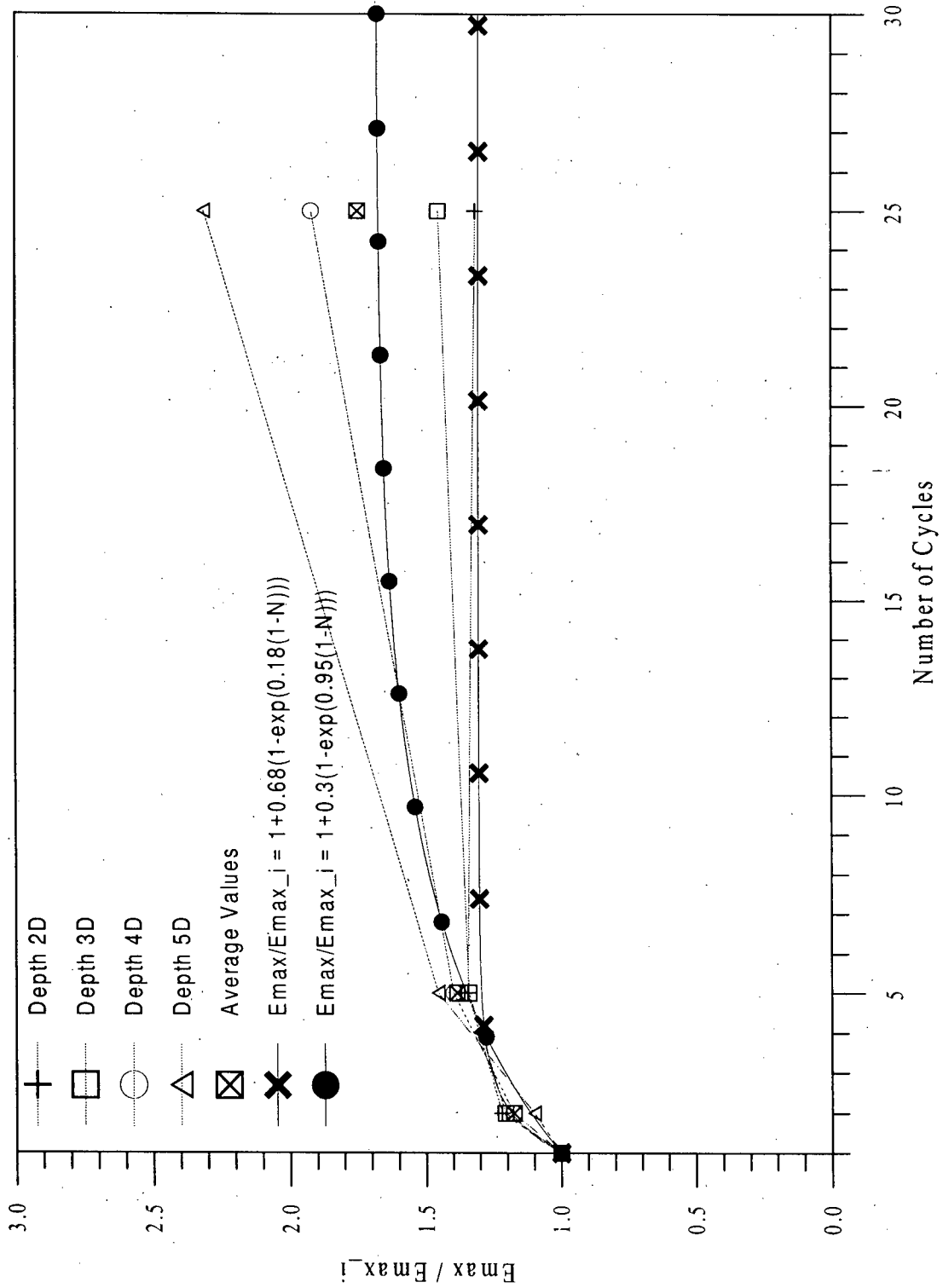


Figure 3.4: Variation of E_{max} with Number of Cycles. Back-calculated from Measured Cyclic P-y Curves (Yan, 1990).

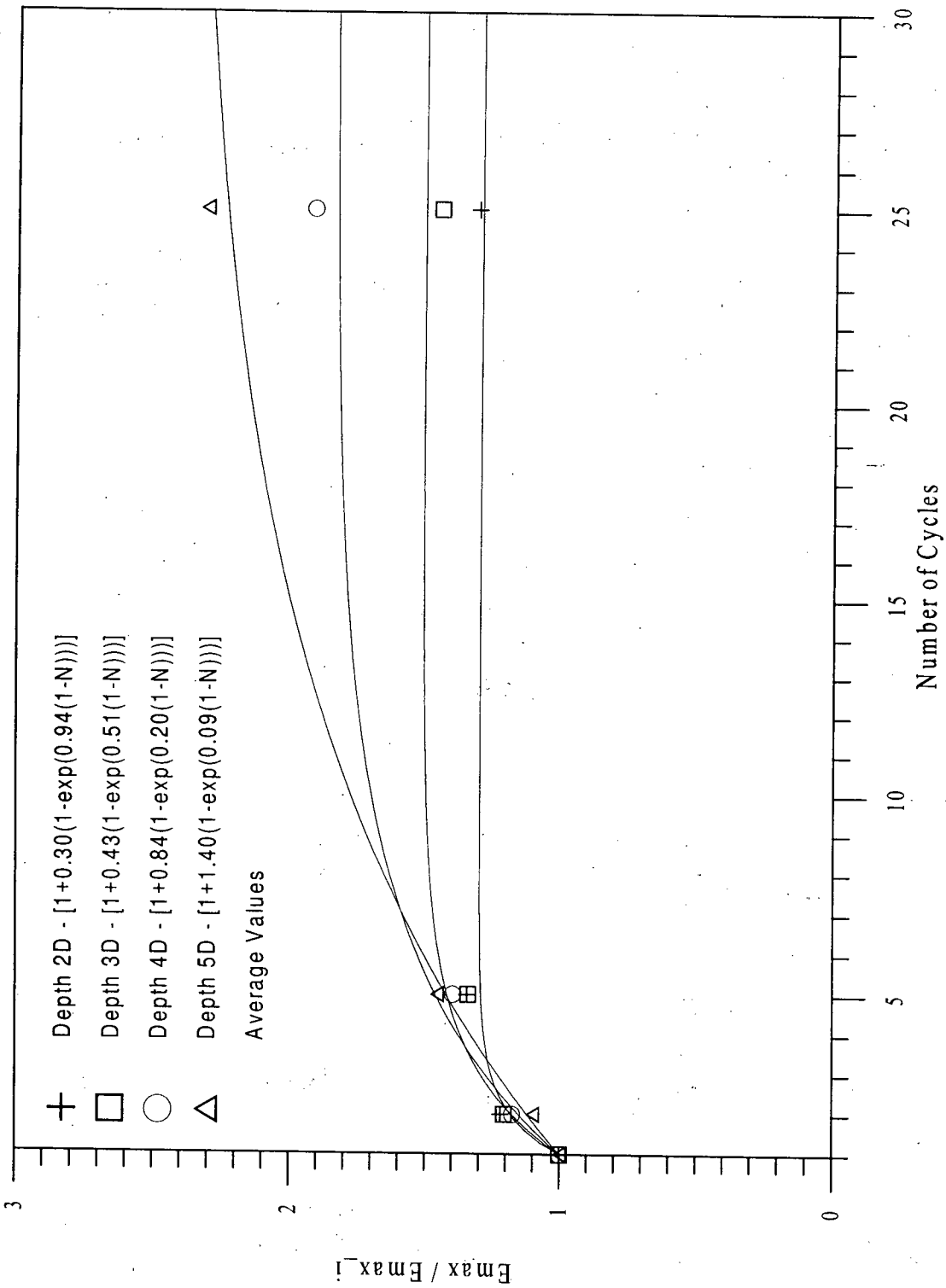


Figure 3.5: Curves Fitted to the Experimental Data for Variation of E_{\max} with Number of Cycles.

where E_{\max} is the soil's maximum Young's modulus at each cycle, $E_{\max i}$ is the E_{\max} at the first cycle, N is the number of cycles, and F_n and F_e are empirical factors which seem to vary with the vertical effective stress according to:

$$F_n = 4.4 e^{-28\left(\frac{\sigma'_{vo}}{Pa}\right)} \quad [3]$$

and,

$$F_e = 0.11 e^{18.4\left(\frac{\sigma'_{vo}}{Pa}\right)} \quad [4]$$

as shown on Figure 3.6. It should be mentioned that we have made a simplifying assumption here by treating the effects of the cyclic loading in the negative and positive directions as equivalent. Although this is different from what is observed at 2 and 3 pile diameter depths, it should introduce little error in predicting the pile head behaviour as the overall differences along the pile length are not significant.

It is noted that the above empirical relationships will give the wrong P-y curves at depths less than three (3) pile diameters. This is important as the pile head response is significantly influenced by the soil resistance at these shallow depths. An examination of the measured P-y curves shown on Figure 3.3 indicate that at a depth of 1 pile diameter, the cyclic P-y curves soften with the number of loading cycles. At a depth of 2 pile diameters, the P-y curves initially harden and then soften with the number of cycles while at a depth of 3 pile diameters and greater, the P-y curves continually harden with the number of loading cycles.

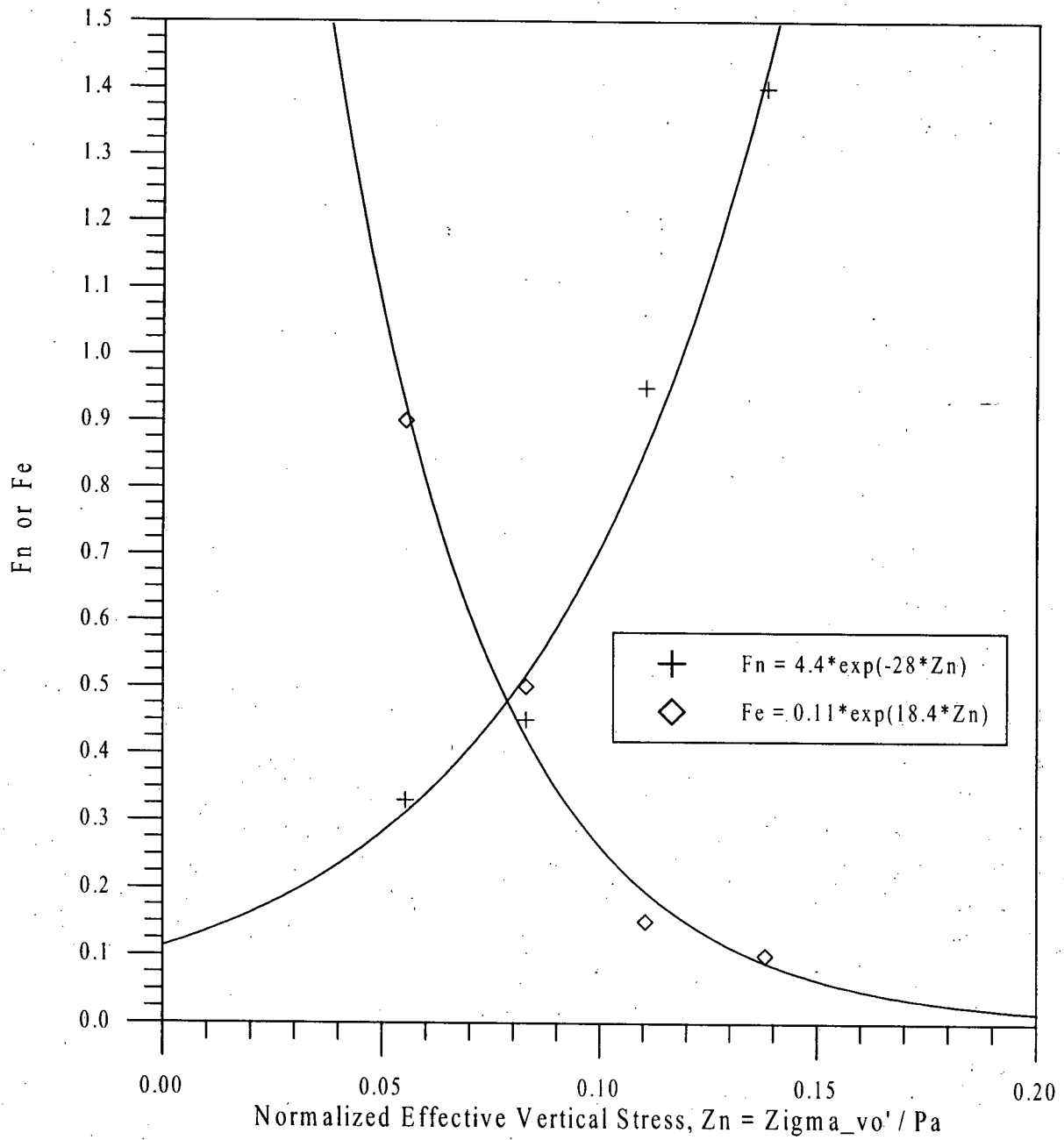


Figure 3.6: Variation of F_n and F_e with Effective Vertical Stress.

The predicted cyclic P-y curves for the various depths are shown on Figure 3.7. As can be seen, the predictions are very good for depths greater than 3 pile diameters. However, at shallower depths the predictions can be in error by as much as 300 percent.

A simple approach to solving this problem would be to use a function which would vary from -1 to 1 in the range of 1 to 3 pile diameters and become asymptotic to -1 and 1 for values less than 1 pile diameters and greater than 3 pile diameters, respectively. We can then multiply F_n by this function and obtain an approximation of the variation of the P-y curves with number of cycles at shallow depths. One such function is

$$f(x) = \tanh(x - 2) \quad [5]$$

where x is the depth in pile diameters. Figure 3.8 shows the predicted P-y curves obtained using this approach. As can be seen, a reasonable agreement with the measured P-y curves (Figure 3.3) is obtained.

3.3.2 Unloading Segments

The unloading portions of the P-y curves shown on Figure 3.3 are very steep and almost linear. The slope of this portion of the P-y curves coincides with the soil's maximum Young's modulus, E_{\max} , as would be expected. Although it is difficult to estimate the change in the unloading modulus with number of cycles from these measurements, it is evident that the unloading modulus would be approximately equal to E_{\max} . The variation of E_{\max} with the number of cycles was discussed above.

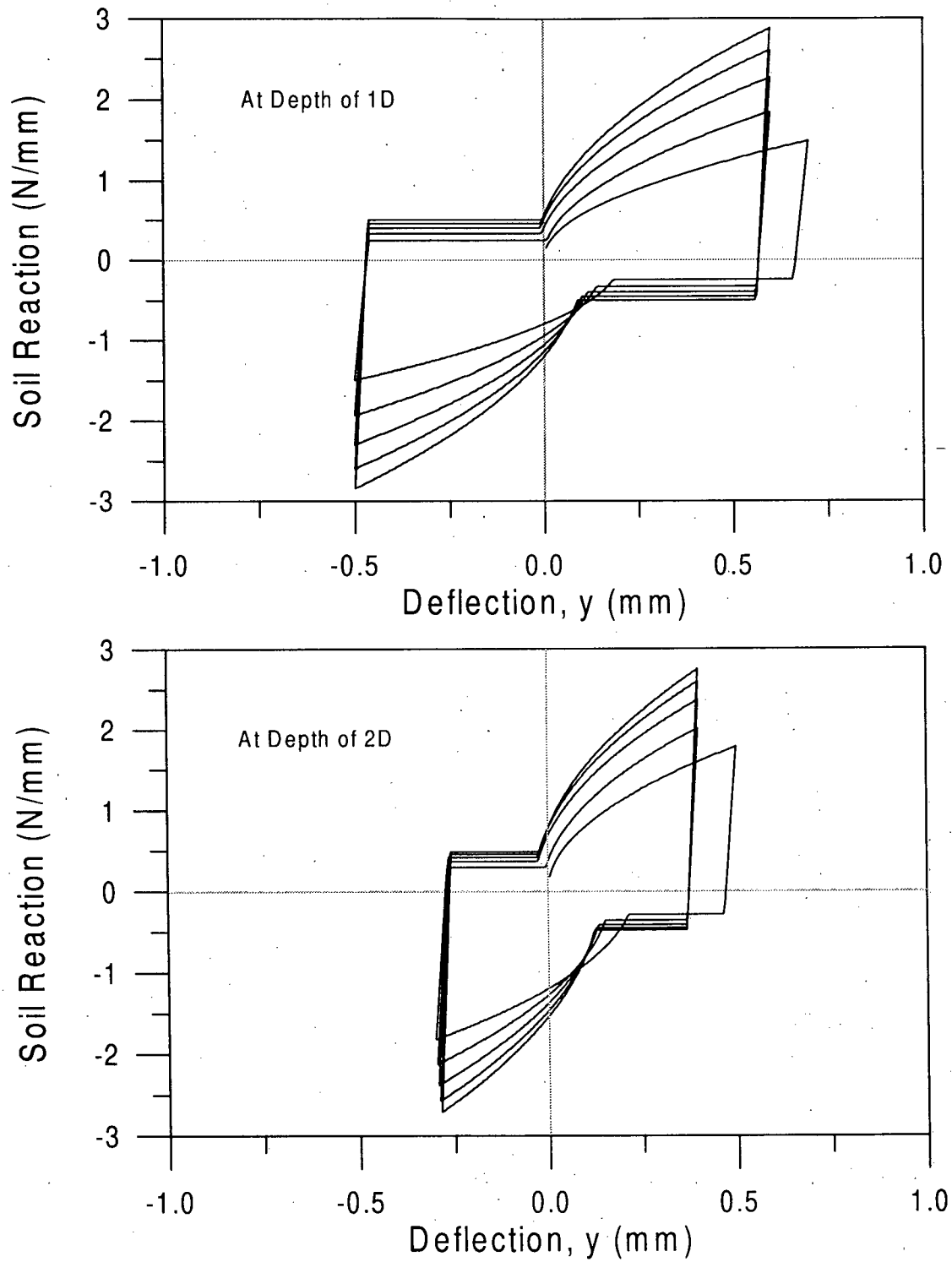


Figure 3.7: Proposed Cyclic P-y Curves Before Adjustments At Shallow Depths.

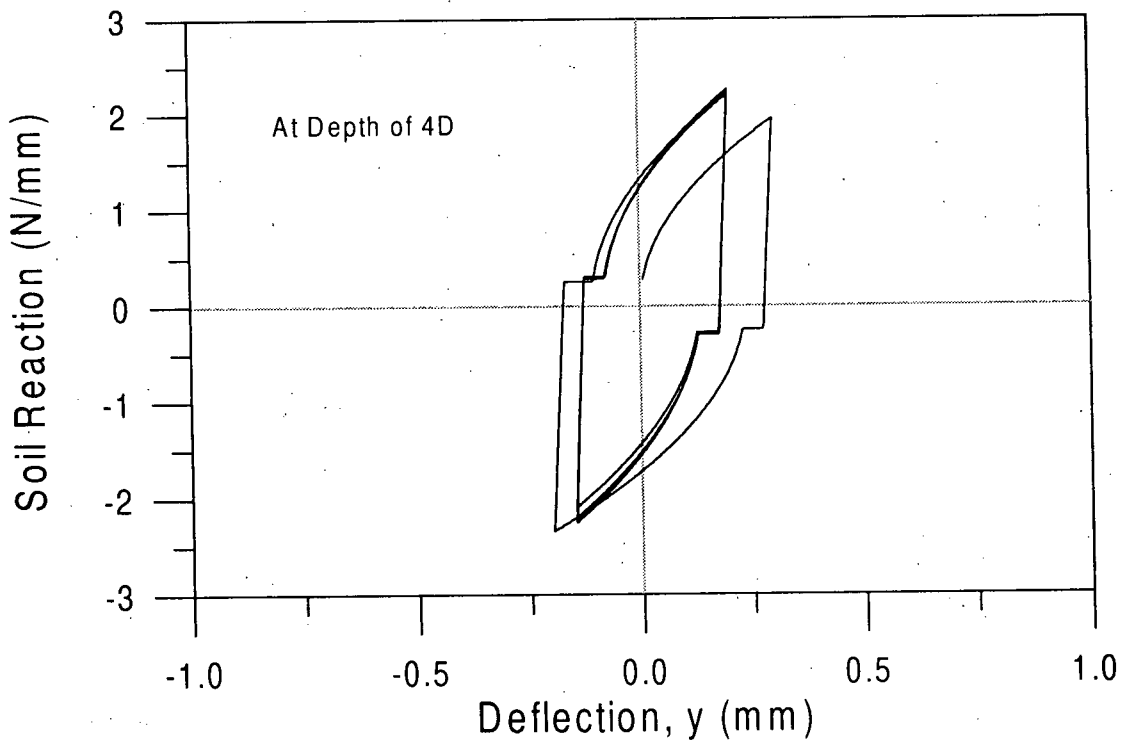
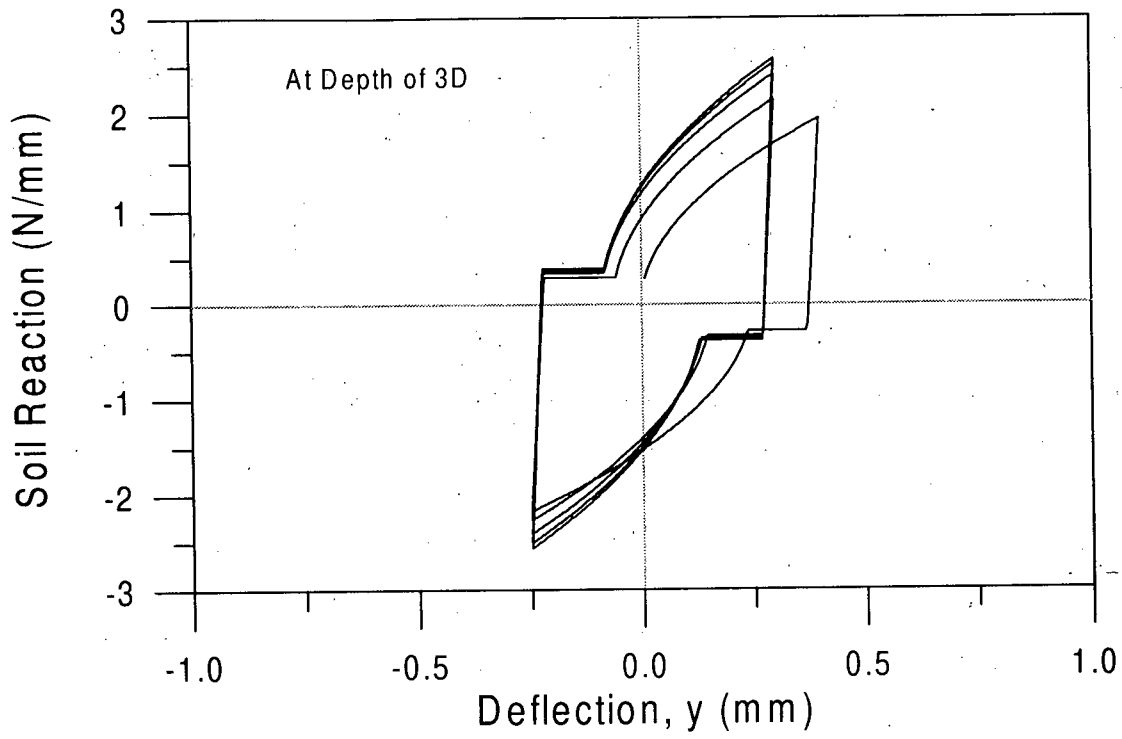


Figure 3.7: Proposed Cyclic P-y Curves Before Adjustments At Shallow Depths.

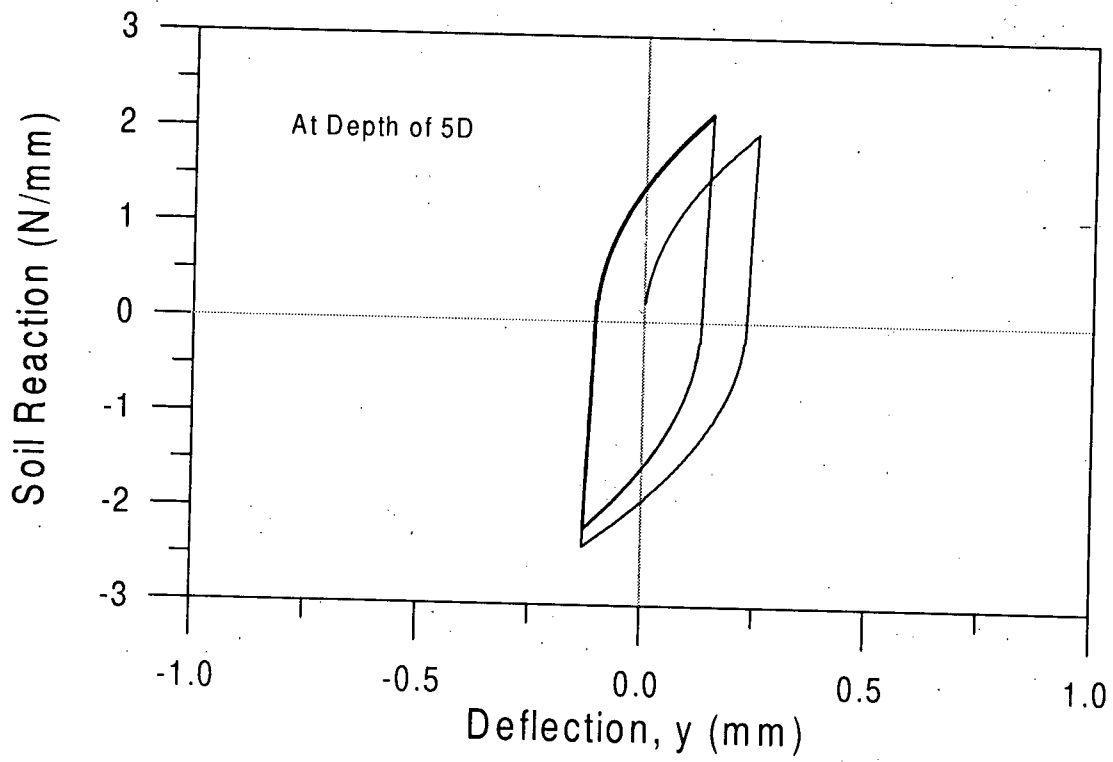


Figure 3.7: Proposed Cyclic P-y Curves Before Adjustments At Shallow Depths.

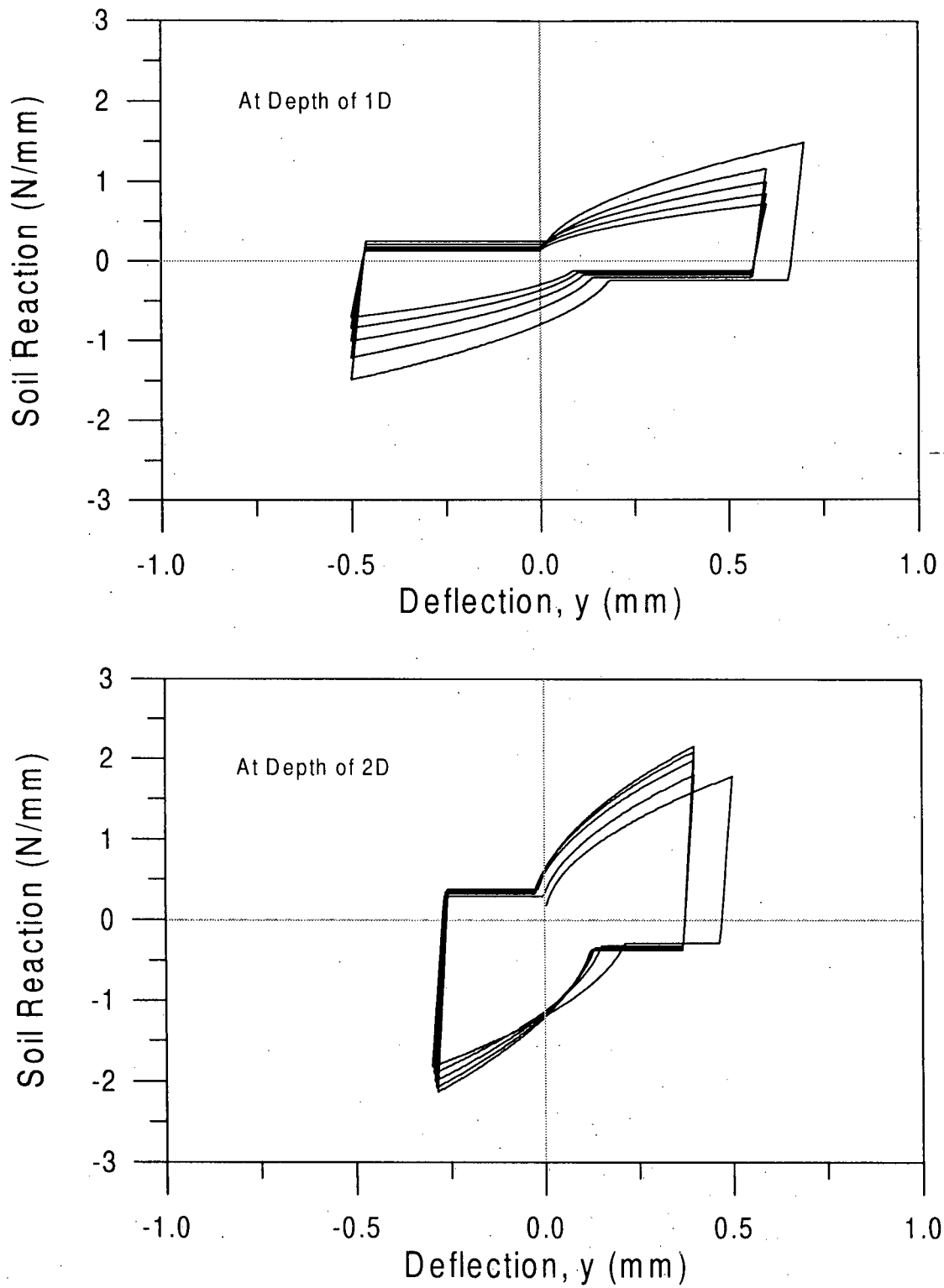


Figure 3.8: Proposed Cyclic P-y Curves with Adjustment At Shallow Depths.

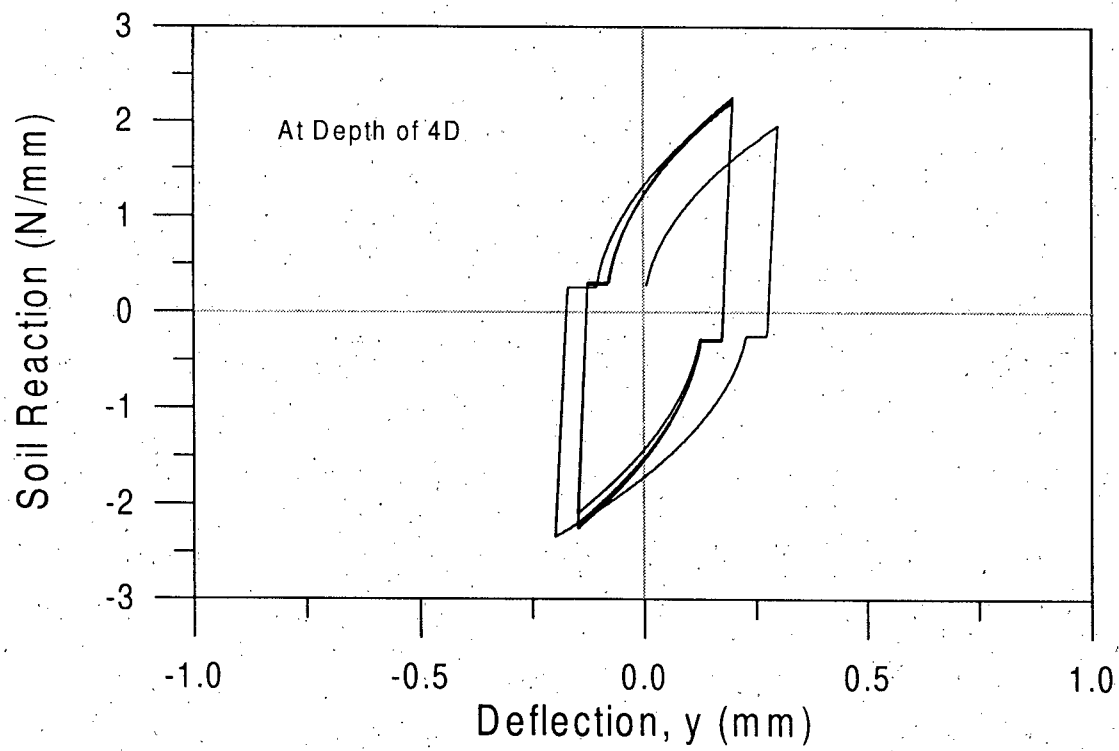
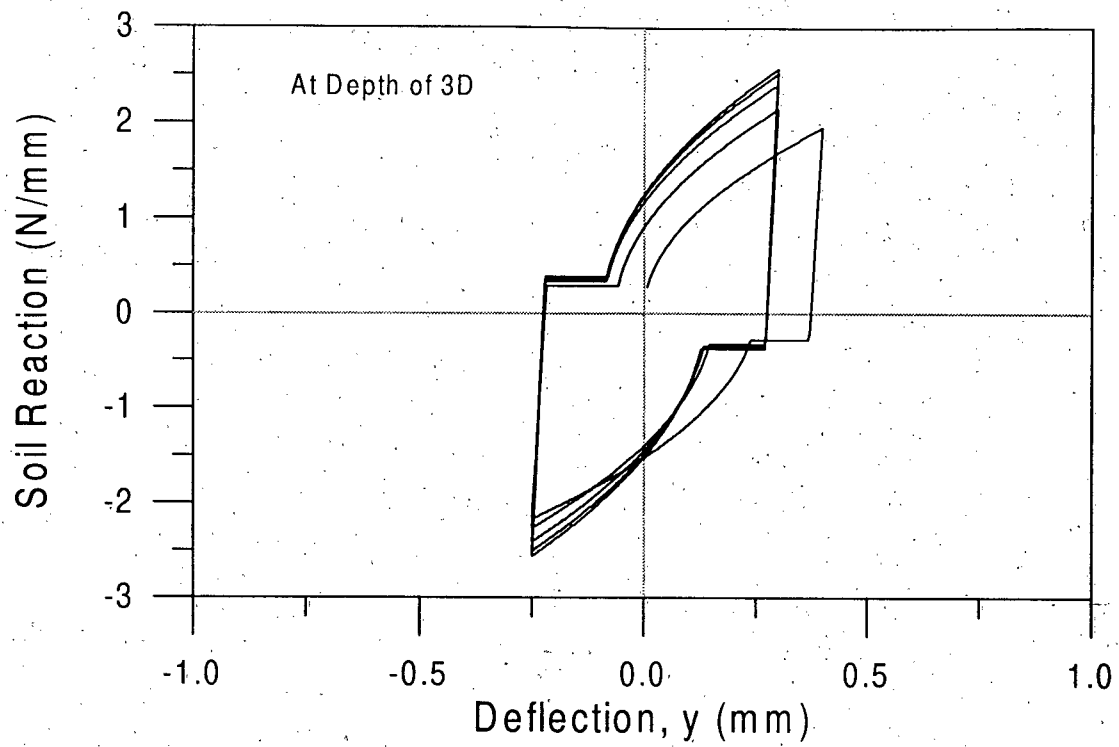


Figure 3.8: Proposed Cyclic P-y Curves with Adjustment At Shallow Depths.

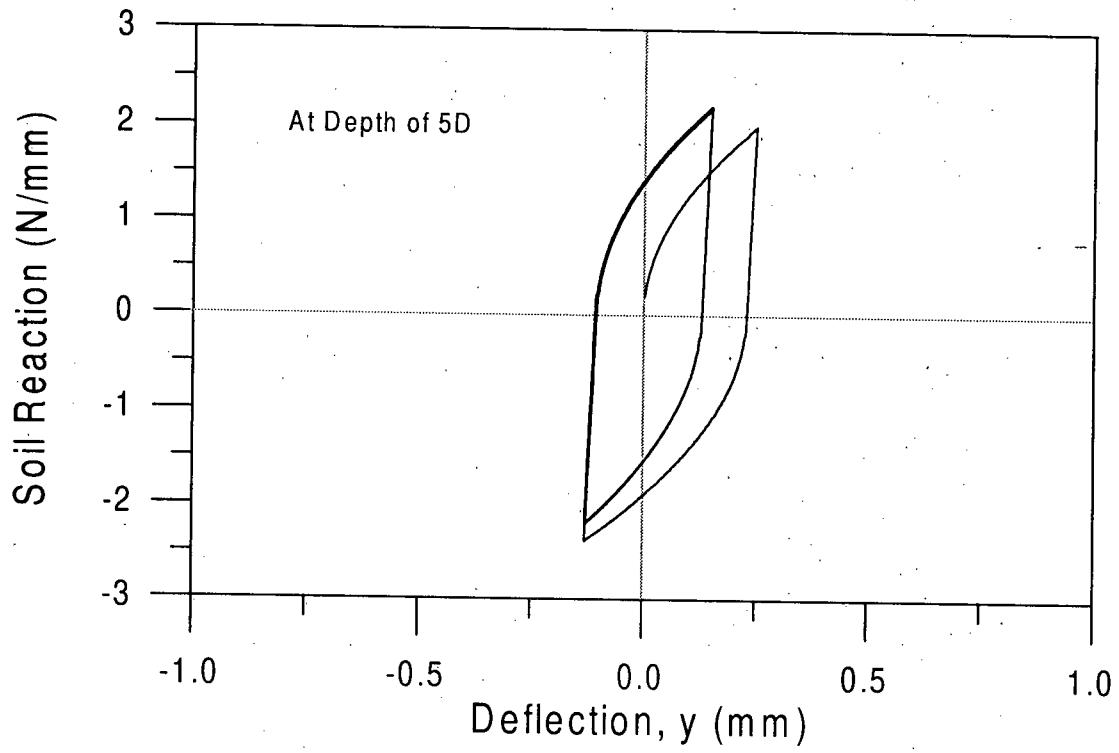


Figure 3.8: Proposed Cyclic P-y Curves with Adjustment At Shallow Depths.

3.3.3 Gap Segments

An examination of the cyclic P-y curves shown on Figure 3.3 reveals that the size of the gaps which form along the pile vary with depth. Relatively large gaps are observed at a depth of 2 pile diameters while there are virtually no gaps observed at 5 pile diameter depth. Figure 3.9 shows the variation of the gaps with stress level. Although there is a variation between the different cycles at each stress level, a generally linear trend with stress level is observed. Figure 3.10 shows linear approximations of this trend for each cycle. The equations of the lines have the form:

$$\frac{\text{gap}}{|\text{max,min } y|} = A_n - B_n \left(\frac{\sigma'_{vo}}{Pa} \right) \quad [6]$$

where

$$A_n = 0.025N + 0.8 \quad [7]$$

and,

$$B_n = 0.2N + 6 \quad [8]$$

as shown on Figure 3.11 where N is the number of loading cycles.

An interesting characteristic of the cyclic P-y curves is that a "full" gap is never developed between the soil and the pile. Upon load reversal, the soil reaction in that direction starts to increase sooner than would be expected. This can be explained by considering the moving soil particles around the pile. As the pile pushes against the soil, the soil fails and moves around the pile to fill

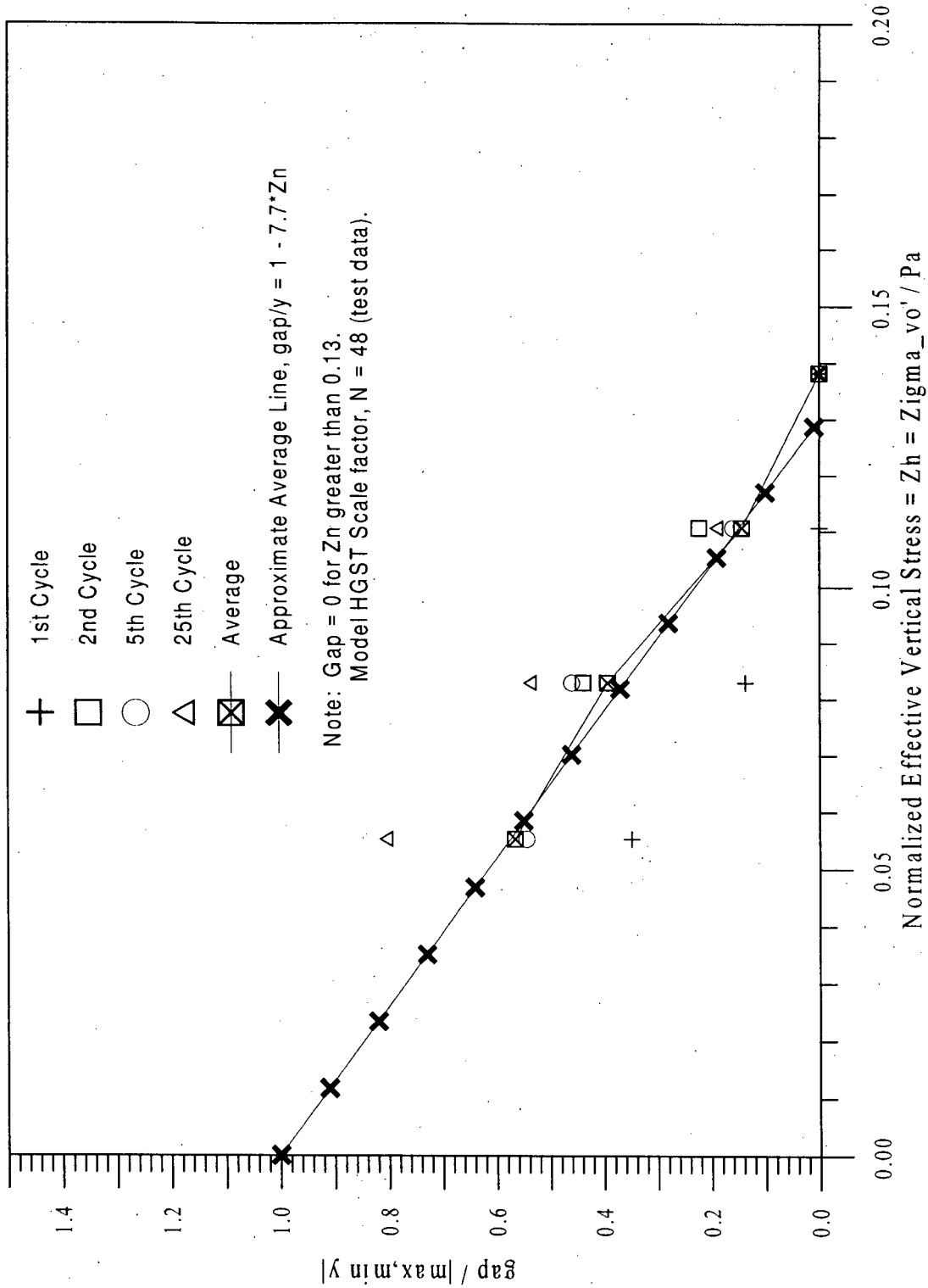


Figure 3.9: Variation of Soil-Pile Gap with Stress Level.

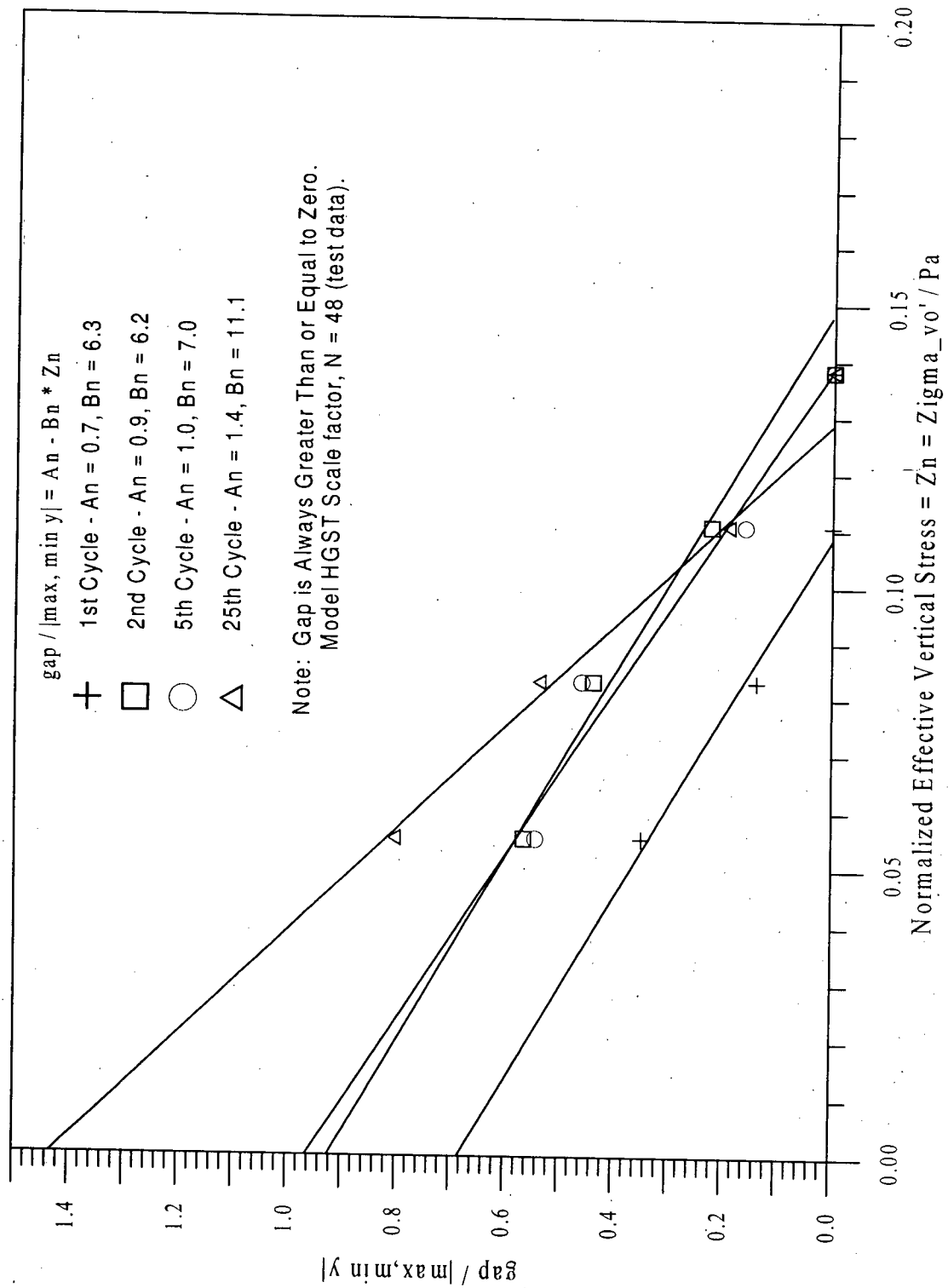


Figure 3.10: Linear Approximations of Variation of the Gap with Soil Stress Level.

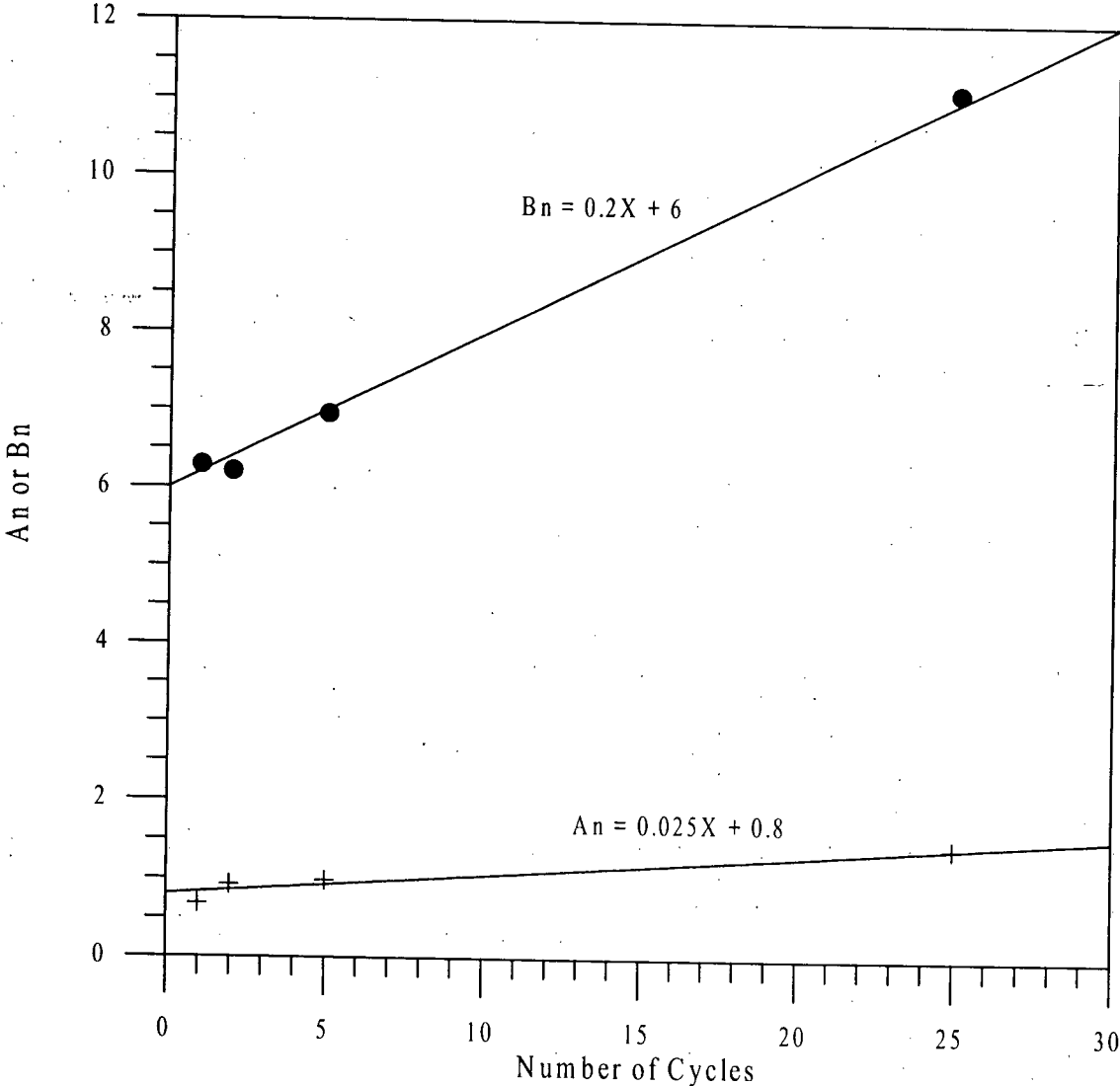


Figure 3.11: Variation of A_n and B_n with Number of Cycles.

in some of the gap that is developed behind it. Similar observations have been made by other researchers (Matlock et al, 1978, Ting et al, 1987).

3.3.4 Residual Soil Reaction

A close examination of the cyclic P-y curves shown on Figure 3.3 indicates that the gap portions of the curves are not generally coincident with the zero soil reaction axis. As discussed earlier, this is perhaps due to the soil-pile friction along the sides of the pile and seems to have a generally constant value at a given depth. Although the soil-pile friction is always present, its effect has been implicitly included in all formulations for other portions of the cyclic, and monotonic, P-y curves. Figure 3.12 shows the variation of the residual soil reaction with the effective vertical stress. A best-fit line yields the dimensionless equation:

$$\frac{P_{res}}{E_{max} D} = 0.10 - 0.50 \left(\frac{\sigma'_{vo}}{Pa} \right) \quad [9]$$

where E_{max} is the soil's maximum Young's modulus, P_{res} is the residual soil reaction, D is the pile diameter, σ'_{vo} is the effective vertical stress and Pa is the atmospheric pressure. Obviously, P_{res} is equal to zero where the soil-pile gap is zero.

Figure 3.8 shows the two-way cyclic P-y curves generated according to the above model. As can be seen, a good agreement is obtained with the measured P-y curves shown on Figure 3.3.

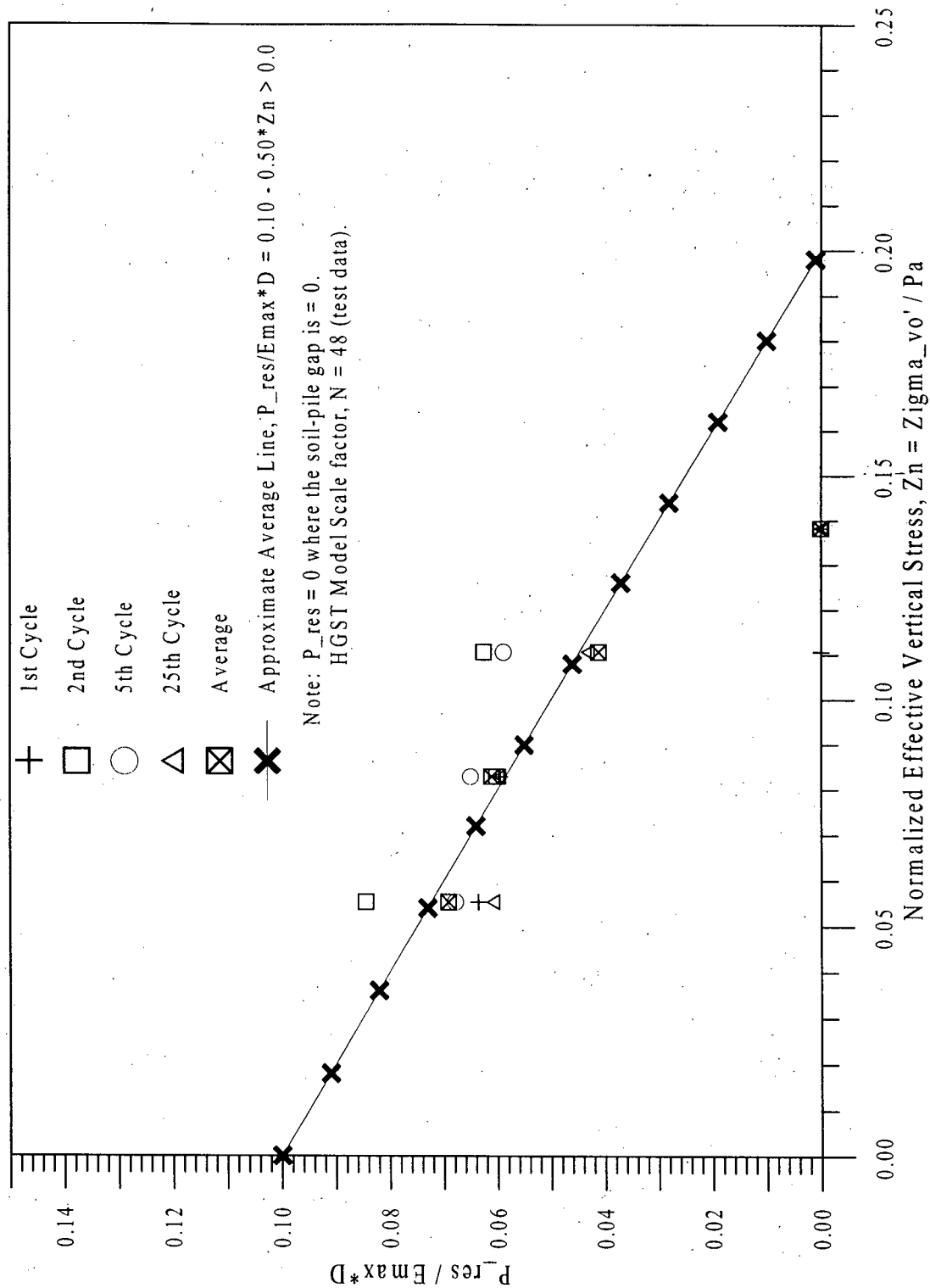


Figure 3.12: Variation of the Residual Soil Reaction with Effective Vertical Stress.

3.4 One-Way Cyclic Loading

Figure 3.13 shows the time histories of applied lateral load and pile head deflections for a free head model pile under the one-way cyclic loading condition. It can be seen that the pile head deflection increases gradually with each loading cycle under the constant amplitude one-way cyclic loading. Further, after the applied lateral load is unloaded to zero, the pile head deflection does not return to zero. Instead, some permanent plastic deformation develops after each loading cycle. The corresponding relation between the applied lateral load and the pile head deflection under one-way cyclic loading is shown on Figure 3.14. It is seen that the largest increment in pile deflection occurs at the first cycle, and then the increment becomes smaller as the soil-pile system tends to become progressively more elastic with the increase of number of cycles. This typical behaviour, however, is expected to depend upon the level of lateral loads. The relation observed in Figure 3.14 is very similar to that for the drained cyclic triaxial tests on a sand sample as shown on Figure 3.15, which indicates that the soil rather than the pile is responsible for the accumulation of plastic pile deflection under the cyclic loading. This conclusion is also supported by the above examination of the two-way cyclic P-y curves. As discussed above, as the pile pushes against the soil, the soil fails and moves around the pile to fill in some of the gap that is developed behind the pile. Therefore, it would be expected that the pile would have a permanently deformed shape when the applied lateral load returns to zero. Therefore, this behaviour can be easily captured with the cyclic P-y curves.

The experimental P-y curves at different depths for a fixed head pile at HGS Scale Factor,

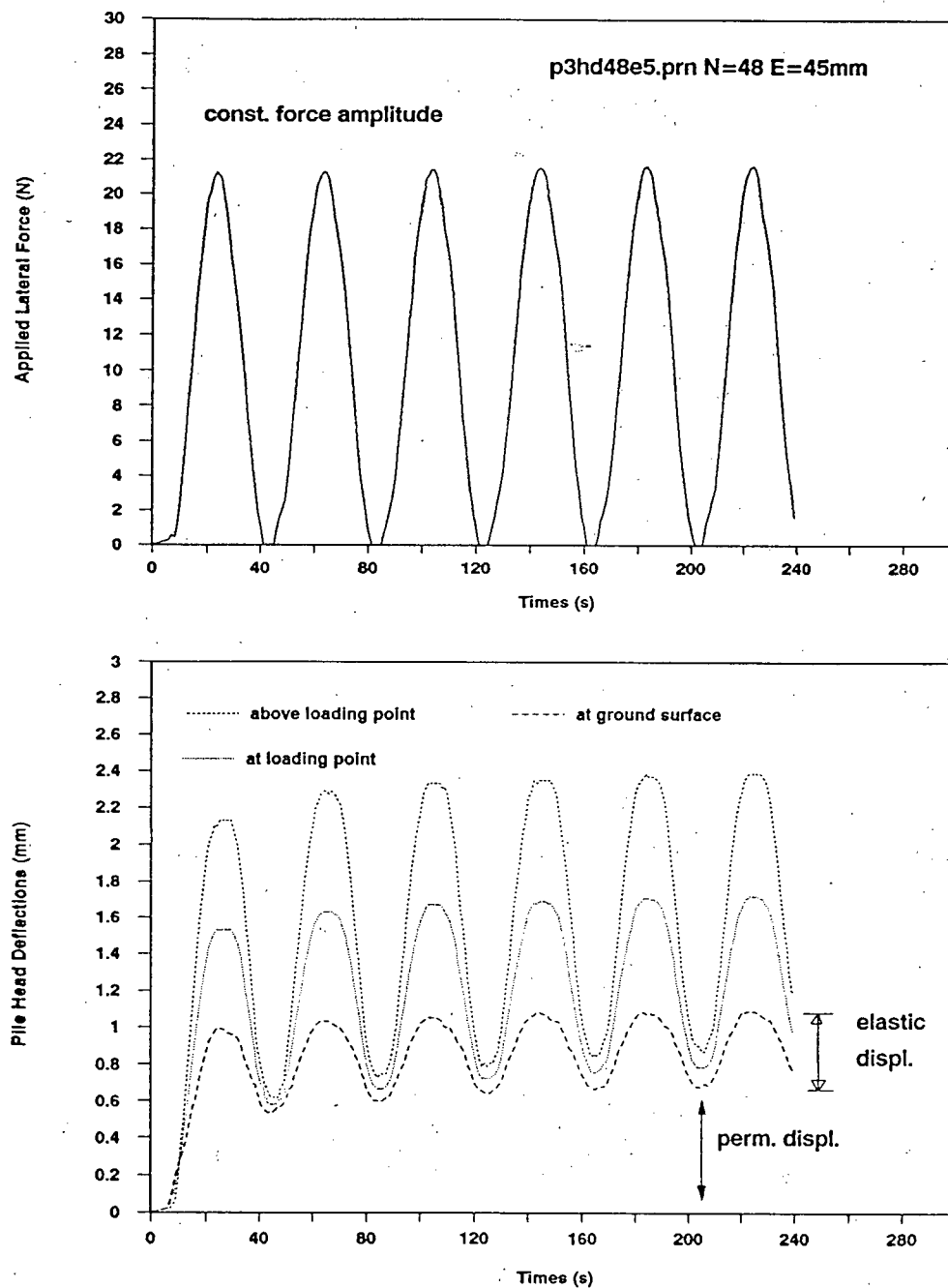


Figure 3.13: Variation of Pile Head Deflection with Time under Constant Amplitude One-Way Cyclic Loading. After Yan (1990).

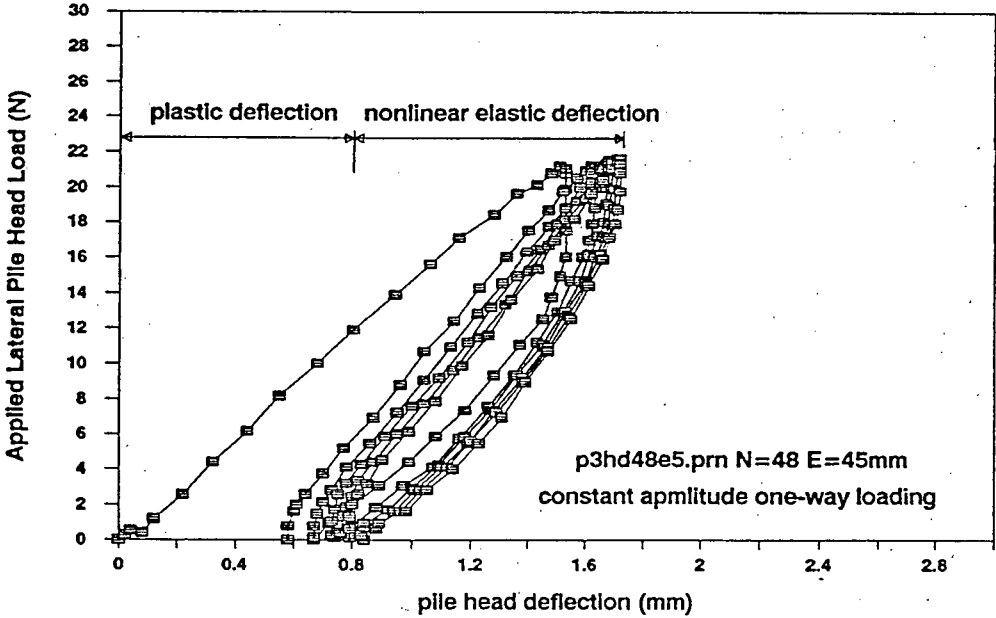


Figure 3.14: Pile Head Response at Loading Point under Constant Amplitude One-way Cyclic Lateral Load. After Yan (1990).

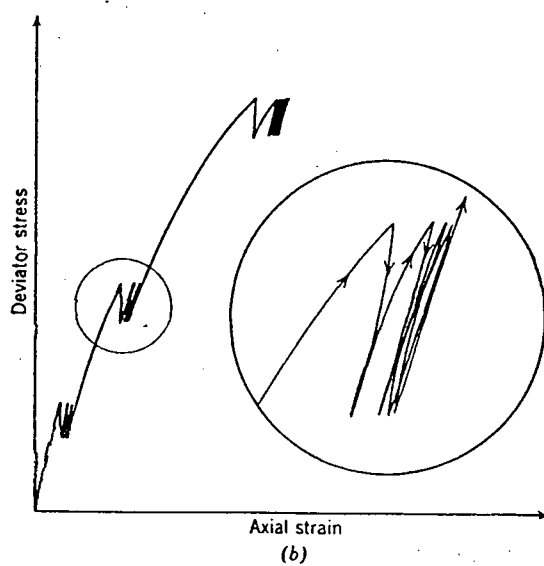


Figure 3.15: Example of Soil Element Response from Drained Cyclic Triaxial Test. After Lamb and Whitman, 1975.

$N=48$, Eccentricity, $E=45\text{mm}$, and a loading amplitude of 40 N , are shown on Figure 3.16. It is seen that the one-way cyclic P-y curves are generally very similar to the two-way cyclic P-y curves. However, a number of differences can be observed in the P-y behaviour. One is that the shapes of one-way cyclic P-y curves do not deteriorate with number of cycles, even at shallow depths. This indicates that without loading the pile in the opposite direction to the first-time loading, the soil's maximum Young's modulus as used in Equation (3.1) is not affected very much by the number of loading cycles. All P-y curves become more linear with number of cycles. In addition, the enclosed area of the hysteretic loop in the cyclic curves decreases with number of loading cycles. These indicate that the soil pile system under the one-way cyclic loading progressively becomes more elastic with number of cycles.

The additional feature of the one-way cyclic P-y curves is the unload-reload portion. Therefore, to capture the pile behaviour under the one-way cyclic loading, we need to develop an unload-reload rule for the cyclic P-y curve formulations presented above.

The modulus of the reload portion of the P-y curves shown on Figure 3.16 are initially much softer than the unload modulus and become stiffer with the number of cycles. It can be noticed from this figure that the reload curve intersects the unload curve at a load, P_{intrsect} , which is lower than the maximum applied load. This intersection point rises closer to the maximum applied load with each cycle. Figure 3.17 shows this variation with the number of cycles. Unfortunately, only two data points can be obtained from Figure 3.16 which makes it difficult to determine how this variation takes place. However, it is anticipated that this variation would have a logarithmic form as indicated

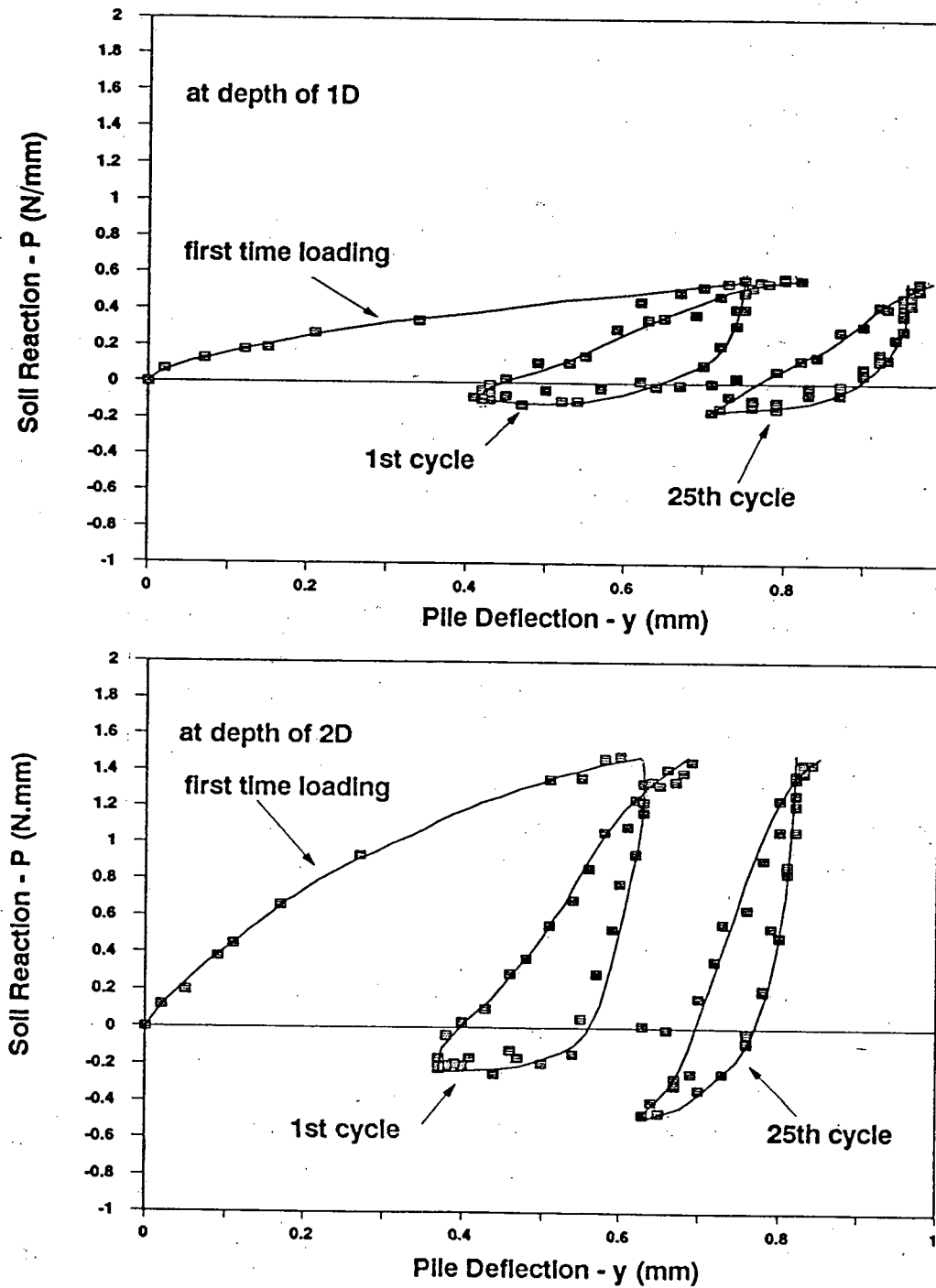


Figure 3.16: P-y Curves under One-way Pile Head Loading at Depths of 1 to 2 Pile Diameters, Fixed Head Pile, HGST Model Scale Factor $N=48$, Eccentricity = 45mm, Load Amplitude = 40 N. After Yan (1990).

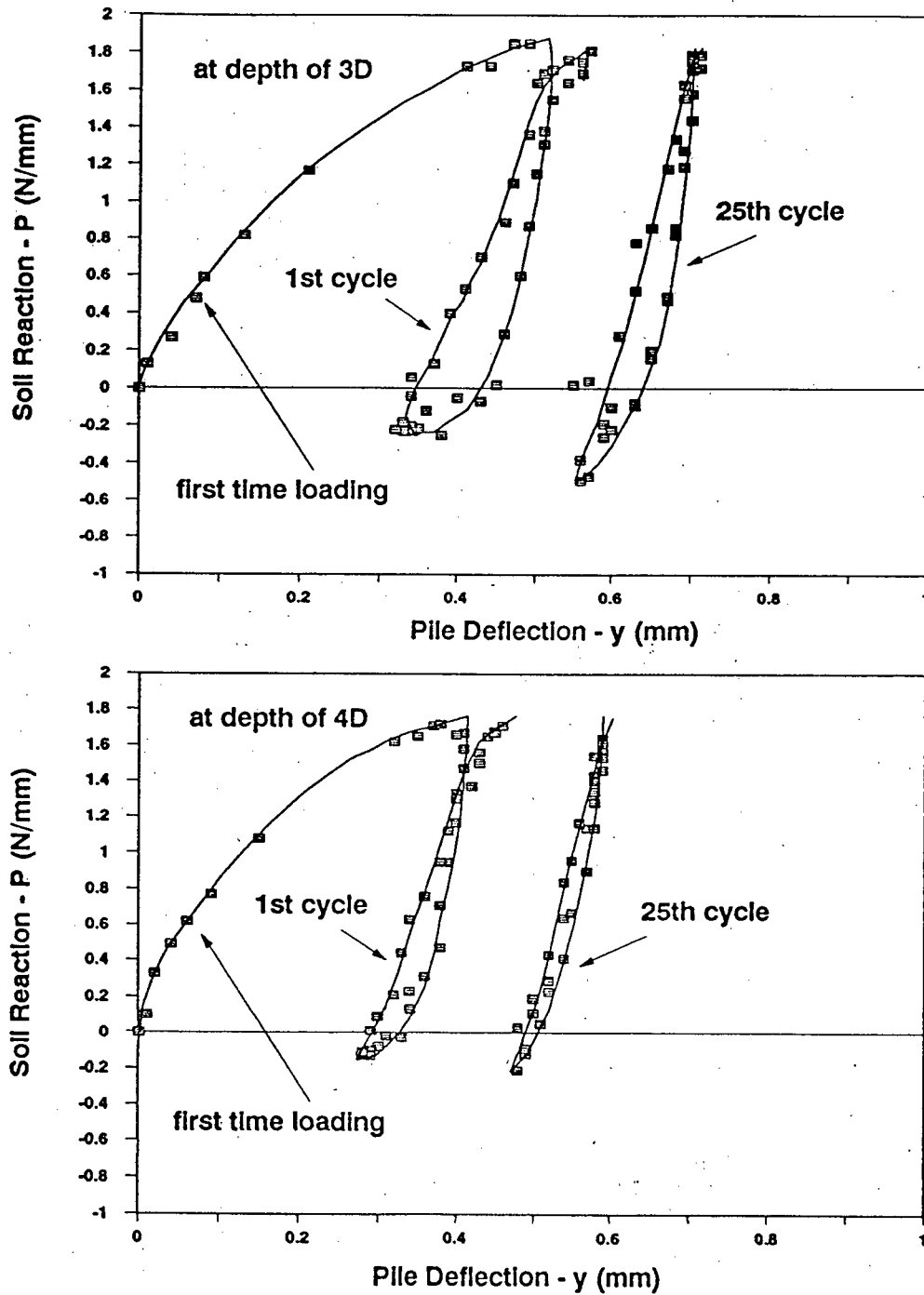


Figure 3.16: P-y Curves under One-way Pile Head Loading at Depths of 3 to 4 Pile Diameters, Fixed Head Pile, HGST Model Scale Factor $N=48$, Eccentricity = 45mm, Load Amplitude = 40 N. After Yan (1990).

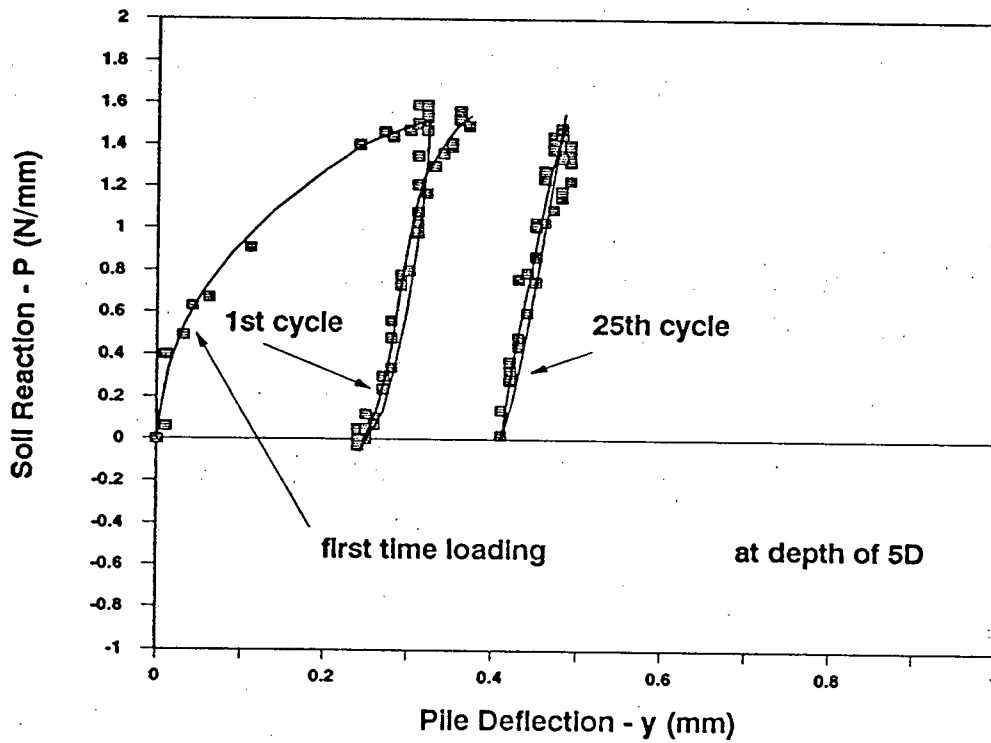


Figure 3.16: P-y Curves under One-way Pile Head Loading at a Depth of 5 Pile Diameters, Fixed Head Pile, HGST Model Scale Factor $N=48$, Eccentricity =45mm, Load Amplitude =40 N. After Yan (1990).

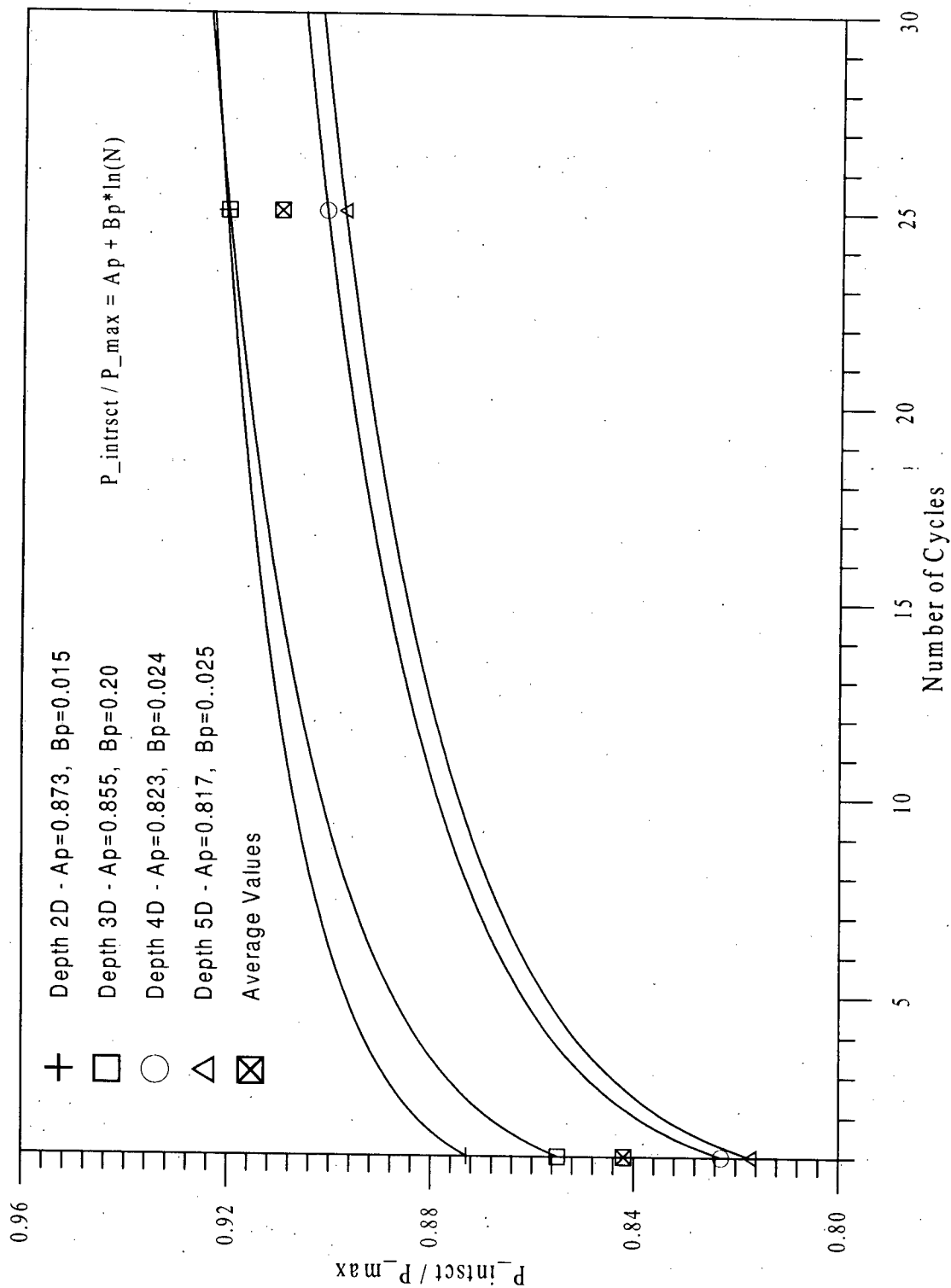


Figure 3.17: Variation with Number of Cycles of Normalized P (Normalized with P_{max}) At Intersection Point of the Reload Portion with the Unload Portion of the P-y Curve

on Figure 3.17 based on observed cyclic loading behaviour of sand in a triaxial test, or an in-situ pressuremeter test. The approximate curves shown on Figure 3.17 have the form:

$$\frac{P_{intrsect}}{P_{max}} = A_p + B_p \ln(N) \quad [10]$$

where N is the number of cycles, $P_{intrsect}$ is the load at the intersection point between the reload and the unload portions of the P-y curve, P_{max} is the maximum applied load for that cycle, and A_p and B_p are empirically fitted variables which depend on the effective vertical stress as shown on Figure 3.18. Straight line approximations of the variables A_p and B_p yield the equations:

$$A_p = 0.77 + 0.72 \left(\frac{\sigma'_{vo}}{Pa} \right) \quad [11]$$

and,

$$B_p = 0.033 - 0.124 \left(\frac{\sigma'_{vo}}{Pa} \right) \quad [12]$$

It should be cautioned that these empirical formulations are based on fewer data points than would be needed to provide a reasonable approximation. The shape of the above curves are based on the assumption that the relationship is logarithmic. Due to the limited number of data points, A_p and B_p may be significantly different from that presented here.

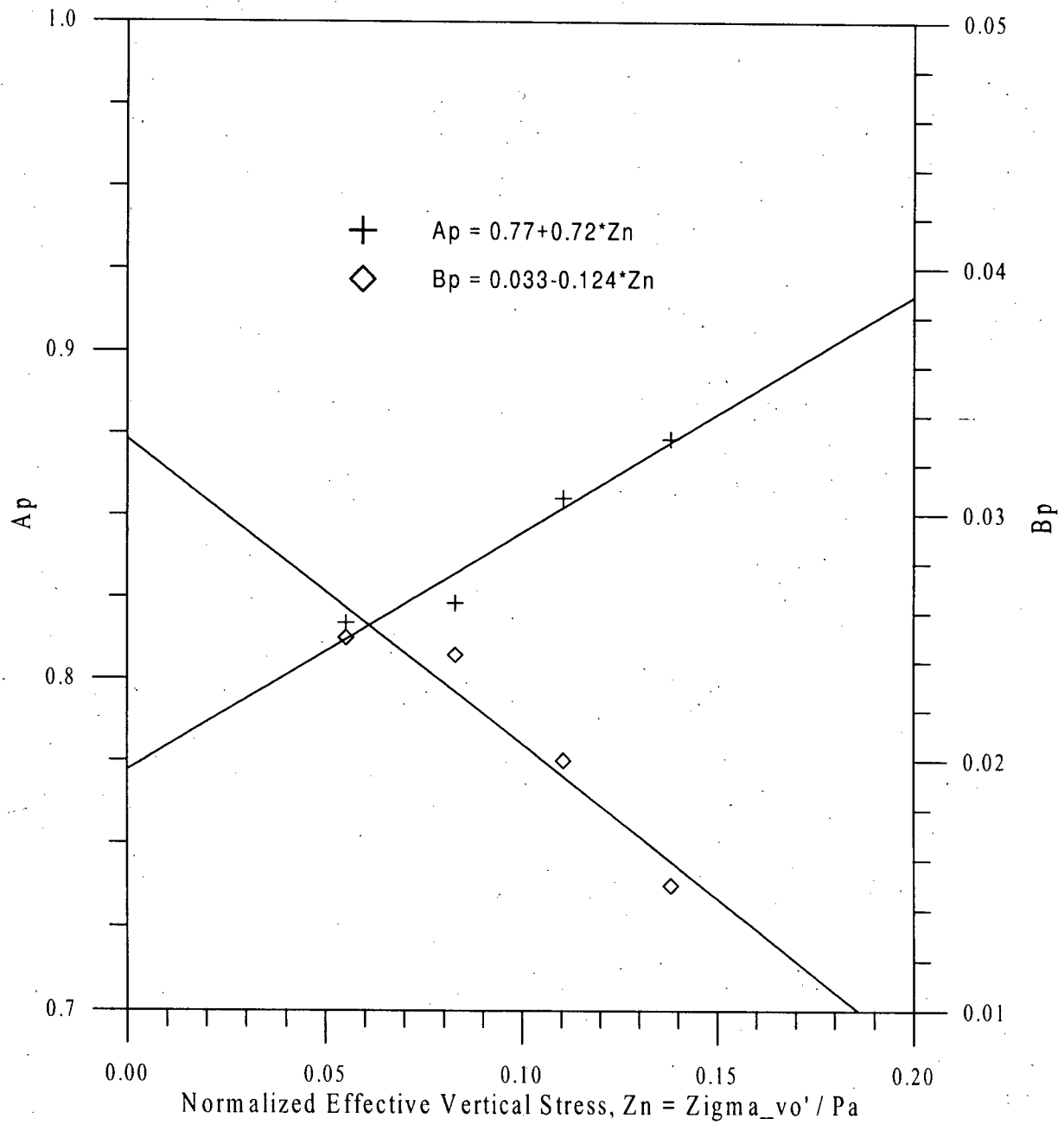


Figure 3.18: Variation of A_p and B_p with the Effective Vertical Stress.

3.5 Summary and Conclusions

Pile response under applied cyclic lateral loads is an important aspect in the design of deep foundations. Although different analytical procedures exist for laterally loaded piles under monotonic conditions, the fundamental aspects of cyclic lateral loading are still poorly understood and very few analytical models are available at this time. The soil parameters which affect the cyclic behaviour of laterally loaded piles have not yet been fully defined and calibrated in a fundamental manner.

In this chapter, the model study of vertical piles embedded in sand under cyclic lateral pile head loading presented by Yan (1990) was studied. The experimental P-y curves were analyzed and various factors which influenced the pile response were investigated. An attempt was made to back-calculate these influencing factors from the experimental P-y curves. The primary purpose of this investigation was to understand the soil-pile interaction under the cyclic lateral pile head loading so that a relatively simple analytical model can be developed to help extrapolate the results of the experimental study to other applications. Empirical relationships were derived based on basic soil properties and observed cyclic P-y behaviour. The empirical relationships are in reasonable agreement with the measured test data.

For the piles under the two-way cyclic loading, it was found that the cyclic P-y curves have four significant features that influence the pile response. These features are the loading segments, the unloading segments, the gap segments and the residual soil reaction. These features were found to depend primarily on the confining stress, the soil's maximum Young's modulus of elasticity, E_{max} , strain level (y), and the number of loading cycles. At depths greater than three pile diameters, the

P-y curves became stiffer with the number of loading cycles indicating densification of the soil surrounding the pile and thereby increasing the E_{\max} of the soil. At shallower depths, the P-y curves become softer with the number of cycles due to the failure of the soil near the ground surface. The size of the soil-pile gaps became smaller with the increasing confining stress and increase in size with the number of loading cycles. The unloading segments of the P-y curves appeared to be approximately equal to the E_{\max} of the soil, as would be theoretically expected. The residual soil reaction is probably due to side friction and varies proportionally with the confining stress.

It was found that the only additional feature of the one-way cyclic P-y curves over the two-way cyclic P-y curves is the unload-reload portion of the curves. Although the unload segment is still consistent with the E_{\max} of the soil, the reload segment was found to depend mostly on the maximum applied load at that cycle. The reload curve was found to intersect the unload curve at a point below the maximum applied load. This intersection point moved closer to the maximum applied load with each cycle. Due to the limited number of data points available, it was assumed that the location of the intersection point with respect to the maximum applied load varies with the number of cycles according to a logarithmic relationship.

In the following chapters a numerical model will be developed based on the empirical relationships derived above. This model will be incorporated into a computer program and will be verified with measured field and laboratory test results.

Chapter 4 Numerical Model

4.1 Introduction

In this chapter, theoretical principles and derivation of a numerical model for the response of single piles to lateral loads are described. The basic model is independent of both the soil and pile stress-strain characteristics and behaviour. This enables us to study different soil and pile stress-strain characteristics. The basic model was first developed by Foschi (1992) for analyzing lateral loading response of nails and bolts in wood. Later, he modified the model to analyze lateral response of simple piles in uniform soils. Khan (1995) has developed this model to include the dynamic response of the pile system. In this chapter, the original model is extended to include a number of soil layers, and variable pile cross-sections and material properties.

4.2 Model Principles

The model proposed here combines the power and versatility of the P-y curve method of representing the soil behaviour with an advanced beam analysis model for the pile. The beam is modelled using a finite element technique often used in structural engineering.

A typical problem is shown in Figure 4.1. The user generally divides the pile into a number of elements the length of which may be variable. As can be seen, the pile may have varying cross-section dimensions and applied loadings along the length of the pile. Since the finite element formulation used is fairly accurate, as will be discussed later, the number of elements can usually be limited to as few as two per soil layer. This helps to reduce computation time. However, if the pile cross-section dimensions change with depth, the element lengths should be small enough to obtain good results. The element lengths in this case should be chosen in order to avoid sharp contrast in the pile dimensions between two adjacent elements unless such contrast is real.

The axial deformations in the pile due to axial and lateral loads are calculated but care must be taken in their interpretation because soil resistance in the axial direction is not taken into account in this model. The effect of axial loads on lateral bending and buckling ($P-\Delta$ effects) is considered.

The Gaussian integration technique (Nakamura, 1992) is used for the finite element representation of the pile. This technique is very accurate in integrating analytical functions and gives exact answers when integrating polynomials of order $2N-1$ or less when using N Gauss quadratures over the integration interval.

A tangent modulus scheme is used to approximate this non-linear model and will be described in the next section. This solution scheme is capable of solving problems where load-reversals need to be taken into account. It is assumed that the unloading modulus is equal to the maximum Young's modulus, E_{max} , as defined by the user. Soil-pile gapping is modelled by assigning zero tensile strength at the soil-pile interface for all $P-y$ curves except that presented in the previous chapter. For this $P-y$ curve, the soil-pile gapping has been integrated into the $P-y$ curve model as a function of pile deflection, depth and number of loading cycles.

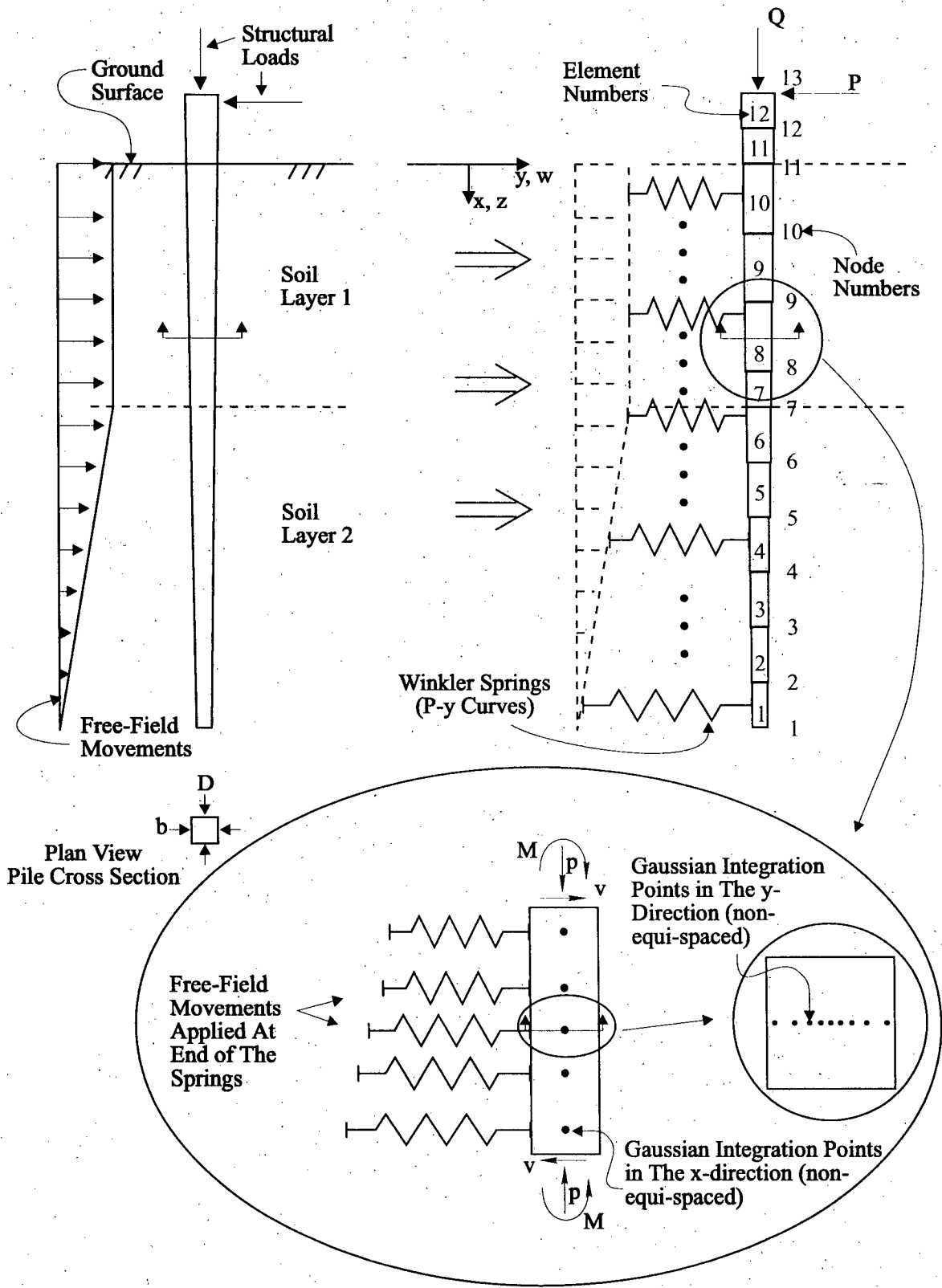


Figure 4.1: General Representation of Soil and Pile in Proposed Model.

4.3 Model Formulation

Consider one pile element as shown in Figure 4.2. The variables used are defined as shown on the figure. We can further define the following variables using generalized or normal coordinates, η , and ξ :

$$\begin{aligned} x &= \bar{x} + \frac{\Delta}{2} \xi ; & \bar{x} &= \frac{x_j + x_i}{2} ; & dx &= \frac{\Delta}{2} d\xi ; \\ y &= \frac{d}{2} \eta ; & dy &= \frac{d}{2} d\eta \end{aligned} \quad (4.1)$$

The degrees of freedom at each node are the lateral displacement, w , slope, w' , curvature, w'' , axial displacement, u , and its first derivative, u' (a ' indicates the first derivative with respect to x , and a '' indicates the second derivative with respect to x). Therefore each element has 10 degrees of freedom, 5 at each node. For simplicity, let us express these degrees of freedom in terms of the vector $\{a\}$:

$$\{a\} = \{w_i, w'_i, w''_i, u_i, u'_i, w_j, w'_j, w''_j, u_j, u'_j\} \quad (4.2)$$

Since moment is proportional to the second differential of displacements, let us approximate w with a fifth degree polynomial, and u with a third degree polynomial to maintain accuracy. That is,

$$w = b_1 x^5 + b_2 x^4 + b_3 x^3 + b_4 x^2 + b_5 x + b_6 \quad (4.3)$$

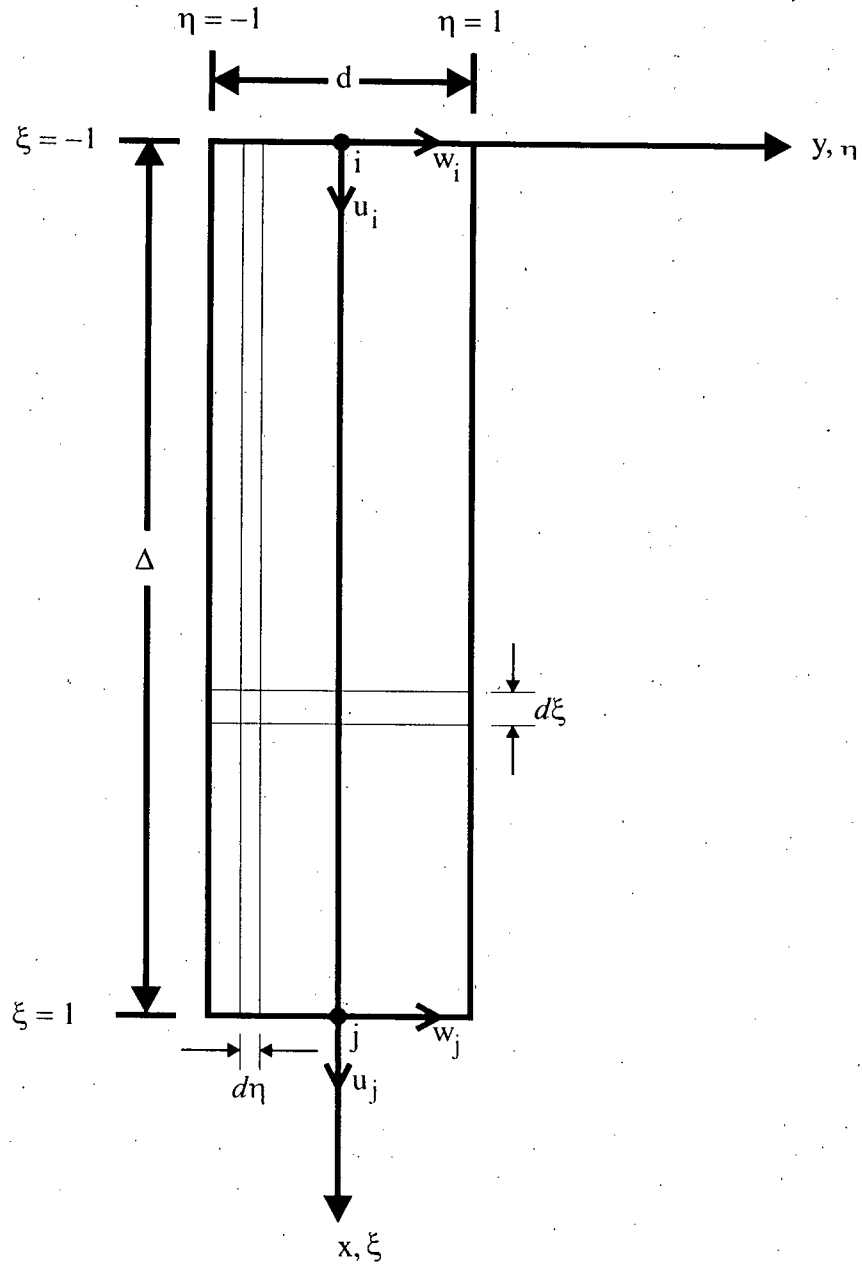


Figure 4.2: A Pile Element Showing Variables and Sign Conventions.

$$u = c_1 x^3 + c_2 x^2 + c_3 x + c_4 \quad (4.4)$$

and the derivatives are obtained by differentiating the above equations. Eliminating b_n and c_n using Equations (4.2) to (4.4), we can express w , w' , w'' , u , and u' at any point ξ within the element, as a function of ξ and $\{a\}$ through shape functions $M_0(\xi)$, $M_1(\xi)$, $M_2(\xi)$, $N_0(\xi)$ and $N_1(\xi)$ such that

$$w(\xi) = M_0^T(\xi)\{a\}; \quad w'(\xi) = M_1^T(\xi)\{a\}; \quad w''(\xi) = M_2^T(\xi)\{a\} \quad (4.5)$$

$$u(\xi) = N_0^T(\xi)\{a\}; \quad u'(\xi) = N_1^T(\xi)\{a\} \quad (4.6)$$

The shape functions are derived and presented in Appendix I.

Based on the principle of virtual work, the total internal work done must be equal to the total external work, i.e.

$$\Psi_{\text{internal}} = \Psi_{\text{external}} \quad (4.7)$$

The total internal work done by an applied virtual strain, $\delta \epsilon$, is given by:

$$\Psi_{\text{internal}} = \int_{\text{vol}} \sigma(\epsilon) \delta \epsilon dV \quad (4.8)$$

where σ is the stress and ϵ is the strain. From beam bending theory (for an Euler beam where plane sections remain plane),

$$\varepsilon = u' - yw'' + \frac{1}{2}(w')^2 \quad (4.9)$$

Substituting u' , w' , w'' from equations (4.5) and (4.6) into the strain equation (4.9) and then substituting again into the internal work equation (4.8) and simplifying, we obtain

$$\Psi_{\text{internal}} = \{\delta a\}^T \int_{-1}^1 \int_{-1}^1 \sigma(\varepsilon) [N_1(\varepsilon) - (\eta \frac{d}{2})M_2(\varepsilon) + M_1(\varepsilon)M_1^T(\varepsilon)\{a\}] b(\eta) d\xi d\eta \quad (4.10)$$

where $b(\eta)$ is the width of the pile perpendicular to the direction of lateral loading. The total external work done is due to all applied external loads. There are four different types of external loads that can be applied to the system (see Figure 4.3):

1. lateral load, Q , at node j (the load applied at node i is accounted for by node j of the adjacent element),
2. axial load P at node j ,
3. lateral soil pressures along the element, $q(w)$,
4. axial soil pressures along the element, $p(u)$, $p(w)$, and $P(u)$. These loads usually have little effect on the lateral behaviour of the pile and will not be considered here.

The external work done by the lateral load, Q , at node j is given by:

$$\Psi_{\text{extl}} = Q \cdot \delta w(x = \Delta) \quad (4.11)$$

If we express $w(x = \Delta)$ as

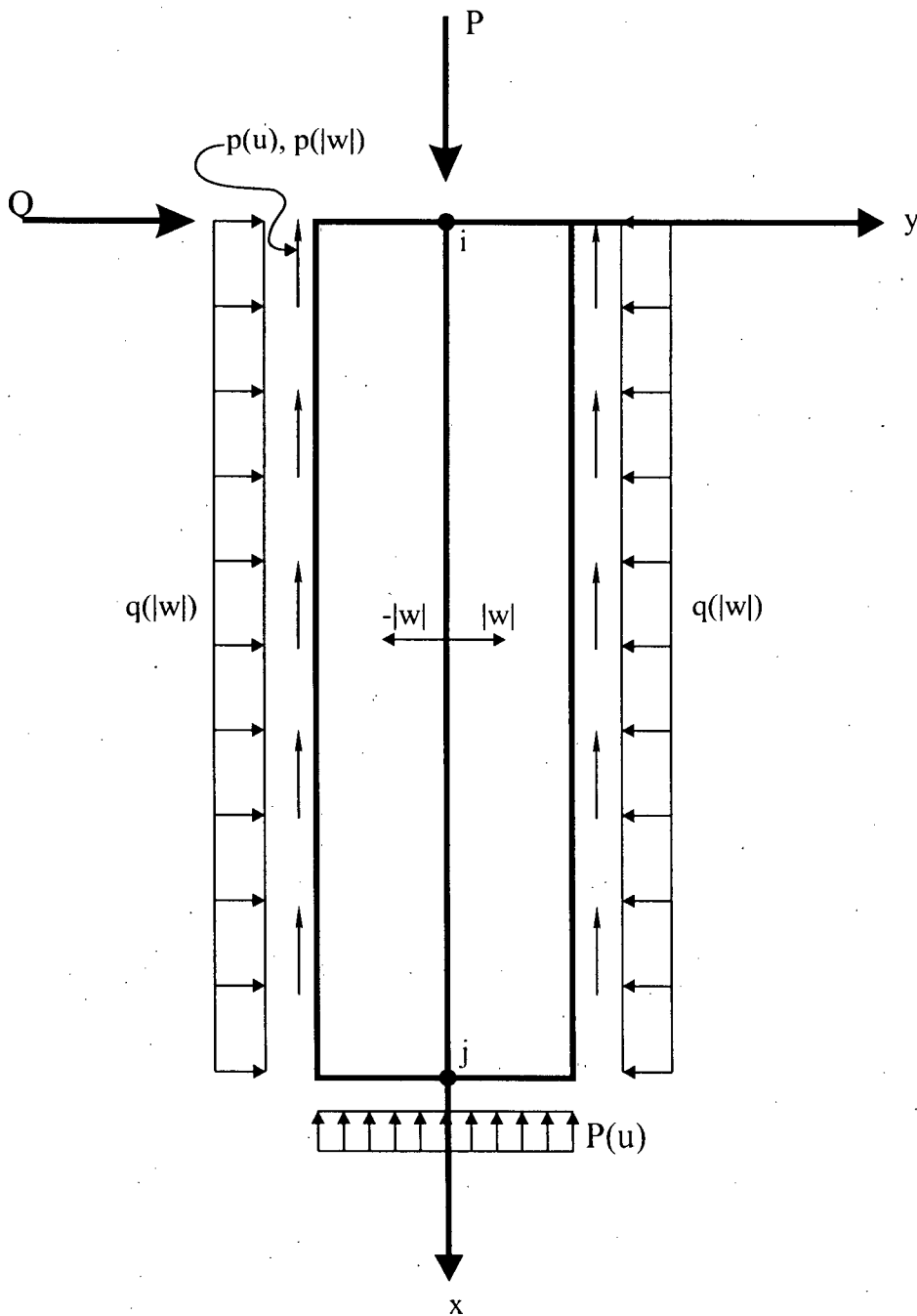


Figure 4.3: The Beam Element with Applied Loads.

$$w(x=\Delta) = \{e_q\}^T \{a\}; \quad \delta w(x=\Delta) = \{e_q\}^T \{\delta a\} \quad (4.12)$$

where

$$\{e_q\} = \{0, 0, 0, 0, 0, 1, 0, 0, 0, 0\} \quad (4.13)$$

and therefore we can write

$$\Psi_{ext1} = \{\delta a\}^T \cdot Q \cdot \{e_q\} \quad (4.14)$$

The external work done by axial load, P , at node j is given by:

$$\Psi_{ext2} = P \cdot \delta u(x=\Delta) \quad (4.15)$$

If we express $u(x=\Delta)$ as

$$u(x=\Delta) = \{e_p\}^T \{a\}; \quad \delta u(x=\Delta) = \{e_p\}^T \{\delta a\} \quad (4.16)$$

where

$$\{e_p\} = \{0, 0, 0, 0, 0, 0, 0, 0, 1, 0\} \quad (4.17)$$

and therefore we can write

$$\Psi_{ext2} = \{\delta a\}^T \cdot P \cdot \{e_p\} \quad (4.18)$$

The external work done by lateral soil pressure, $q(|w|)$, along the element is given by

$$\Psi_{\text{ext3}} = \int_0^{\Delta} -q(|w|) \delta(|w|) dx = \int_{-1}^1 -q(|w|) \delta(|w|) d\xi \quad (4.19)$$

After some algebra and substituting for w from equation (4.5) we obtain

$$\Psi_{\text{ext3}} = \frac{-\Delta}{2} \{\delta a\}^T \int_{-1}^1 q(|w|) \frac{w}{|w|} M_0(\xi) d\xi \quad (4.20)$$

The total external work would be the sum of each of the above external work relations.

Therefore,

$$\Psi_{\text{external}} = \{\delta a\}^T \cdot [Q\{e_\rho\} + P\{e_p\} - \frac{\Delta}{2} \int_{-1}^1 q(|w|) \frac{w}{|w|} M_0(\xi) d\xi] \quad (4.21)$$

Equating the internal and external work equations, we get

$$\begin{aligned} \frac{\Delta \cdot d}{4} \int_{-1}^1 \int_{-1}^1 \sigma(\epsilon) [N_1(\xi) - (\eta \frac{d}{2}) M_2(\xi) + M_1(\xi) M_1^T(\xi) \{a\}] b(\eta) d\xi d\eta \\ = Q\{e_\rho\} + P\{e_p\} - \frac{\Delta}{2} \int_{-1}^1 q(|w|) \frac{w}{|w|} M_0(\xi) d\xi \end{aligned} \quad (4.22)$$

and if we let

$$\begin{aligned} \{\Psi\} = & \frac{\Delta \cdot d}{4} \int_{-1}^1 \int_{-1}^1 \sigma(\epsilon) \left[N_1(\xi) - \left(\eta \frac{d}{2} \right) M_2(\xi) + M_1(\xi) M_1^T(\xi) \{a\} \right] b(\eta) d\xi d\eta \\ & + \frac{\Delta}{2} \int_{-1}^1 q(|w|) \frac{w}{|w|} M_0(\xi) d\xi \end{aligned} \quad (4.23)$$

and

$$\{R\} = Q \{e_o\} + P \{e_p\} \quad (4.24)$$

we can define

$$\{\theta\} = \{\theta(\{a\})\} = \{\Psi\} - \{R\} = \{0\} \quad (4.25)$$

We can now calculate $\{a\}$ by iteratively solving equation (4.25) using the Newton-Raphson method until $\{\theta\}$ is equal to zero within a specified tolerance. As mentioned earlier, the Gaussian integration technique is used to solve for the integrals in equation (4.23). This means that ξ and η represent the Gaussian integration points in the x- and y-directions within the beam element, respectively (see Figure 4.2) not the nodes.

The stress (σ) and soil reaction (q) are obtained directly from the pile stress-strain and soil-pile interaction P-y curves where q is used instead of P in the present formulation. Q is the applied lateral load at node j, and, P , is the applied axial load at node j. The free-field displacements are accounted for when calculating $q(|w|)$ by simply subtracting the free-field displacement at a Gaussian integration point in the x-direction from w before calculating $q(|w|)$ (Byrne et al, 1984).

We can approximate $\{\theta\{a\}\}$ by

$$\{\theta\{a\}\} = \{\theta\{a^0\}\} + \frac{d\{\theta\}}{d\{a\}}[\{a\} - \{a^0\}] = \{0\} \quad (4.26)$$

where $\{a^0\}$ is the initial guess or the solution from the previous iteration for $\{a\}$. Therefore,

$$\{a\} = \{a^0\} - \left(\frac{d\{\theta\}}{d\{a\}}\right)^{-1} \{\theta\{a^0\}\} \quad (4.27)$$

where

$$\frac{d\{\theta\}}{d\{a\}} = [\nabla\theta] \quad (4.28)$$

and,

$$\begin{aligned} [\nabla\theta]_y = \frac{\partial \Psi_i}{\partial a_j} = \frac{\Delta \cdot d}{4} \int_{-1}^1 \int_{-1}^1 \left\{ \left(\frac{\partial \sigma(\epsilon)}{\partial \epsilon} \right) [N_{1j}(\xi) - (\eta \frac{d}{2}) M_{2j}(\xi) + [M_1(\xi) M_1^T(\xi)]_j] \{a\} \right. \\ \left. [N_{1i}(\xi) - (\eta \frac{d}{2}) M_{2i}(\xi) + [M_1(\xi) M_1^T(\xi)]_i] \{a\} + \sigma(\epsilon) [M_1(\xi) M_1^T(\xi)]_y \right\} b(\eta) d\xi d\eta \\ + \frac{\Delta}{2} \int_{-1}^1 \frac{dq(|w|)}{d(|w|)} M_{0i}(\xi) M_{0j}(\xi) d\xi \end{aligned} \quad (4.29)$$

The above arrays and matrices for each element are assembled into the global arrays and matrices by adding the terms for the common nodes of adjacent elements in the left-hand side of the

equation. The array $\{a\}$, representing the degrees of freedom of the two nodes of each element, is assembled into the global array, $\{a_g\}$, where

$$\{a_g\} = \{w_1, w_1', w_1'', u_1, u_1', w_2, w_2', \dots, w_{N+1}, w_{N+1}', w_{N+1}'', u_{N+1}, u_{N+1}'\} \quad (4.30)$$

and N is the total number of elements in the problem. Note that the size of the array $\{a_g\}$ is $5(N+1)$ and the size of the global matrix, $[\nabla\theta_g]$, is $5(N+1)$ by $5(N+1)$. For example, the terms in the 6th through 10th columns and 6th through 10th rows in $[\nabla\theta_g]$ are the result of the term by term summation of the 6th through 10th columns and 6th through 10th rows of $[\nabla\theta]$ of the first element and the 1st through 5th columns and 1st through 5th rows of $[\nabla\theta]$ of the second element.

From Equations (4.27) and (4.28) we can write

$$[\nabla\theta_g] \cdot \{a_g - a_g^0\} = -\{\theta_g^0\} \quad (4.31)$$

and solve for $\{a_g - a_g^0\}$ and add to $\{a_g^0\}$ after each iteration until the ratio between each term of the former and the latter arrays is less than a specified tolerance. For the first iteration of each time step, $\{a_g^0\}$ is equal to the final calculated values from the previous time step.

The values of q and σ are obtained directly from the P-y and σ - ϵ curves, respectively, and the tangent modulus is used in calculating the derivatives.

It should be mentioned here that when analyzing problems which include load-reversals, the time step chosen should be small enough to avoid large changes in the deflections which can introduce significant errors in the calculated derivatives in Equation (4.29).

4.4 Summary

A model was presented in this chapter for analyzing the response of vertical piles to lateral and free-field loading conditions. No presumptions have been made regarding the stress-strain behaviour of the pile so any stress-strain model can be incorporated into the above formulation. Although the model assumes that soil-pile interaction is in form of a P-y relationship, there is no limitation on shape, form, or coupling effects on the P-y relationships. This provides an extremely versatile tool for analyzing lateral loading of single piles, even though it is rather complicated for simple hand calculations.

It is necessary to check and verify the model with closed-form solutions and test data to check the validity of the basic assumptions. A computer program, CYCPILE has been developed that uses the above model with the following assumptions:

- ◆ the pile is linear-elastic-perfectly-plastic,
- ◆ the soil-pile interaction P-y curves are uncoupled,
- ◆ the unloading part of the P-y curves is linear with a modulus equal to the E_{max} of the soil,
- ◆ soil-pile gapping is modelled by assuming that soil is incapable of carrying tensile loads, or as described in Chapter 3.

In the following chapter the model will be checked and verified using the computer program CYCPILE. Next a complete documentation of this computer program (written using Microsoft FORTRAN Power Station Compiler version 1.0), along with some examples, can be found in Appendix II.

Chapter 5 Model Verification and Validation

5.1 Introduction

In this chapter, the model presented in the previous chapter is first verified by checking with other known solutions. Then, the model is validated by applying it to known case histories and real test data. Various test data including those presented in Chapter 2 are used. The computer program CYCPILE which has been developed based on this model is employed. Comparison is also made with the well known computer program LATPILE where the capabilities of the two programs overlap. The model verification will be carried out in the following way:

1. comparison with closed-form solutions for a rigid beam on an elastic foundation (Scott, 1981),
2. comparison with LATPILE for monotonic loading, and,
3. comparison with LATPILE for monotonic free-field loading.

The model validation will be carried out using:

1. comparison with Yan's (1990) test results from HGS model tests on monotonic lateral loading behaviour; adjustments made if necessary,
2. comparison with Yan's (1990) test results from HGS model tests on cyclic lateral loading behaviour,
3. comparison with BC Hydro's (Lee et al, 1992) laboratory tests on timber piles, and,

4. prediction of results from BC Hydro's (Lee et al, 1992) field test on single timber piles; comparison with actual results to draw conclusions about the accuracy of the model.

5.2 Closed-Form Solutions

As mentioned in an earlier chapter, closed-form solutions are available for rigid and flexible beams on an elastic foundation. For the cases of constant and linearly varying foundation moduli, the vertical deflection of these closed form solutions is analogous to the lateral deflection of the pile. The solution for the deflection, w , of a rigid beam on a constant-modulus foundation is (Scott, 1981):

$$w(x) = \frac{2P}{kl} \left[2 - \frac{3a}{l} - 3 \left(1 - \frac{2a}{l} \right) \frac{x}{l} \right] \quad (5.1)$$

where k is the modulus of elasticity of the subgrade. Figure 5.1a compares equation (5.1) with CYCPILE results obtained using for a 6.1m long beam, a foundation modulus of 84 kPa, load P equal to 134 kN, and a/l of 0.3. The comparison is excellent. This is not surprising as CYCPILE effectively approximates the deflected shape of the beam with a ninth-degree polynomial over each element. Since the closed-form deflected shape of the beam is a linear function here, the exact matching would be expected.

The solution for a rigid beam on a linear-modulus foundation is (Scott, 1981; Note: the formulation presented by Scott is incorrect and the correct formulation is presented here):

$$w = A + Bx \quad (5.2)$$

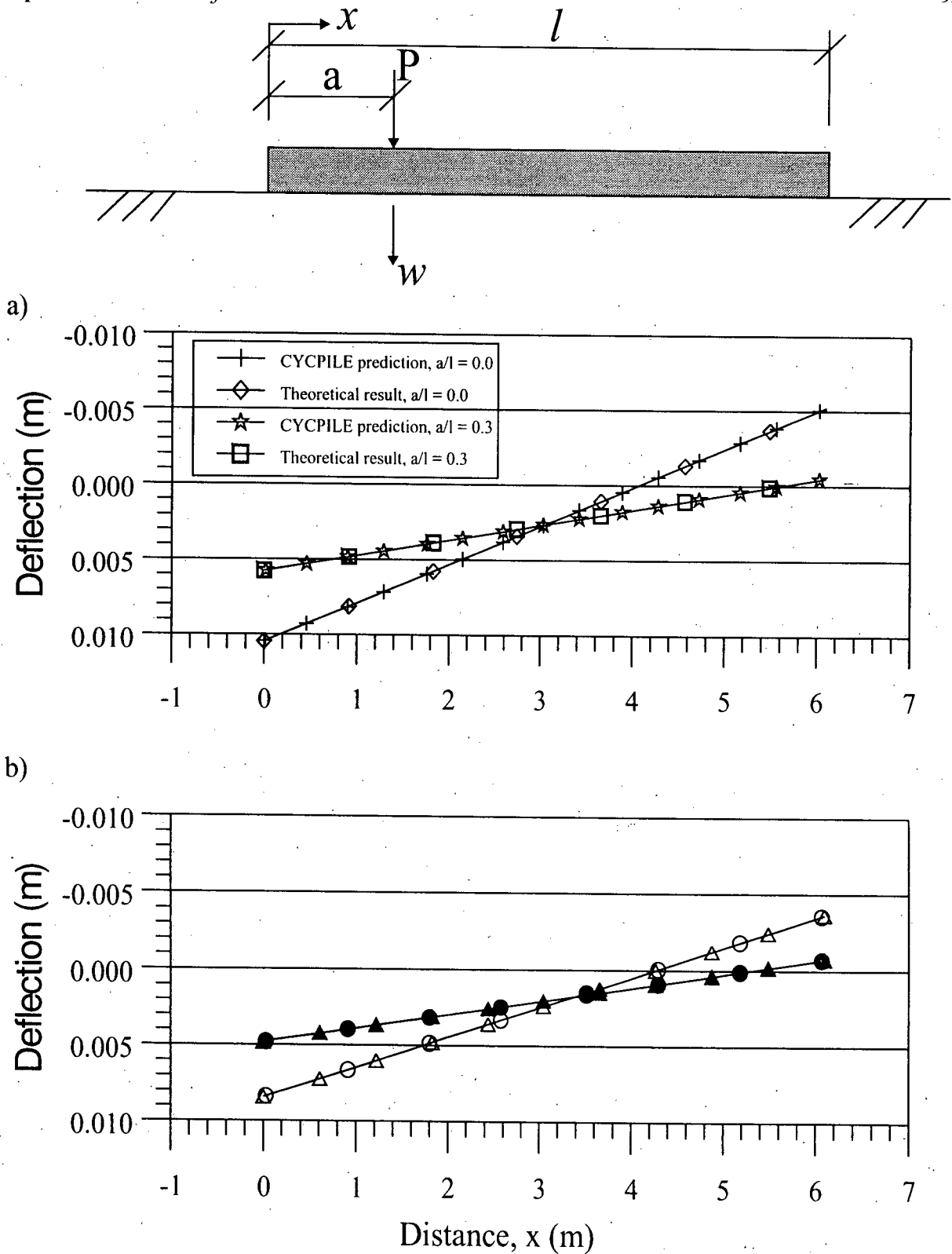


Figure 5.1: Comparison of CYCPILE with Closed-Form Solutions, a) Rigid Beam on a Constant Foundation, b) Rigid Beam on a Linear Foundation.

where

$$A = \frac{P \left[a \left(\frac{k_1}{2} + \frac{k_2 l}{3} \right) - \left(\frac{k_1 l}{3} + \frac{k_2 l^2}{4} \right) \right]}{\left[\left(\frac{k_1}{2} + \frac{k_2 l}{3} \right) \left(\frac{k_1 l^2}{2} + \frac{k_2 l^3}{3} \right) - \left(k_1 l + \frac{k_2 l^2}{2} \right) \left(\frac{k_1 l}{3} + \frac{k_2 l^2}{4} \right) \right]}, \quad (5.3)$$

and

$$B = \frac{P - A \left(k_1 l + \frac{k_2 l^2}{2} \right)}{\frac{k_1 l^2}{2} + \frac{k_2 l^3}{3}} \quad (5.4)$$

where k_1 and k_2 are defined as

$$k = k_1 + k_2 x \quad (5.5)$$

Similar to the constant-modulus foundation problem, CYCPILE gives an exact answer to the problem of linear-modulus foundation as the theoretical deflected shape of the rigid beam is still a linear function. Using results obtained from CYCPILE Figure 5.1b shows that an exact agreement is in fact obtained for the same loading conditions as the previous example.

The basic assumptions and formulation of the model have been checked with closed form solutions for an elastic foundation. Unfortunately, no such solutions exist for non-linear soil behaviour. Therefore a different approximation technique which has been proven to give accurate results is used to verify the results of CYCPILE.

5.3 Finite Difference Solutions

For non-linear soil behaviour, CYCPILE will be checked against another model in the areas where this model is known to be accurate. This model is a finite difference formulation which uses an equivalent elastic approach and has been incorporated into the computer program LATPILE (Reese, 1980; Byrne and Janzen, 1984), as discussed earlier. LATPILE is capable of analyzing vertical piles with lateral monotonic loads at the top and with free-field movements along the length of the pile.

Some of LATPILE's limitations are:

- ◆ only one load can be analyzed at one time,
- ◆ cyclic loading is not included,
- ◆ non-linear pile behaviour (yielding) is not accounted for,
- ◆ lateral loads can only be applied at the top.

Another computer program, SPASM, also based on a finite difference formulation is available, and is capable of analyzing cyclic loads including soil-pile gapping and dynamic effects. However, SPASM is also limited to linear-elastic piles (no yielding) which is not any more suitable for comparing with CYCPILE than LATPILE. Also, because SPASM accounts for dynamic effects, which is not the solution objective of CYCPILE, it is not selected for comparison. The following comparisons are made using LATPILE.

A generic soil-pile condition consisting of a 5 meter long pile embedded in a uniform dense sand with a lateral load of 14 kN and an axial load of 89 kN (for P- Δ effects) at the top is used. The same set of P-y curves were used at the same locations (depths of 0.0, 0.25, 0.5, 0.75, 1.25, 3.0, 4.0

and 5.0m) assuming a relative density of 75% for the sand. The pile used was a pipe pile with an outer diameter of 0.273 m, inner diameter of 0.2637 m and a modulus of elasticity of 300 GPa which give an EI of 10.6 MN-m². Figure 5.2 compares the moments and deflections calculated by the two programs. As can be seen, the comparison is very good, although there are small differences. It is likely that more elements in the LATPILE analysis would be required to achieve the same level of accuracy as CYCPILE. In this example, 100 elements were used in LATPILE and 20 elements were used in CYCPILE. Another comparison under free-field loading conditions is shown on Figure 5.3. A similarly good comparison is obtained in this case.

The observed differences would be expected because the two programs have different basic assumptions for the pile behaviour. However, the differences are very small and we can conclude that CYCPILE is capable of duplicating the calculations of LATPILE.

We now need to see how well CYCPILE predicts model pile behaviour where the input parameters for the non-linear P-y curves have been derived from the same model test results. This will ensure that little error is introduced by assuming that the soil reaction can be represented by uncoupled, non-linear Winkler springs and also ensure that the P-y curve implementation in the program is free of error.

5.4 Model Tests

5.4.1 Monotonic Loading

Yan's (1990) model tests using the Hydraulic Gradient Similitude (HGS) testing method was presented and discussed in an earlier chapter. The proposed P-y curves which are derived based on

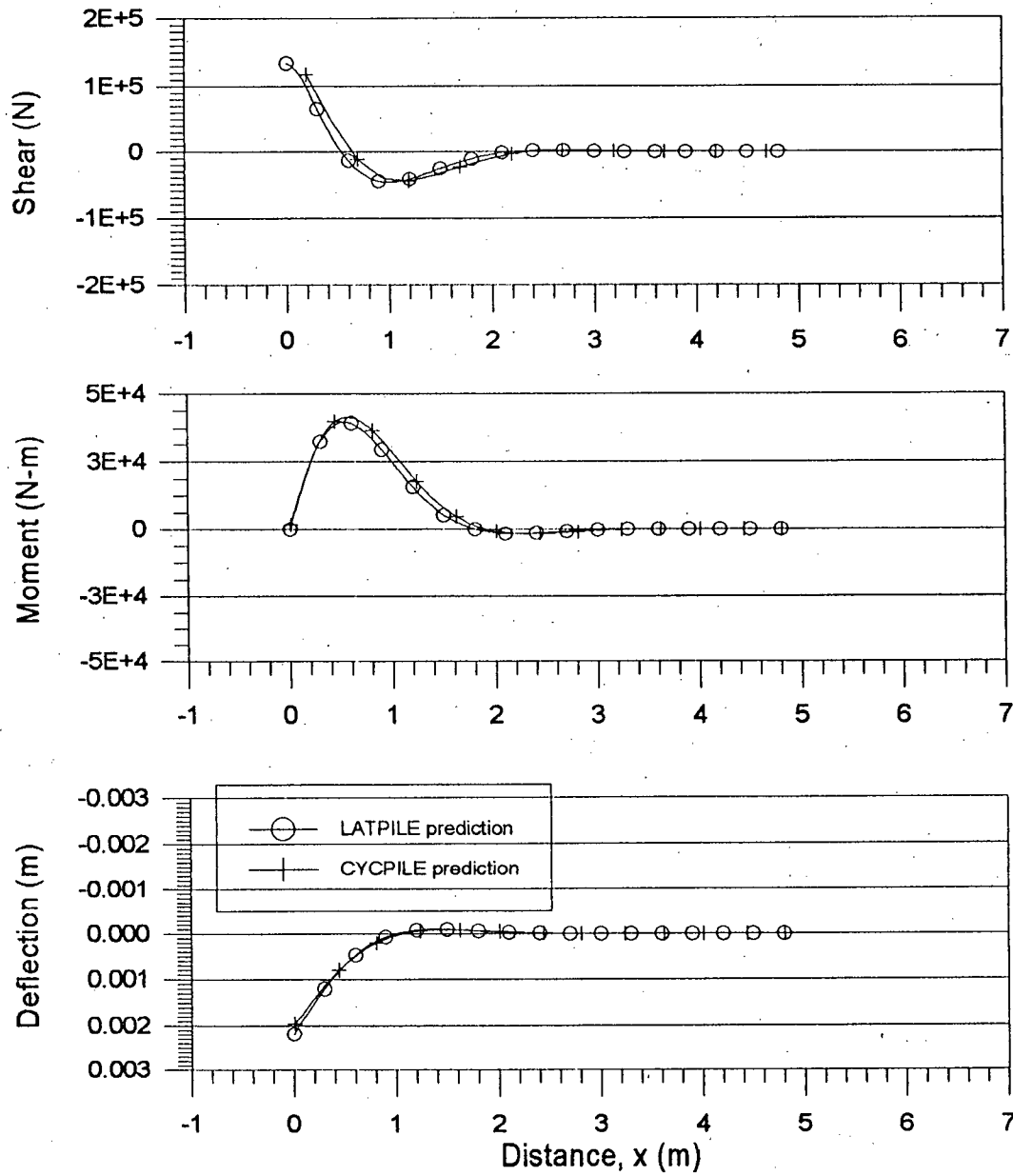


Figure 5.2: Comparison of Results of CYCPILE with LATPILE for Arbitrary Soil and Pile Conditions.

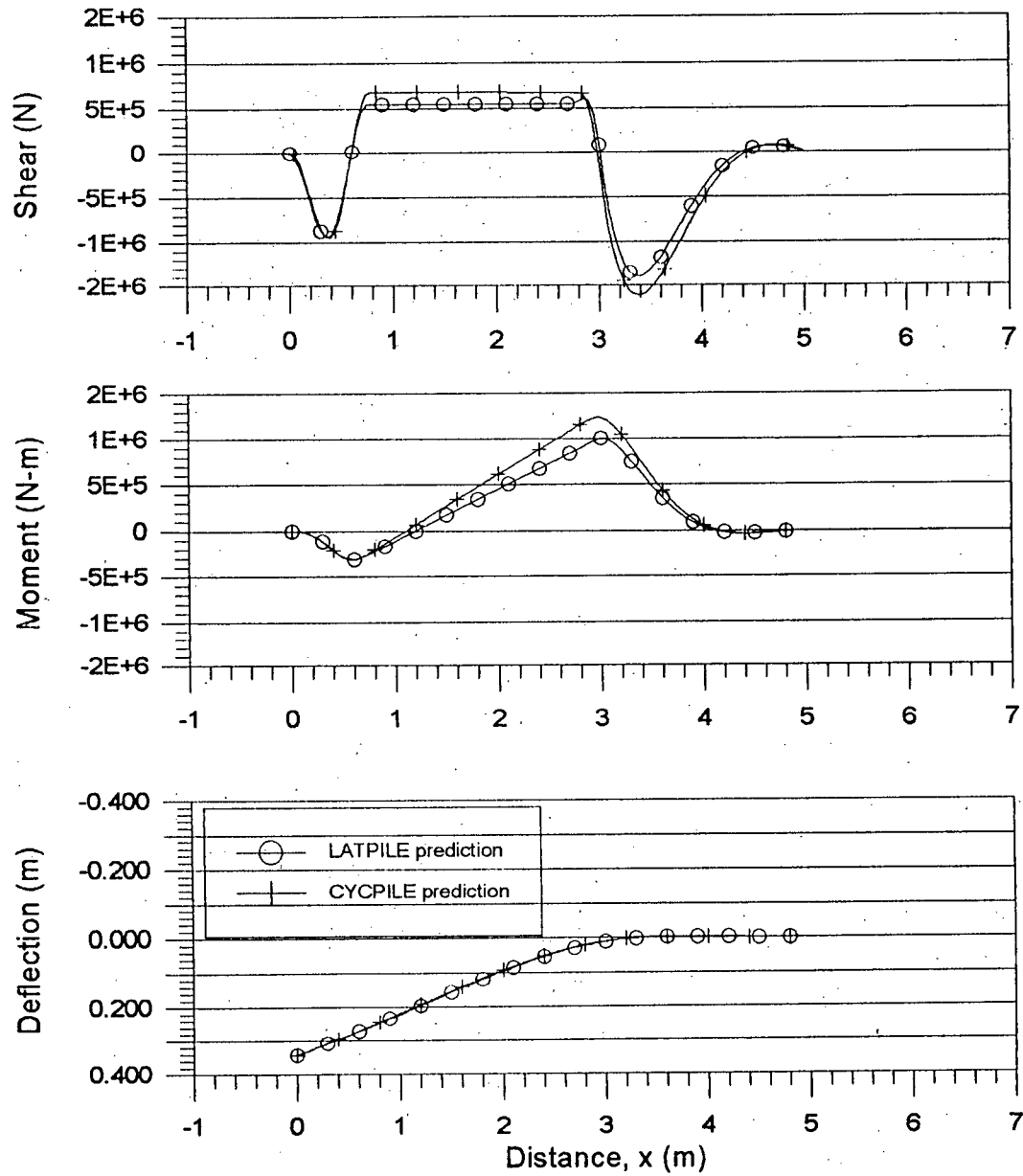


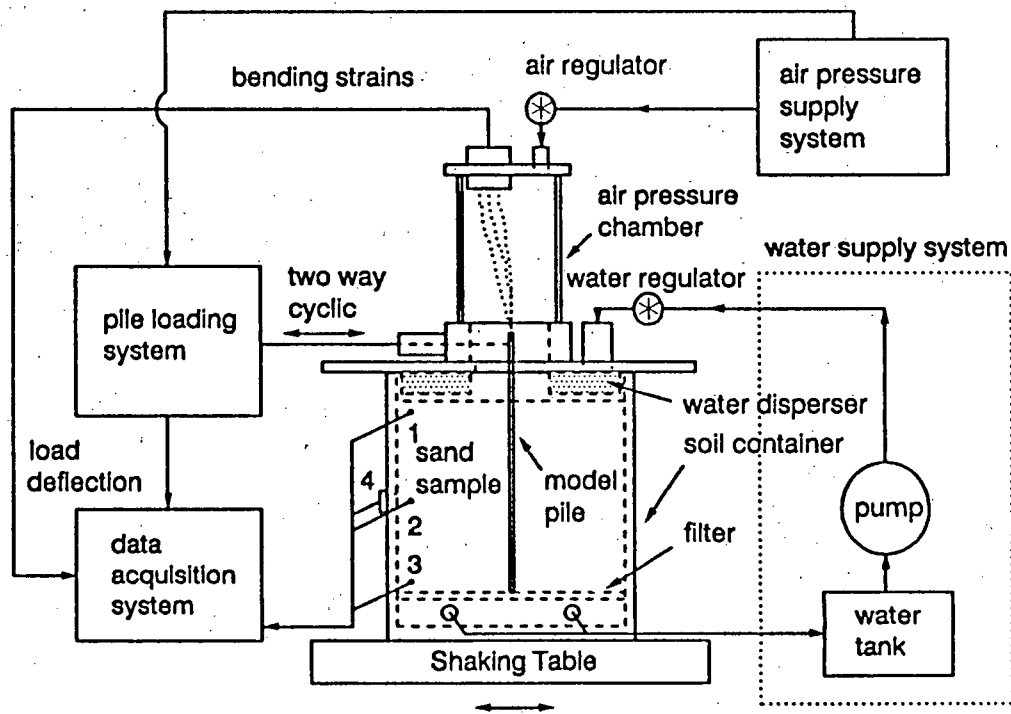
Figure 5.3: Comparison Between CYCPILE and LATPILE Under Free-Field Loading Conditions.

the test results were also discussed. A typical test setup is shown on Figure 5.4. These tests were modelled with CYCPILE using the actual physical dimensions shown but with the unit weight of sand increased by the HGS scale factor, N , for the particular test (Yan and Byrne, 1992).

Figure 5.5a compares the calculated pile head deflection for a free head pile with the measured data. The bending moments along the pile at a load level of 22 N is shown on Figure 5.5b. The comparisons here are excellent. Figure 5.6a and Figure 5.6b compare the pile head deflections and bending moments for a fixed head pile and show that CYCPILE's predictions are very good, although there are minor differences. The differences in these cases can be attributed to the fact that in reality it is very difficult to test a pile under a "true" fixed head condition. This problem will be encountered again when considering the full-scale field tests. Some pile rotation at the top will take place resulting in the measured deflections and moments being slightly different than those calculated by CYCPILE.

Generally speaking, the above comparisons are excellent, confirming that the basic assumptions on which CYCPILE is based introduce little error in predicting the soil-pile interaction behaviour. Therefore, the accuracy of predicted results by CYCPILE would generally be governed by the choice of input P-y curves.

It would be interesting to compare LATPILE's calculations of the same test data with CYCPILE. It would also be interesting to do the same calculations using API code (1987) P-y curves in CYCPILE. The results of these calculations are shown on the same figures as above. It can be seen that 1) CYCPILE's predictions are better than LATPILE; and 2) the API code P-y curves do not provide a good comparison with the measure data. The observation that CYCPILE's predictions are better than LATPILE is more or less expected here. Not only is CYCPILE capable



Note: 1,2,3 - pore water pressure transducer #PWP1,#PWP2,#PWP3
 4 - lateral soil stress transducer LATP

Soil Container Dimension: 445x230x420mm

Figure 5.4: Typical Model Test Setup in Yan's (1990) HGS Tests. After Yan (1990).

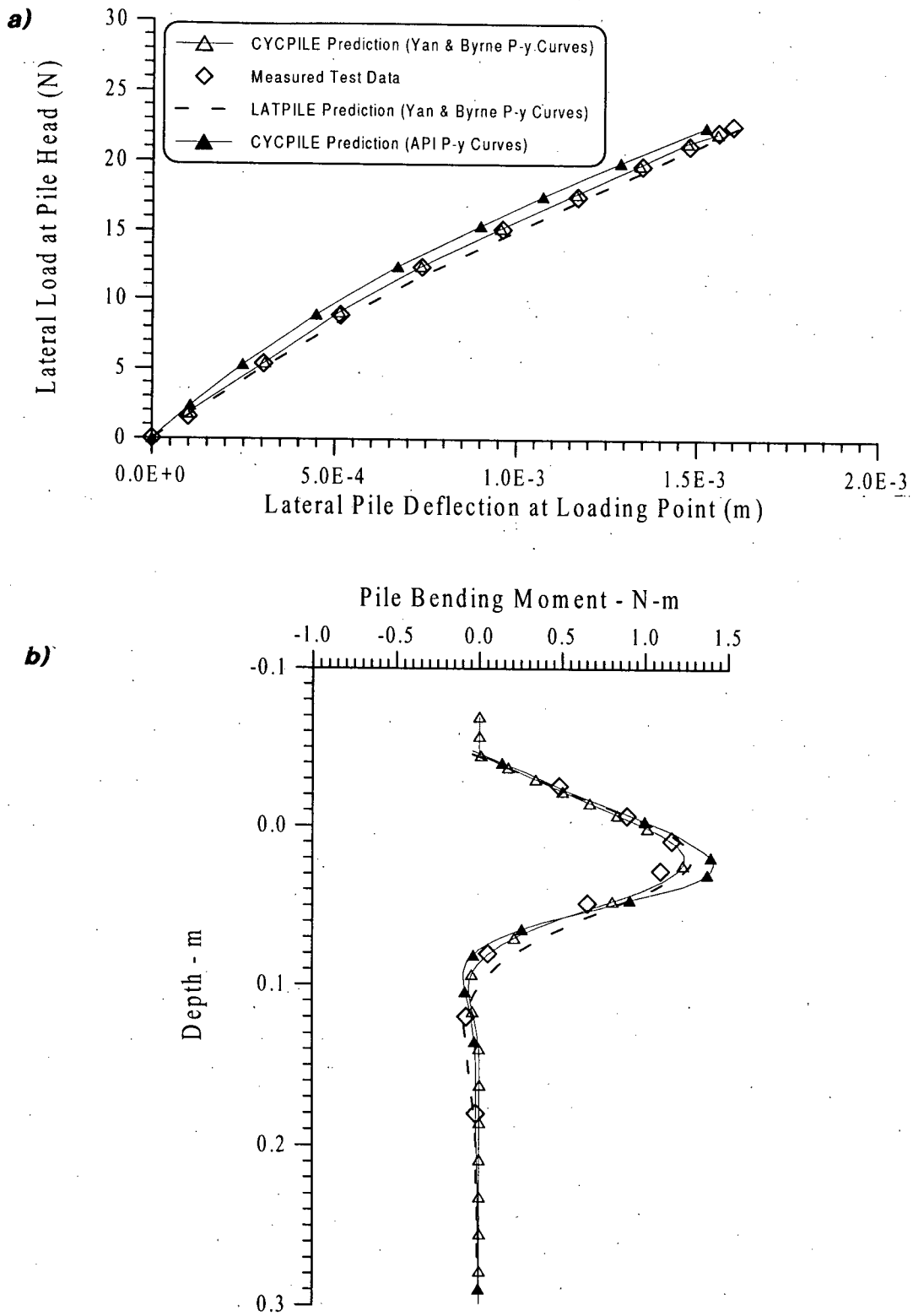


Figure 5.5: a) Prediction of Pile Head Deflection (Model Test, Free Head). b) Prediction of Pile Bending Moment Distribution (Model Test, Free Head).

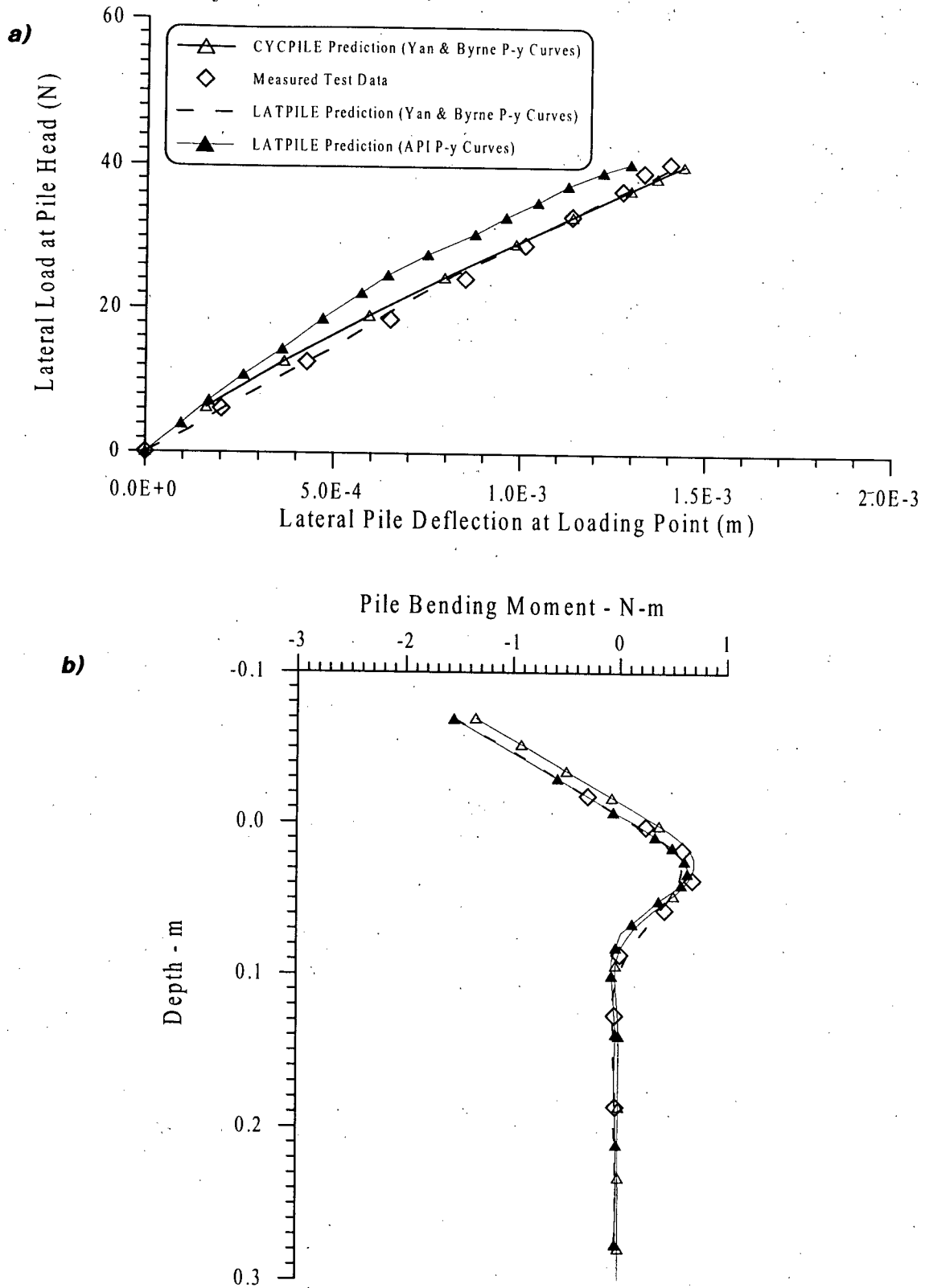


Figure 5.6: a) Prediction of Pile Head Deflection (Model Test, Fixed Head). b) Prediction of Pile Bending Moment distribution (Model Test, Fixed Head).

of accounting for pile yielding, it also gives a more accurate shape for the deformed pile elements than LATPILE.

5.4.2 Cyclic Loading

Cyclic loading and soil-pile gapping is modelled in CYCPILE by either using the cyclic P-y curves described in Chapter 3, or, by assuming that the unloading modulus is equal to the soil's maximum Young's modulus, E_{max} , and that soil is incapable of carrying tension.

As mentioned earlier, lateral cyclic loading can be divided into one-way and two-way cyclic loads. The key factor in capturing cyclic behaviour is the assumptions about material and mechanical degradations as discussed in an earlier chapter. Although CYCPILE is currently incapable of modelling material degradation, the mechanical degradation is accounted for in the unload-reload and soil-pile gapping assumptions.

Figure 5.7 shows the applied loading and measured pile head deflections for a 6.35 mm diameter model pile subjected to a load-controlled, constant amplitude, two-way cyclic loading in the HGS Testing device (after Yan, 1990). This pile was modelled with CYCPILE using the cyclic P-y curves presented in Chapter 3 and the results are shown on Figure 5.8. As can be seen the comparison is very good although there are minor differences between the predicted and measured results in the negative loading direction. The differences here can be attributed to the assumption in the cyclic P-y curve model that the variations with the number of cycles in both the positive and negative portions of the cyclic P-y curves are identical. This, however, is not the case in reality as evidenced by the measured cyclic P-y curves discussed in Chapter 3. Nevertheless, the results

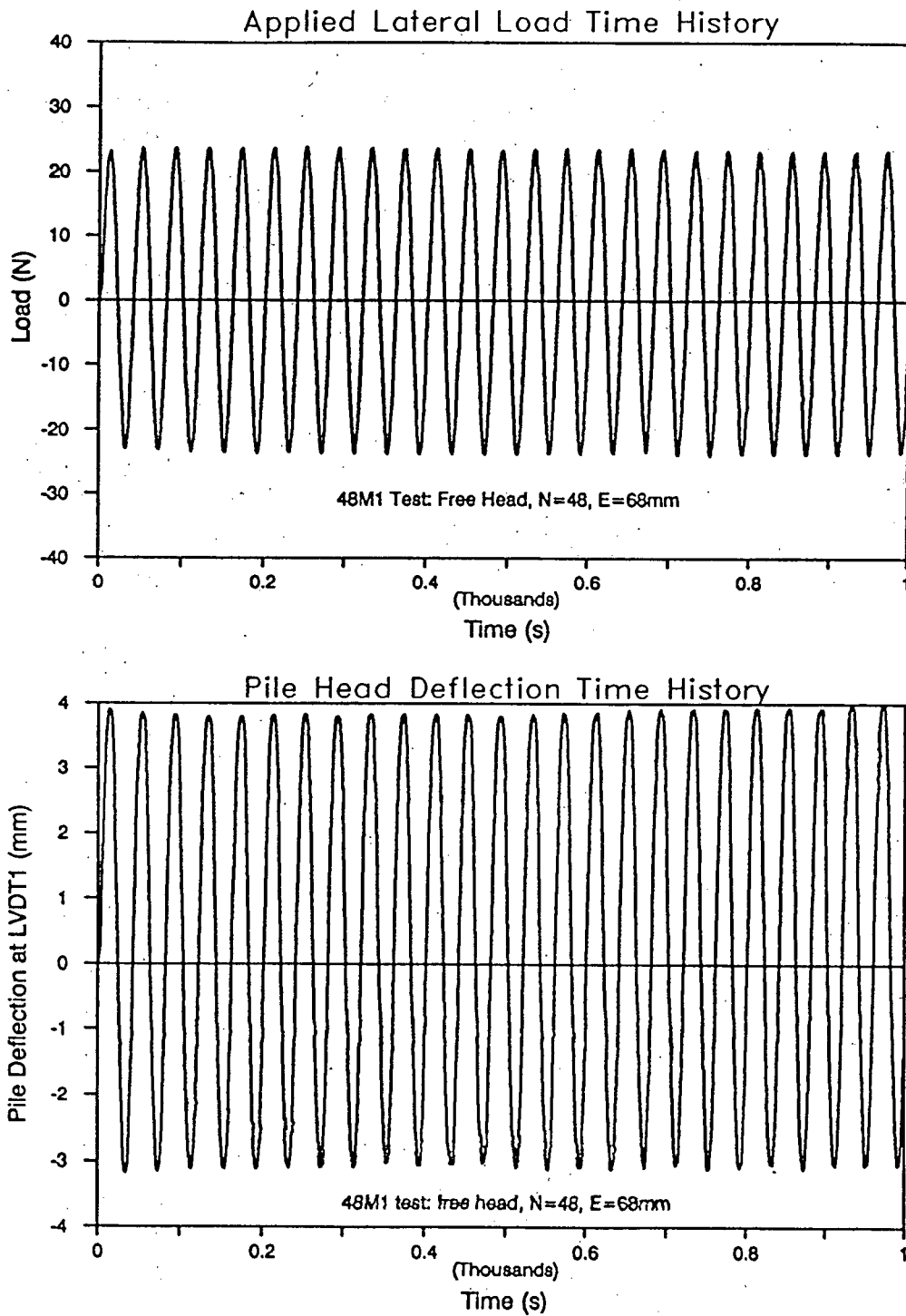


Figure 5.7: Applied Lateral Pile Head Loading and Measured Pile Head Deflections under Two-way Constant Amplitude Cyclic Loading. After Yan (1990).

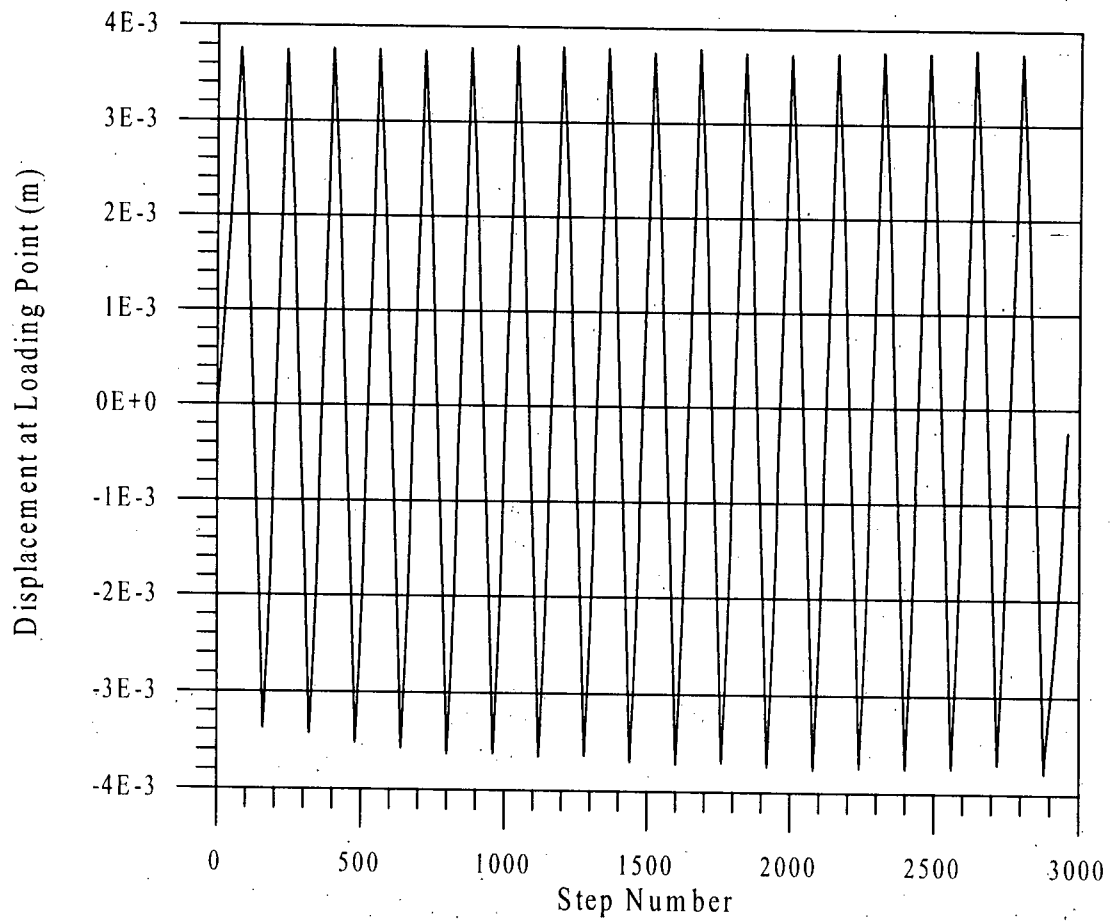


Figure 5.8: CYCPILE Prediction of The Pile Head Response under Two-way Cyclic Loading.

shown on Figure 5.8 indicate that the above assumption introduces little error in calculations for practical applications.

Figure 5.9 shows the applied loading and measured pile head deflections for the same pile as above subjected to a load-controlled, one-way cyclic loading (after Yan, 1990). The results of the CYCPILE analysis are shown on Figure 5.10. The comparison is excellent. It is worthwhile noting that CYCPILE correctly predicts the permanent pile head deflections and the increase in pile head deflections with the number of loading cycles, as observed from the test results.

5.5 Full Scale Tests

5.5.1 BC Hydro Laboratory Tests on Timber Piles

The BC Hydro laboratory tests on timber piles was described in Chapter 2. The response of a particular pile test will be presented here first to confirm that the model can in fact capture the pile behaviour both before and after yielding occurs. Then, we will attempt to match the 25th, 50th and 75th percentile of the moment-curvature relationships from the test data based on the corresponding moduli and yield stresses that were measured.

Figure 5.11 shows the moment-curvature and load-deflection curves as measured. During the test, some pile material degradation with strain was observed. The modulus of elasticity used in the CYCPILE analysis corresponds to that of the final loading cycle before loading to failure. It was found that to obtain the match as shown on the figure a yield stress of 22.7 MPa had to be used. The modulus of rupture (MOR) which is an indication of the yield stress was reported to be 40 MPa

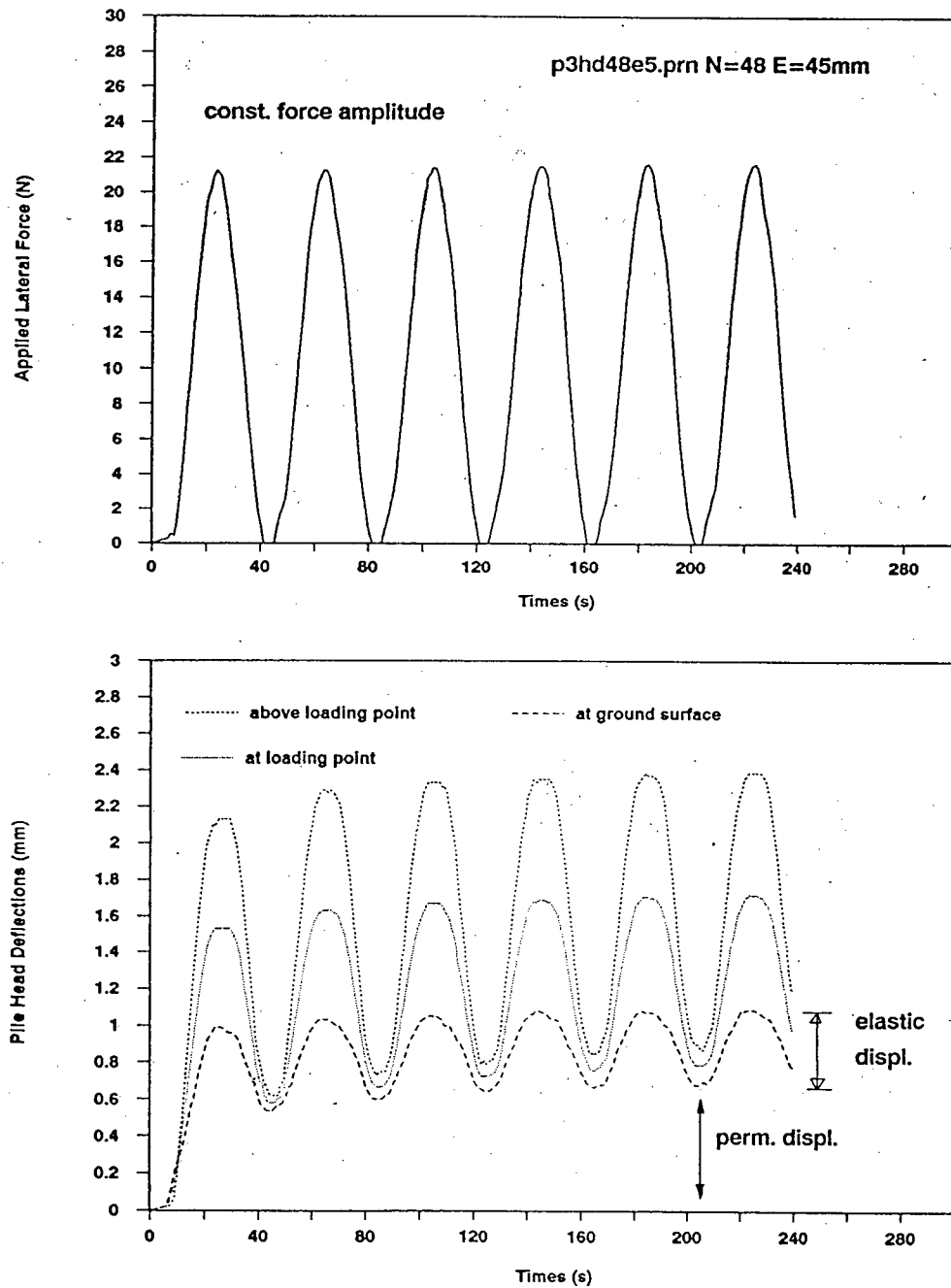


Figure 5.9: Applied Pile Head Loading and Measured Pile Head Deflections under Constant Amplitude One-way Loading. After Yan (1990).

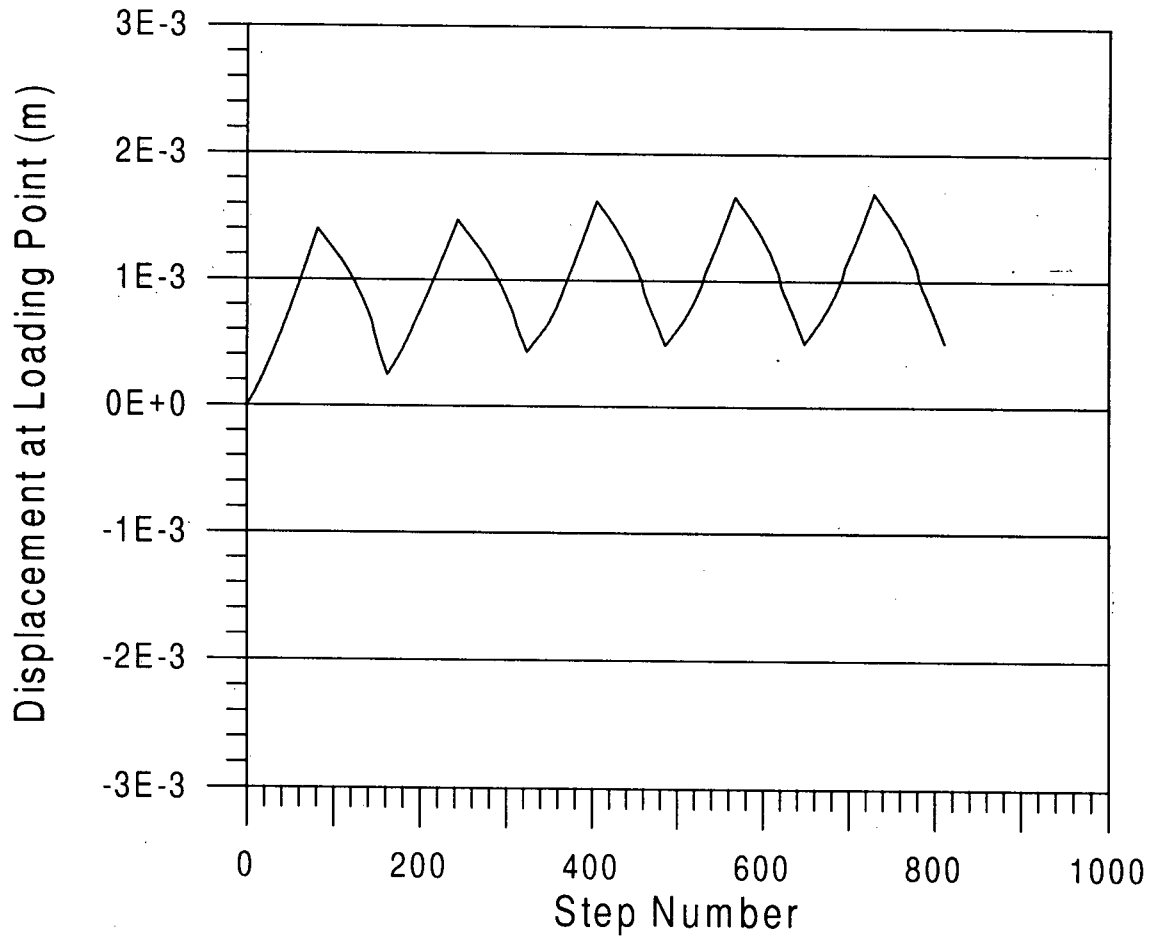


Figure 5.10: CYCPILE Prediction of The Pile Head Deflections under Constant Amplitude One-way Loading.

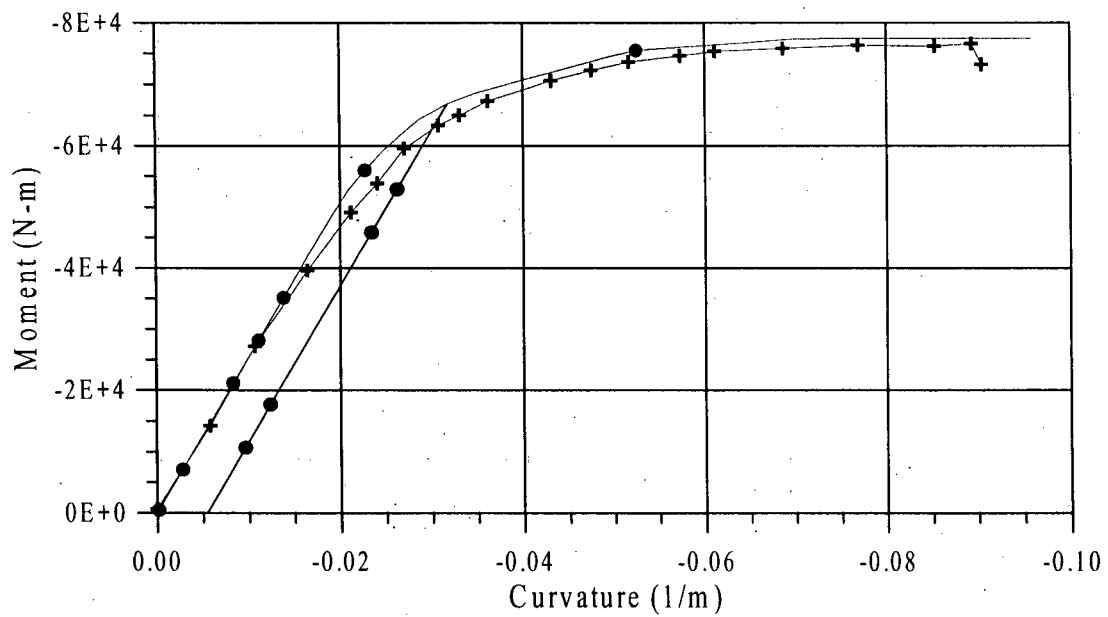
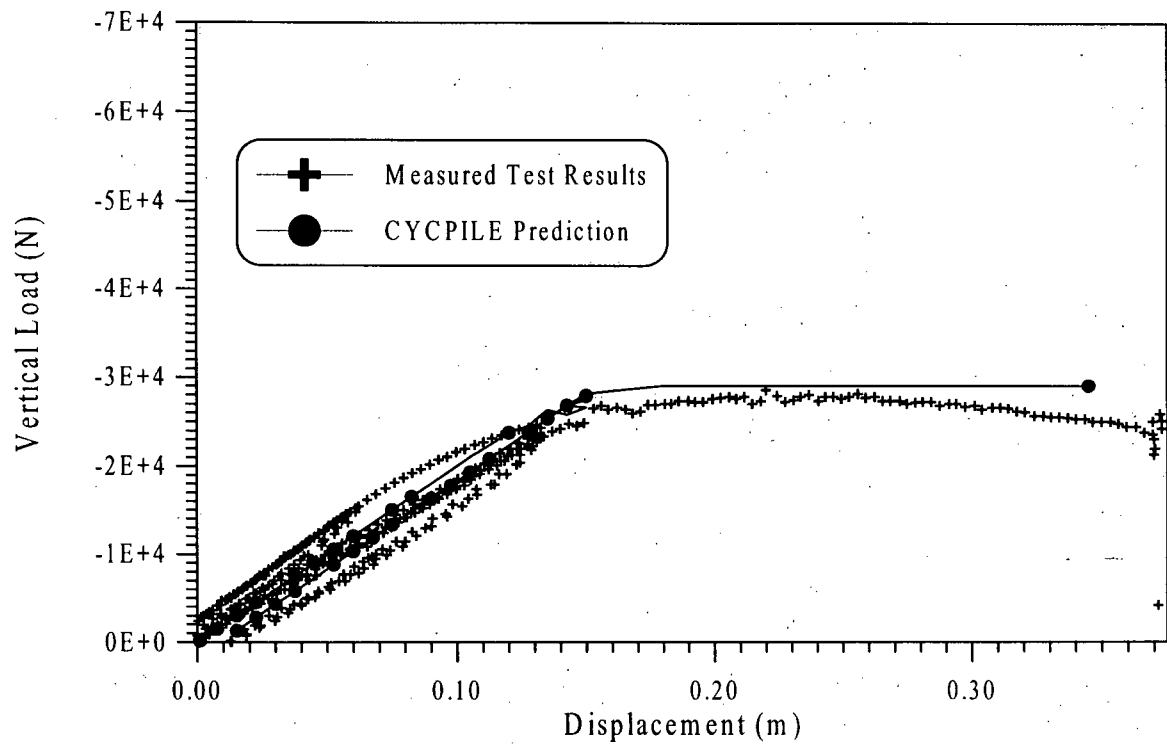


Figure 5.11: Comparison of Moment-Curvature and Load-Deflection from BC Hydro Laboratory Tests and CYCPILE.

on average. This MOR was about twice as much as the yield stress of 22.7 MPa. Interestingly, the recommended MOR by the Canadian Standards Association (CSA) CAN/CSA-086.1-M89 is 20.1 MPa which is close to that needed to match the BC Hydro test results. It is too early to make any conclusions about the test results until the different percentile moment-curvature curves are predicted using CYCPILE.

The comparison between measured data and CYCPILE's prediction is nevertheless excellent as shown on the figure.

To match the 50th percentile data points, corrected to 270mm diameter pile as shown on Figure 5.12, an elastic modulus of 9.0 GPa and a yield stress of 24.0 MPa was used in the CYCPILE analysis. The moduli and yield stress values used for the remaining curves were proportional to the percentile values and the parameters used to match the 50th percentile curve.

The above observations indicate that the yield stress of the timber piles are generally about one-half of the measured MOR values and close to the recommended MOR value in CAN/CSA-086.1-M89. Evidently, the computer program CYCPILE correctly captures the pile bending behaviour even well beyond the yield point. However, the final test for verifying the program, and the numerical model, is to predict field response of timber piles. Assuming that the soil stratigraphy, pile dimensions, and pile stress-strain parameters are known, CYCPILE should provide a fairly accurate prediction and this is attempted in the next section.

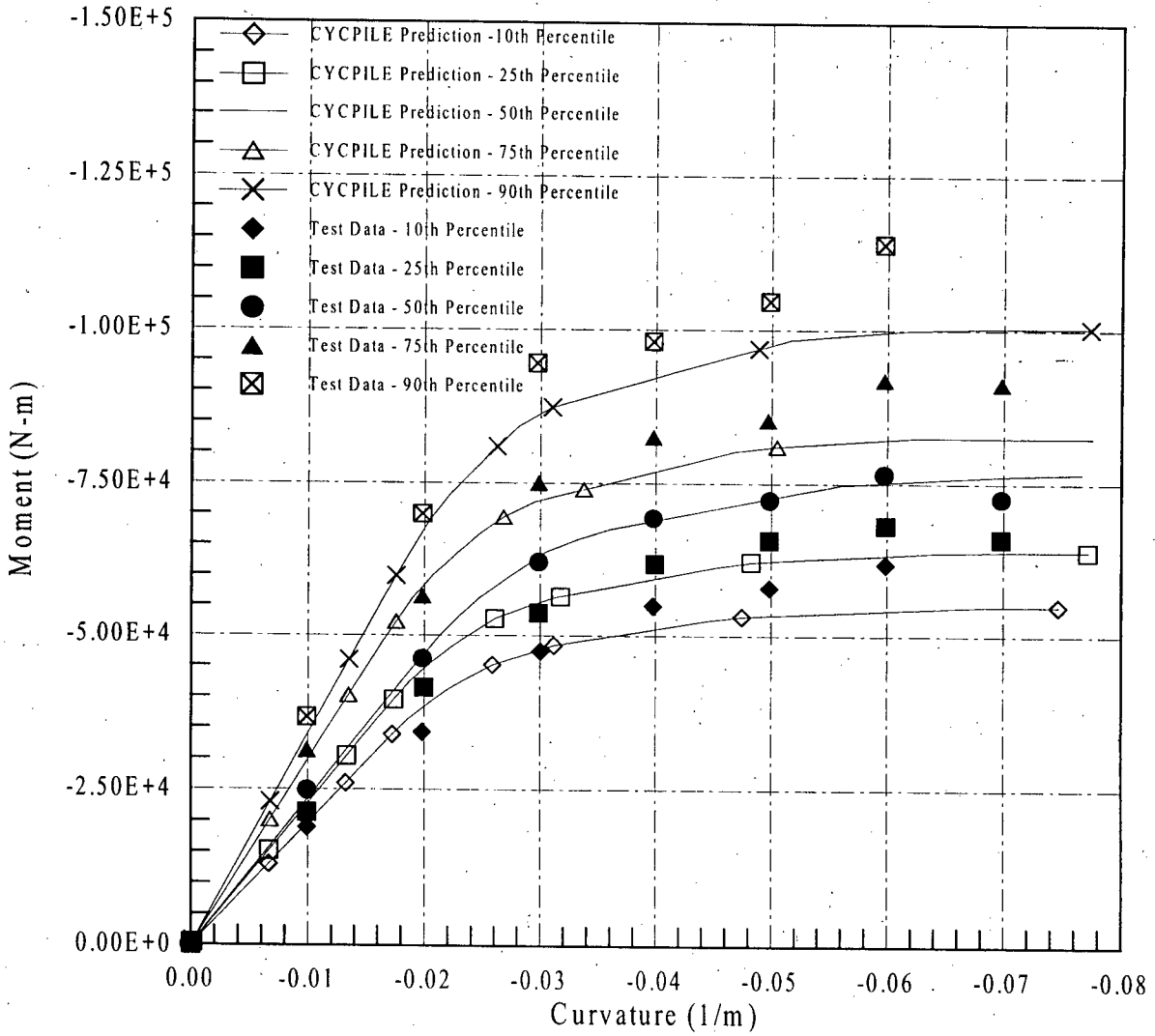


Figure 5.12: Comparison of Moment-Curvature Curves Adjusted to 270mm Pile Diameter from BC Hydro Laboratory Tests on Timber Piles and CYCPILE's Predictions.

5.5.2 BC Hydro Full Scale Field Tests on Timber Piles

The BC Hydro Full Scale Field Tests on Timber Piles were discussed in chapter 2 although not all of their results were presented there. In summary, three size 14 piles were tested with an attempt to keep the pile cap fixed against rotation. Figure 5.13 shows the typical test setup for these piles along with a summary of the parameters used in the CYCPILE analyses. The soil P-y curves were calculated based on the Cone Penetrometer Tests carried out at each pile location. The P-y curves presented in Chapter 3 were used in the analyses. The assumed soil stratigraphy for the analyses are also shown on Figure 5.13. The soils' relative densities and unit weights were the only soil parameters used in the generation of the P-y curves. The soil's E_{max} values were estimated from the relative densities as shown by Yan (1992). The displacement-controlled loading pattern was one-way cyclic with the amplitude of applied loading increasing at each cycle as shown on Figure 5.14 for a typical test.

The predicted load-deflection curves for all three piles is compared with the measured data on Figure 5.15. As can be seen, CYCPILE's predictions are very close to the measured values. The input parameters for the soils were obtained from Cone Penetration Tests performed prior to pile driving. The pile's elastic modulus was back-calculated from the elastic portion of the available moment-curvature curves for each pile. The initial estimate at yield stress was the median 25 MPa that was estimated from back-calculation of the laboratory test results. The actual values used to obtain the match for each test case is shown on the figure. Also shown on the figure for comparison are the predicted curves for a yield stress of 24 MPa. As can be seen from the figures, the comparisons are excellent.

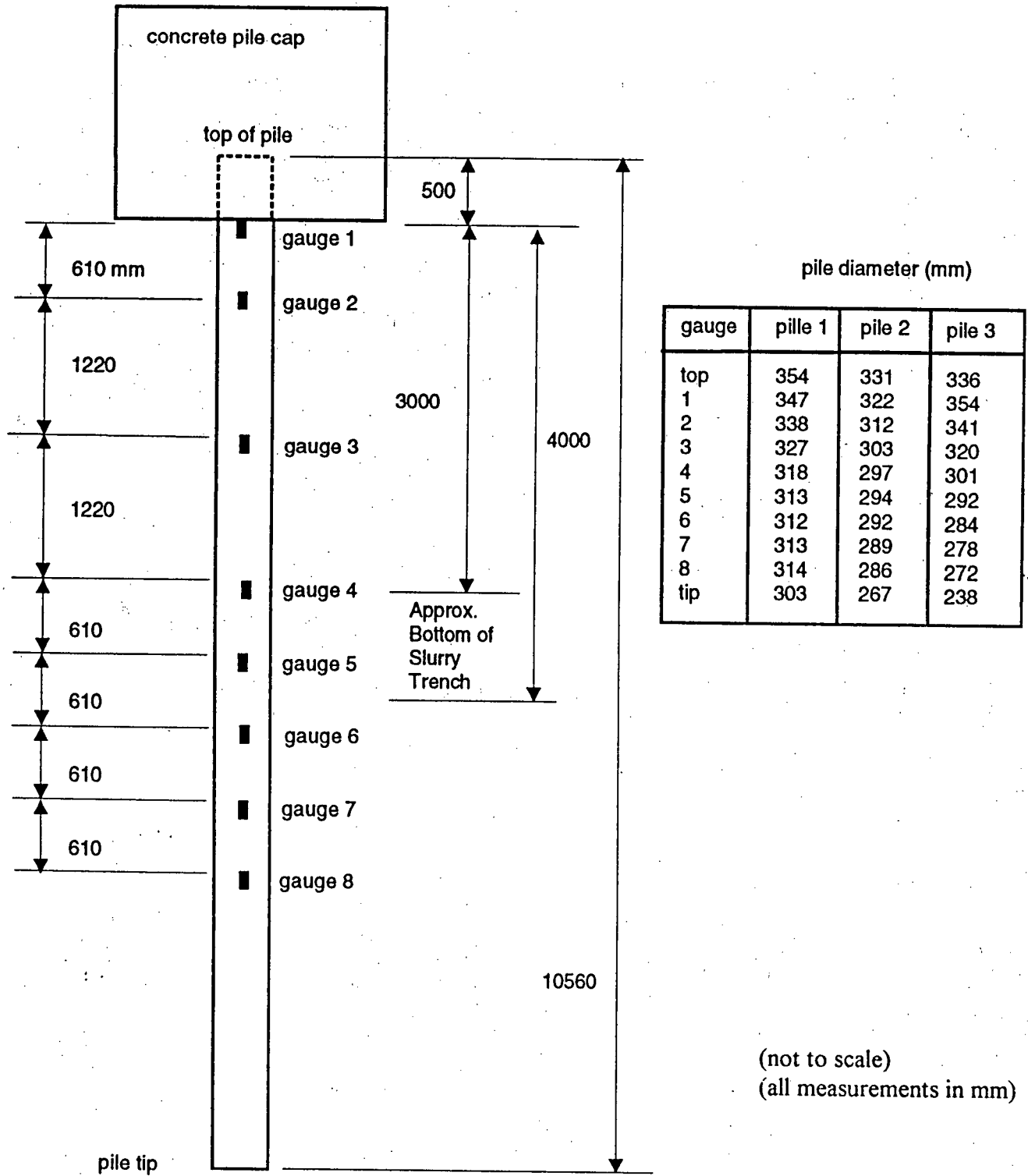


Figure 5.13: Typical Test Setup, BC Hydro Field Tests. After Wong (1992).

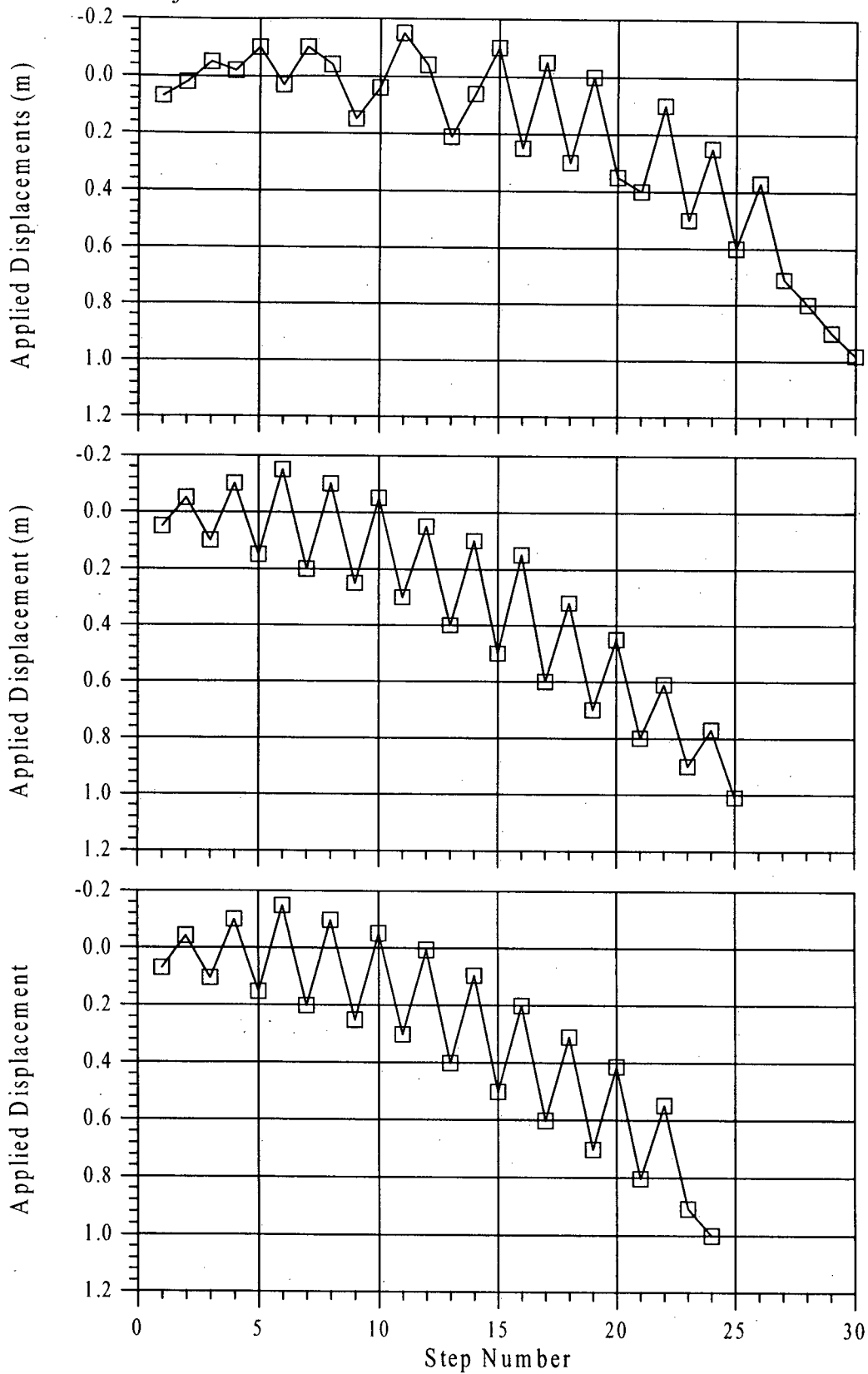


Figure 5.14: Applied Loading Sequence For The BC Hydro Field Tests. After Wong (1992).

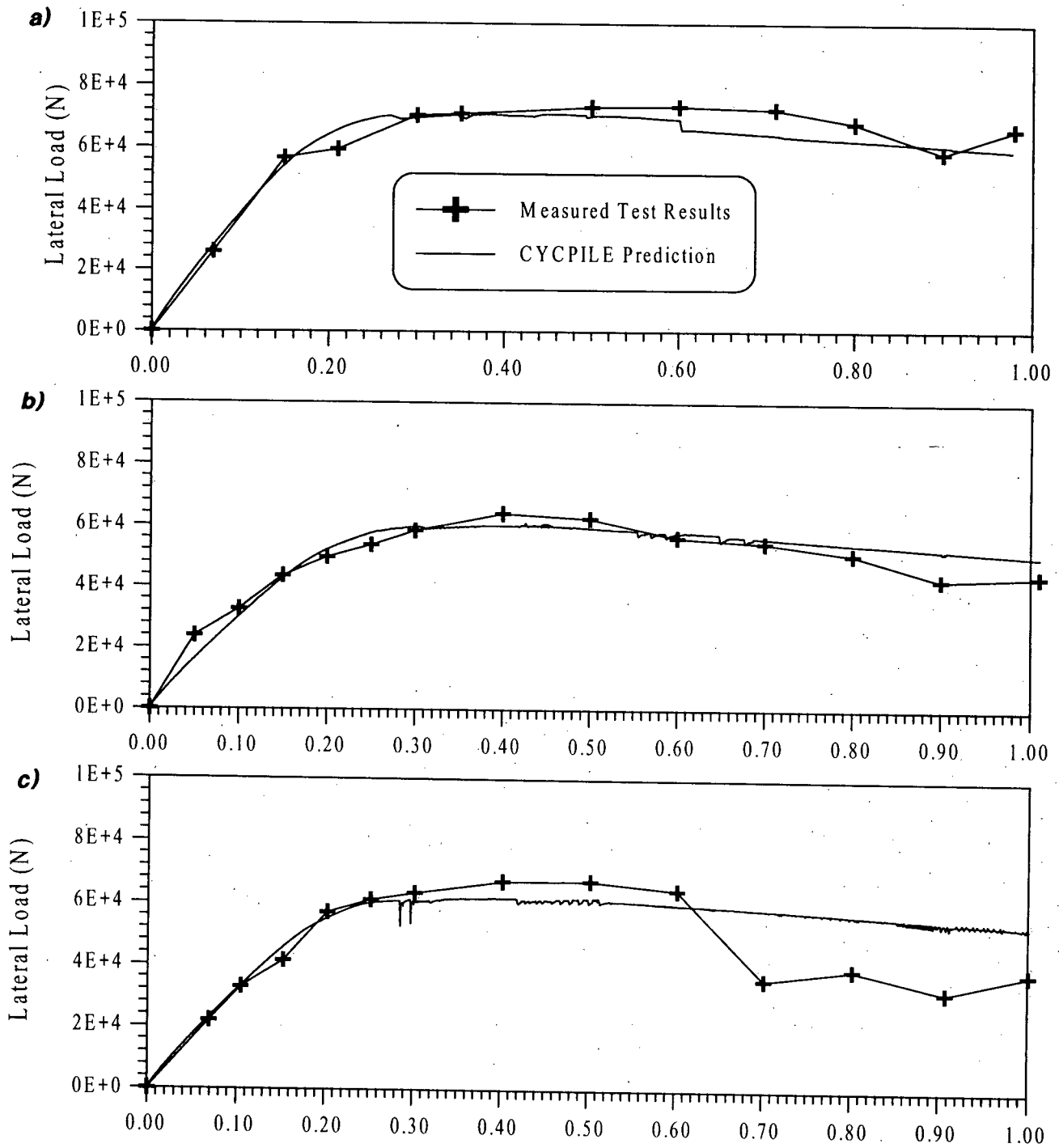


Figure 5.15: Comparison of Predicted versus Measured Load-Deflection Curves at Pile Cap for the BC Hydro Field Tests on Timber Piles. a) Test Pile 1; b) Test Pile 2; c) Test Pile 3.

For the moment-curvature curves (Figure 5.15, adjusted to Pile Diameter = 270 mm), however, the comparisons at first glance are not as good. The moments at the connection between the loading frame and the pile cap were measured using a moment cell. Moments in the pile section just below the pile cap can be estimated based on statics (Lee et al, 1992). A reason for the discrepancies can be found by examining the deflected shapes of the piles as shown on Figure 5.16. It can be easily seen that the pile caps were not effectively held against rotation and the yielding of the constraint would have somewhat significant effects on the measured moments. This would also explain the observed scatter in the moment-curvature curves at the bottom of the pile cap adjusted to 270mm diameter pile as shown on Figure 5.17. In fact, if we adjust the moments further based on rigid body motions and statics, we find that the moment-curvature curves fall within a narrow range, consistent with CYCPILE predictions and laboratory test results as shown on Figure 5.18. The rotation of the pile cap would induce an additional moment in the moment cell, mounted on the side of the pile cap, due to the additional eccentric loading and the weight of the pile cap. This additional moment can be calculated from the plots of the deflected shapes (Figure 5.16) and the knowledge of the weight of the pile cap (89 kN). The adjusted moments can be roughly approximated by multiplying the moments shown on Figure 5.17 by one minus the slope of the measured pile deflection within the pile cap.

In this case, it is very difficult to obtain a point by point comparison between the predicted and measured deformed shapes of the test piles due to the variability of timber and soil materials. However, it is envisaged that the effects of pile cap rotation on the deformed shape are not significant: the measured and predicted shapes of the deformed piles compare well as shown on Figure 5.16.

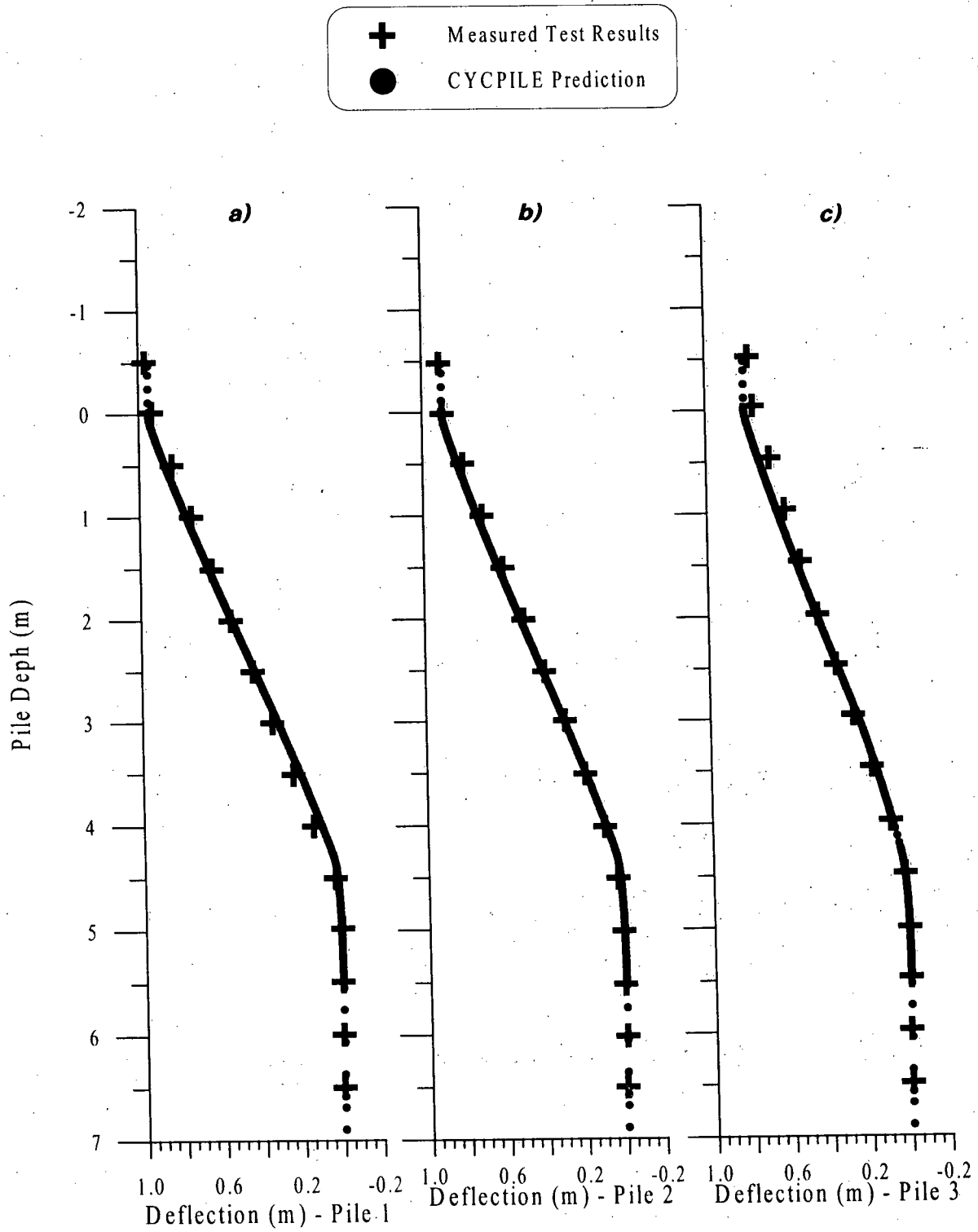


Figure 5.16: Predicted and Measured Deformations Along the Length of The Test Piles (BC Hydro's Field Tests on Timber Piles, 1992). a) Test Pile 1; b) Test Pile 2; c) Test Pile 3.

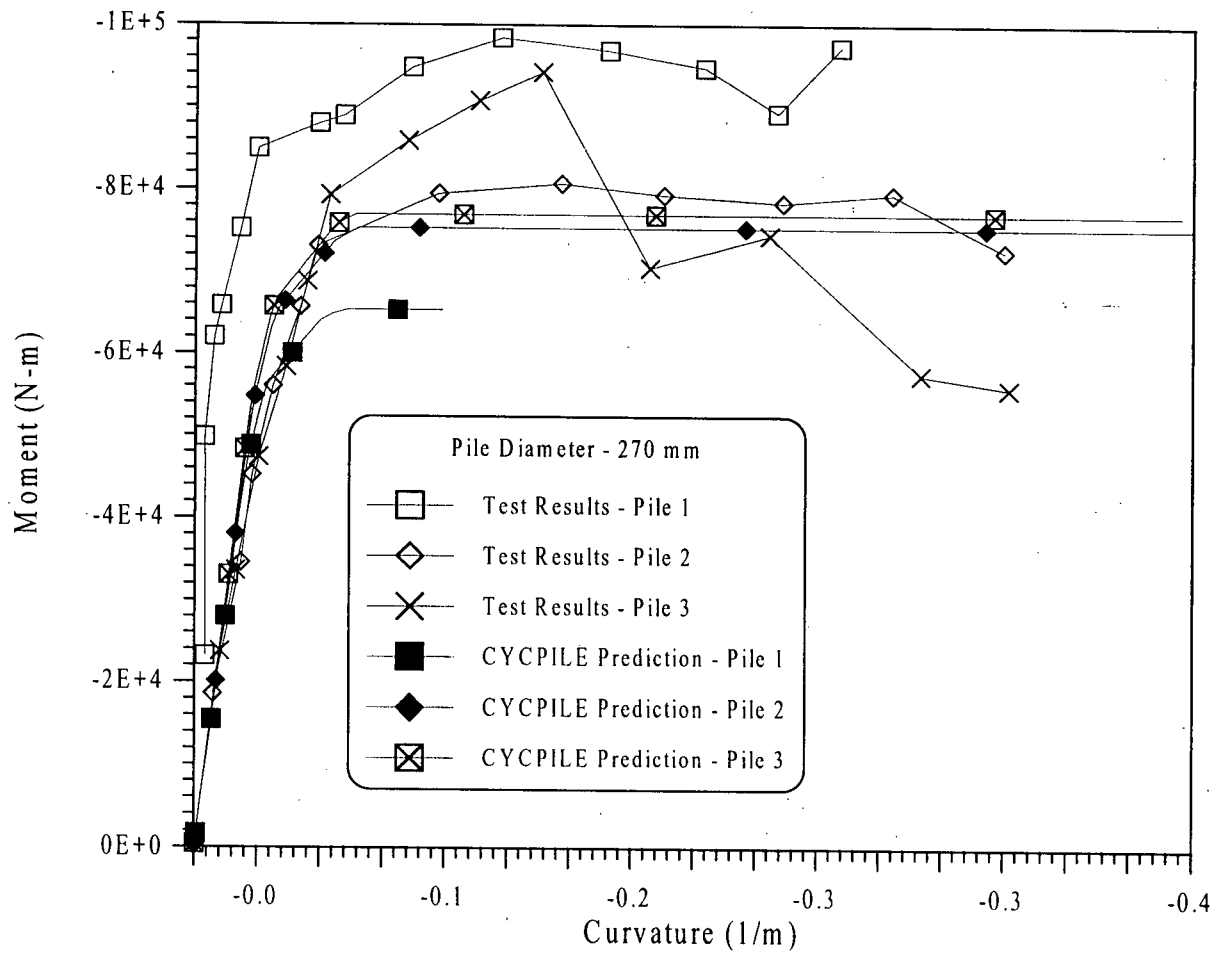


Figure 5.17: Moment vs. Curvature Adjusted to 270mm Pile diameter. After Lee et al (1992).

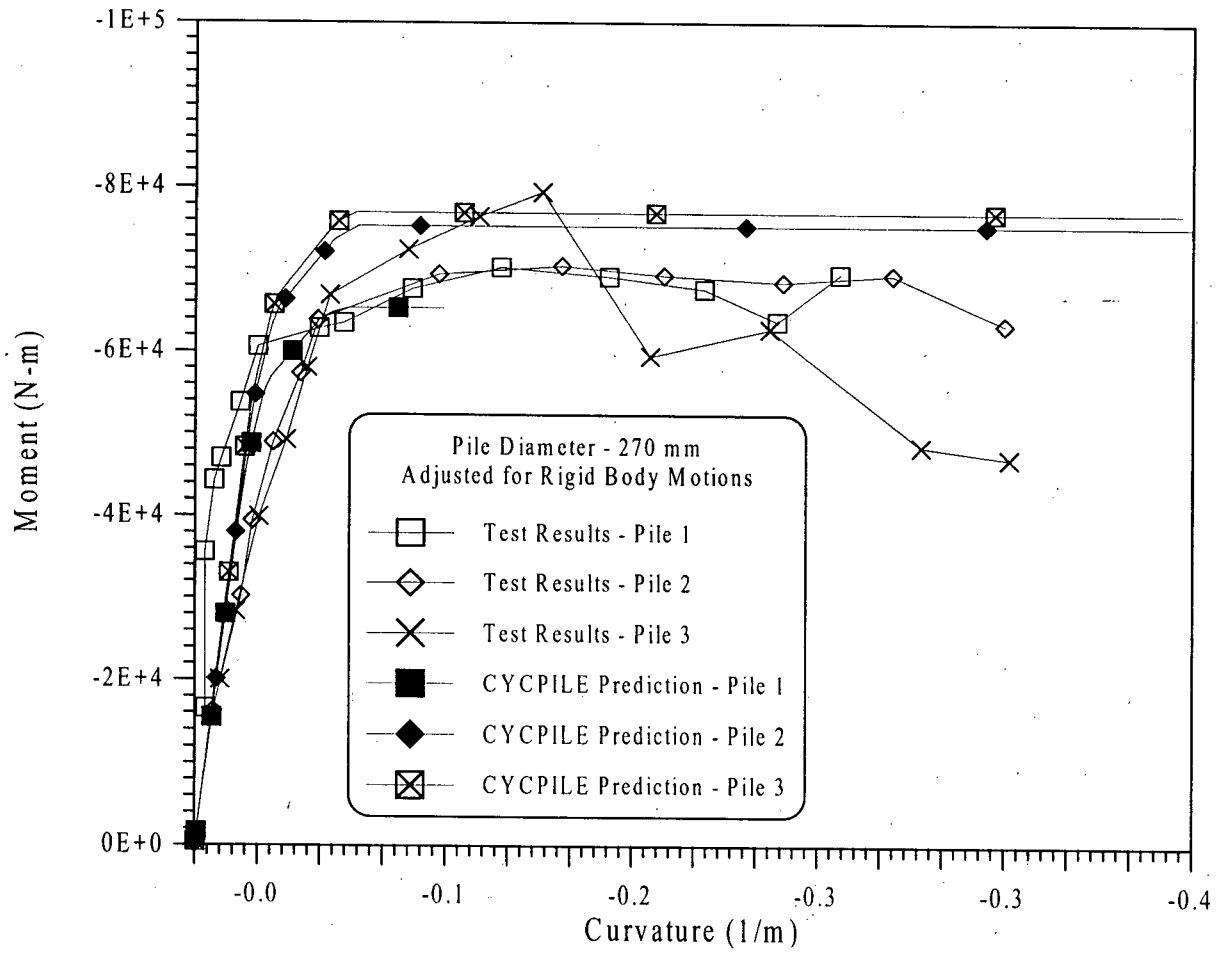


Figure 5.18: Moment vs. Curvature Curves Further Adjusted for Rigid Body Motions Caused by Rotation of Pile Caps.

5.6 Summary

The proposed model on which the computer program CYCPILE is based was first checked with closed-form solutions and found to be in excellent agreement as would be expected. The non-linear soil-pile interaction part of the model was then successfully verified with Hydraulic Gradient Similitude Test data (Yan, 1990, 1992). Using test data from the BC Hydro Laboratory tests on timber piles, it was ensured that CYCPILE was capable of correctly capturing the pile behaviour in both linear and non-linear, post-yield regions as well as in both monotonic and cyclic loading problems. Finally, the results of BC Hydro's field tests were predicted and found to be in excellent agreement with the measured data. However, it was necessary to make some adjustments to the test data in order to present them in a form that could be compared with CYCPILE's output.

The proposed model along with computer program CYCPILE have proven to be a very versatile and robust tool for analyzing monotonic and cyclic lateral loading of single vertical piles. The model and CYCPILE can be used for analyzing response of piles to lateral loads for different soil types as long as an appropriate P-y curve is specified. Information is now available for the behaviour of both fine-grained (API, 1987; Matlock, 1970; Reese et al, 1974) and granular soils (Yan, 1990; Yan and Byrne, 1992).

Chapter 6 Summary and Conclusions

Although to date a great deal of research effort has focussed on the analysis of laterally loaded piles, no comprehensive model had been developed to capture the behaviour of these piles based on experimental data. The availability of experimental data in the last five years (Yan, 1990, 1992, Lee et al, 1992, Naesgaard et al, 1992) has allowed for the development of a new model which accurately captures the response of vertical piles subjected to lateral loads. A review of the available test data indicated that soil-pile interaction is highly non-linear and is dependent on various factors such as stress level, soil density, and level of loading. A review of the present modelling methods revealed that a new model was required to capture the cyclic P-y curves. Of all the modelling methods reviewed in this thesis, those that employed the non-linear P-y curve technique were found to be the most versatile and powerful in capturing soil-pile interaction.

A new cyclic P-y curve model was developed based on available test data. A new numerical model was also developed for the analysis of laterally loaded vertical piles which incorporated the new cyclic P-y curve model. The proposed numerical model employs a robust finite element formulation for modelling the pile. P-y curves are used to represent the soil. The computer program CYCPILE was developed to perform the numerical analysis based on this model.

The proposed model was tested, calibrated and verified using a linear-elastic-perfectly-plastic stress-strain relationship for the pile and P-y curves presented here. The results were compared with available test data, and was found to give very accurate predictions. It was found

that for granular soils in general, Yan and Byrne (1992) P-y curves provided a much better match with measured data than the API code (1987) P-y curves.

The proposed model and the program allow the extension of the recent test results to more general problems. For specific problems, some testing may still be required to ensure appropriate P-y curves are used for the soil and the proper stress-strain behaviour for the pile. For example, the behaviour of concrete piles may not be accurately represented by a simple linear-elastic-perfectly-plastic model.

In conclusion, it is recommended that further research be carried out to:

1. obtain accurate stress-strain behaviour of different materials used for pile construction,
2. include material degradation for the pile in the computer program CYCPILE,
3. obtain an accurate mathematical model for cyclic P-y curves,
4. include dynamic effects from superstructure and surrounding ground,
5. include pile group interaction, and,
6. effect of vertical side friction.

Research on dynamic effects from superstructure and surrounding ground is ongoing at UBC (Dou, 1991; 1996; Khan, 1995). Also, some experimental research on pile group interaction has been performed at UBC (Panwalkar, 1994). These data suggest that pile group interaction can possibly be accounted for by applying an additional free-field movement to the ends of the springs (P-y curves) connected to each pile in the pile group. Free-field movements for any pile would include the effects of the adjacent piles. With some effort, such method of pile group interaction can

be added to the numerical model presented here. Panwalkar's (1994) research has shown that the amount of free-field movement depends primarily on the distance between each pair of piles being considered and the direction of loading which is consistent with observations of other researchers (Poulos & Davis, 1987). With more model test data now available, the effect of pile groups can be included in the numerical model in the future. However, some field testing would still be required in order to verify such a model.

Bibliography

- [1] Aboustit, B.L. and Reddy, D.V. (1980), "Finite Element Linear Programming Approach to Foundation Shakedown", International Symposium on Soils under Cyclic and Transient Loading, Swansea, Vol. 2, pp 727-738.
- [2] Alizadeh, M. and Davisson, M.T. (1970), "Lateral Load Tests on Piles - Arkansas River Project", Journal of Soil Mechanics and Foundation Division, ASCE, Vol. 96, SM5, pp 1583-1604.
- [3] API-RP2 (1987), *Recommended Practice for Planning, Designing and Constructing Fixed Offshore Platforms*. American Petroleum Institute, Washington, D.C. 17th Edition, April 1, 1987.
- [4] Atukorala, U., Byrne, P.M., and She, J. (1986), "Prediction of P-y Curves from Pressuremeter Tests and Finite Element Analyses", Version 2, Soil Mechanics Series No. 108, Department of Civil Engineering, University of British Columbia, Vancouver, B.C.
- [5] Baguelin, F., Frank, R. and Said, Y.H. (1977), "Theoretical Study of Lateral Reaction Mechanism of Piles", *Geotechnique*, Vol. 27, No. 3, pp 405-434.
- [6] Briaud, J.L., Smith, T.D., and Meyer, B. (1982), "Design of Laterally Loaded Piles using Pressuremeter Test Results," Proc. Symp. Pressuremeter and Its Marine Application, IFP-LPC, pp377-395, Paris.

- [7] Broms, B.B. (1964), "Lateral Resistance of Piles in Cohesionless Soils," *Jnl. Soil Mech. Found. D.V.*, ASCE, Vol. 90, SM3, pp123-156
- [8] Brown, D.A., Morrison, C. and Reese, L.C. (1987), "Response of A Single Pile in Sand subjected to Cyclic Lateral Loading,' *Symp. on Offshore and Arctic Operations*, The American Society of Mechanical Engineers, New York, pp139-143
- [9] Byrne, P.M., Chang, H. and Yan, L. (1987), "Soil Parameters for Deformation Analysis of Sands," *Canadian Geotechnical Journal*, Vol. 24, No. 3, pp.366-376.
- [10] Byrne, P.M., Anderson, D.L., Janzen, W. (1984) "Response of Piles and-Casings to Horizontal Free-field Soil Displacements", *Canadian Geotechnical Journal*, Vol. 21, No. 4, pp.720-725.
- [11] Cox, W.R., Reese, L.C. and Grubbs, B.R. (1974), "Field Testing of Laterally Loaded Piles in Sand," *Proc. 6th Annual OTC*, Houston, Texas, Vol. 2, Paper No. OTC2079, pp459-472.
- [12] Davis, M.P. (1987), M.A.Sc. Thesis, Dept. of Civil Engineering, The University of British Columbia, Vancouver, B.C.
- [13] Desai, C.S. (1977), Chapter 9, *Numerical Methods in Geotechnical Engineering*, ed. by Desai, C.S. and Christian, J., McGraw-Hill.
- [14] Desai, C.S. (1981), "Behavior of Interfaces between Structural and Geological Media," *Int. Conf. on Recent Advances in Geotech. Earthquake Engineering and Soil Dynamics*, Vol.II, St. Louis, MO. 1981.
- [15] Desai, C.S., Zaman, M.M., Lighter, J.G. and Siriwardane, H.J. (1984), "Thin-layer Element for Interface and Joints," *International Journal of Numerical Analysis Methods in Geomechanics* Vol. 8, pp19-43.

- [16] Dou, H.R. (1991), "Response of Pile Foundation Under Simulated Earthquake Loading", M.A.Sc. Thesis, Dept. of Civil Engineering, The University of British Columbia, Vancouver, B.C.
- [17] Duncan, J.M. and Chang, C.Y. (1970), "Nonlinear Analysis of Stress and Strain in Soils," J. of the Soil Mech. Found. Div., ASCE, Vol. 96, No. SM5, Sept. 1970.
- [18] Duncan, J.M., Byrne, P.M., Wong, K.S. and Mabry, P. (1980), "Strength, Stress-strain and Bulk Modulus Parameters for Finite Element Analysis of Stresses and Movements in Soil Masses," University of California, Berkeley, CA, Report No. UCB/GT/80-01.
- [19] Faruque, M.O. and Desai, C.S. (1982)) "3-D Material and Geometric Nonlinear Analysis of Piles," Proc. 2nd Int. Conf. on Num. Methods in Offshore Piling, Univ. of Texas, TX., pp553-575.
- [20] Foschi, R.O. (1992), Personal Communications.
- [21] Gambin, M. (1979), "Calculation of Foundations Subjected to Horizontal Forces using Pressuremeter Data," Sols Soils, No.30-31, 1971.
- [22] Gleser, S.M. (1953), "Lateral Load Tests on Vertical Fixed-Head and Free-Head Piles," Sym. on Lateral Load Tests on Piles, ASTM STP 154, Atlantic City, N.J., pp75-94.
- [23] Habibagahi, K. and Langer, J. (1983), "Horizontal Subgrade Modulus of Granular Soils," *Laterally Loaded Deep Foundations: Analysis and Performace*, ASTM STP 835, J.A. Langer, E.T. Mosley, and C.D. Thompson, eds., pp21-34.
- [24] Heytenyi, M. (1946), "Beams on Elastic Foundations," Ann Arbor, Mich. U.S.A.

- [25] Khan, A. (1995), "A New Non-linear Analysis of Layered Soil-Pile-Superstructure Seismic Response", M.A.Sc. Thesis, Department of Civil Engineering, University of British Columbia, Canada.
- [26] Kubo, K. (1965), "Experimental Study of the Behavior of Laterally Loaded Piles," Proc. 6th Int. Conf. SMEF., Montreal, Vol.II. pp275-279.
- [27] Kuhlemeyer, R.L. (1979), "Static and Dynamic Laterally Loaded Floating Piles," Jnl. Geot. Eng. Div., ASCE, Vol. 105, GT2, pp289-304.
- [28] Lee, M.K., Stewart, R.A., Imrie, A.S., "Timber Pile Lateral Test Program, Seismic Withstand of Timber Piles, Volume 1 of 2, Evaluation of Practise versus Theory", BC Hydro, Hydroelectric Engineering Division, Report No. H2607, April, 1992.
- [29] Leshchinsky, D. and Rawlings, D.L. (1988), "Stress Path and Permanent Deformations in Sand subjected to Repeated Load," Geotechnical Testing Journal, Vol. 11, No. 1, March 1988, pp.36-43.
- [30] Madson, B. (1992) "Report on Laboratory Testing of Timber Piles for BC Hydro Geotechnical Department", Timber Engineering Ltd., February 11, 1992.
- [31] Matlock, H. (1970), "Correlations for Design of Laterally Loaded Piles in Soft Clay," Proc. 2nd OTC, Houston, Paper OTC1204, pp577-594.
- [32] McClelland, B. and Focht, J.A. (1956), "Soil Modulus for Laterally Loaded Piles," Transactions, ASCE, Paper No.2954, pp.1049-1086.
- [33] Murchison, J.M. and O'Neill, M.W. (1984), "Evaluation of P-y Relationships in Cohesionless Soils," Proc. Symp. on Analysis and Design of Pile Foundations, San Francisco, Calif. Oct. 1984.

- [34] Naesgaard, E. (1992), "Lateral Load Tests to Examine Large-Strain (Seismic) Behaviour of Piles" Canadian Geotechnical Journal, Vol. 29, pp. 245-252.
- [35] Nakamura, S., *Applied Numerical Methods in C*, PTR Prentice Hall, Englewood Cliffs, New Jersey, 1993.
- [36] Oh-Oka, H. (1976), "Drained and Undrained Stress-strain Behavior of Sands Subjected to Cyclic Shear Stress under Nearly Plane Strain Condition," Soils and Foundations, Vol. 16, No.3.
- [37] Pande, G.N., Abdullah, W.S. and Davis, E.H. (1980), "Shakedown of Elasto-plastic Continuum with Special Reference to Soil-rock Structures," Int. Symp. Soils under Cyclic and Transient Loading, Swansea, pp-739-746, G.N. Pande and O.C. Zienkiewicz, eds., A.A. Balkema, Rotterdam.
- [38] Panwalkar, A. (1994), M.A.Sc. Thesis, Department of Civil Engineering, University of British Columbia, Canada.
- [39] Poulos, H.G. (1971), "Behaviour of Laterally Loaded Piles: I - Single Piles", Jnl. SMFE Div. ASCE, Vol.97, SM5, pp733-751.
- [40] Poulos, H.G. (1974), "Analysis of Pile Groups subjected to Vertical and Horizontal Loads," Aust. Geomechs., Jnl, Vol.G4, No.1:26-32.
- [41] Poulos, H.G. and Davis, E.H. (1980), *Pile Foundation Analysis and Design*, John Wiley and Sons, New York, 397pp.
- [42] Poulos, H.G. (1981), "Behavior of Single Piles Subjected to Cyclic Lateral Load," Civil Engineering Research Report R385, University of Sydney, Australia.

- [43] Poulos, H.G. (1982), "Developments in the Analysis of Static and Cyclic Lateral Response of Piles," Proc. 4th Int. Conf. on Num. Meth. in Geomech., Edmonton, Alberta, Canada, Vol.3, pp.1117-1135.
- [44] Poulos, H.G. (1987), "From Theory to Practice in Pile Design," Research Report No. R559, The University of Sydney, Australia.
- [45] Randolph, M.F. (1981), "The Response of Flexible Piles to Lateral Loading," *Geotechnique*, Vol.31, No-2, pp247-259.
- [46] Reese, L.C., Cox, W.R. and Koop, F.D. (1974), "Analysis of Laterally Loaded Piles in Sand," Proc. 6th OTC, Houston, Paper OTC2080, pp.473-483.
- [47] Reese, L.C. (1977), "Laterally Loaded Piles: Program Documentation," *Jnl. Geot. Engng. Div., ASCE*, Vol.103, NoC.T4, 287-305.
- [48] Reese, L.C. (1979), "Design of Evaluation of Load Tests on Deep Foundations," *Behavior of Deep Foundations*, ASTM STP 670.
- [49] Reese, L.C. et al (1988), "Experimental Research into the Behavior of Piles and Pile Groups subjected to Lateral Loads," U.S. Army Corps of Engineers Waterways Experiment Station, Vicksburg, June 1988, WES/MO/GL-86-10.
- [50] Robertson, P.K., Campanella, R.G., Gillespie, D., and Rice, A. (1984), "Seismic CPT to Measure In-Situ Shear Wave Velocity," Proc. Measurement and Use of Shear Wave Velocity for Evaluating Dynamic Soil Properties, Geotechnical Engineering Div., ASCE, Denver, Colorado, April 1984.

- [51] Robinson, K.E. (1970), "Horizontal Subgrade Reaction Estimated from Lateral Loading Tests on Timber Piles", Symp. on Behaviour of Deep Foundations, ASTM STP 670, ed. by R. Lundgren, pp.520-536.
- [52] Scott, R.F. (1981), *Foundation Analysis*, Prentice-Hall, Inc. Englewood Cliff, N.J.
- [53] Shaw, P. and Brown, S.F. (1986), "Cyclic Simple Shear Testing of Granular Materials," *Geotechnical Testing Journal*, Vol. 9, No. 4, Dec. 1986, pp213-220.
- [54] Smith, T. (1983), "Pressuremeter Design Method for Single Piles subjected to Static Lateral Load," Ph.D. Thesis, Texas A & M University.
- [55] Swane, I.C. and Poulos, H.G. (1982), "A Theoretical Study of the Cyclic Shake-down of Laterally Loaded Piles," Research Report No.R415, School of Civil and Mining Engineering, The University of Sydney, Australia, July, 1982.
- [56] Terzaghi, K. (1955), "Evaluation of Coefficients of Subgrade Reaction," *Geotechnique*, Vol.5, No.4, pp297.
- [57] Ting, J.M., Kauffman, C.R. and Lovicsek, M. (1987), "Centrifuge Static and Dynamic Lateral Pile Behaviour," *Can. Geot. J.* Vol. 24, pp.198-207.
- [58] Wagner, A.A. (1953), "Lateral Load Tests on Piles for Design Information," Sym. on Lateral Load Tests on Piles, ASTM STP 154, Atlantic City, N.J., pp.59-73.
- [59] Wong, J., (1992) "Timber Pile Lateral Test Program, Summary of Field Tests", Powertech Labs Inc., July, 1992.

- [60] Yan, L. (1986), "Numerical Studies on Some Aspects with Pressuremeter and Laterally Loaded Piles," M.A.Sc. Thesis, Dept. of Civil Engineering, University of British Columbia, Vancouver, Canada.
- [61] Yan, L. (1990) "Hydraulic Gradient Similtude Method for Geotechnical Modelling Tests with Emphasis on Laterally Loaded Piles" Ph.D. Thesis, Department of Civil Engineering, University of British Columbia, Canada.
- [62] Yan, L. and Byrne, P.M. (1992), "Lateral Pile Response to Monotonic Pile Head Loading", Canadian Geotechnical Journal, Vol. 29, pp. 955-970.
- [63] Yegian, M. and Wright, S.G. (1973), "Lateral Soil Resistance Displacement Relationships for Pile Foundations in Soft Clay," OTC, paper No. 1893, Dallas, Texas, U.S.A.
- [64] Yoshida, I. and Yoshinaka, R. (1972), "A Method to Estimate Modulus of Horizontal Subgrade for a Pile," Soils and Foundations, Vol.12, No.3.

Appendix I - Shape Functions Used in The Numerical Model

The shape functions, $M_0(\xi)$, $M_1(\xi)$, $M_2(\xi)$, $N_0(\xi)$, $N_1(\xi)$, are derived by considering (see Chapter 4):

$$\{a\} = \{w, w', w'', u, u', w, w', w'', u, u'\} \quad (\text{I.1})$$

$$w = b_1 x^5 + b_2 x^4 + b_3 x^3 + b_4 x^2 + b_5 x + b_6 \quad (\text{I.2})$$

$$u = c_1 x^3 + c_2 x^2 + c_3 x + c_4 \quad (\text{I.3})$$

Differentiating w and u with respect to x :

$$w' = 5b_1 x^4 + 4b_2 x^3 + 3b_3 x^2 + 2b_4 x + b_5 \quad (\text{I.4})$$

$$w'' = 20b_1 x^3 + 12b_2 x^2 + 6b_3 x + 2b_4 \quad (\text{I.5})$$

Using local coordinates such that $x_i = 0$, $x_j = \Delta$, and define ξ such that $x = (1+\xi)(\Delta/2)$, we can evaluate Equations (I.2) through (I.6) at x_i and x_j to solve for b_n and c_n in terms of $\{a\}$. Substituting for b_n and c_n in Equations (I.2) through (I.6), we can re-write these equations in terms of $\{a\}$:

$$u' = 3c_1x^2 + 2c_2x + c_3 \quad (\text{I.6})$$

$$w(\xi) = M_0^T(\xi)\{a\}; \quad w'(\xi) = M_1^T(\xi)\{a\}; \quad w''(\xi) = M_2^T(\xi)\{a\} \quad (\text{I.7})$$

$$u(\xi) = N_0^T(\xi)\{a\}; \quad u'(\xi) = N_1^T(\xi)\{a\} \quad (\text{I.8})$$

where shape functions, $M_0(\xi)$, $M_1(\xi)$, $M_2(\xi)$, $N_0(\xi)$, and $N_1(\xi)$ are given by

$$\begin{aligned} M_0(1,\xi) &= (8-15\xi+10\xi^3-3\xi^5)/16 \\ M_0(2,\xi) &= (5-7\xi-6\xi^2+10\xi^3+\xi^4-3\xi^5)(\Delta/32) \\ M_0(3,\xi) &= (1-\xi-2\xi^2+2\xi^3+\xi^4-\xi^5)(\Delta^2/64) \\ M_0(4,\xi) &= 0 \\ M_0(5,\xi) &= 0 \\ M_0(6,\xi) &= (8+15\xi-10\xi^3+3\xi^5)/16 \\ M_0(7,\xi) &= (-5-7\xi+6\xi^2+10\xi^3-\xi^4-3\xi^5)(\Delta/32) \\ M_0(8,\xi) &= (1+\xi-2\xi^2-2\xi^3+\xi^4+\xi^5)(\Delta^2/64) \\ M_0(9,\xi) &= 0 \\ M_0(10,\xi) &= 0 \end{aligned} \quad (\text{I.9})$$

$$\begin{aligned}
M_1(1,\xi) &= (-15 + 30\xi^2 - 15\xi^4)(2/16\Delta) \\
M_1(2,\xi) &= (-7 - 12\xi + 30\xi^2 + 4\xi^3 - 15\xi^4)/16 \\
M_1(3,\xi) &= (-1 - 4\xi + 6\xi^2 + 4\xi^3 - 5\xi^4)(\Delta/32) \\
M_1(4,\xi) &= 0 \\
M_1(5,\xi) &= 0 \\
M_1(6,\xi) &= (15 - 30\xi^2 + 15\xi^4)(2/16\Delta) \\
M_1(7,\xi) &= (-7 + 12\xi + 30\xi^2 - 4\xi^3 - 15\xi^4)/16 \\
M_1(8,\xi) &= (1 - 4\xi - 6\xi^2 + 4\xi^3 + 5\xi^4)(\Delta/32) \\
M_1(9,\xi) &= 0 \\
M_1(10,\xi) &= 0
\end{aligned} \tag{I.10}$$

$$\begin{aligned}
M_2(1,\xi) &= (60\xi - 60\xi^3)(4/16\Delta^2) \\
M_2(2,\xi) &= (-12 + 60\xi + 12\xi^2 - 60\xi^3)(2/16\Delta) \\
M_2(3,\xi) &= (-4 + 12\xi + 12\xi^2 - 20\xi^3)/16 \\
M_2(4,\xi) &= 0 \\
M_2(5,\xi) &= 0 \\
M_2(6,\xi) &= (-60\xi + 60\xi^3)(4/16\Delta^2) \\
M_2(7,\xi) &= (12 + 60\xi - 12\xi^2 - 60\xi^3)(2/16\Delta) \\
M_2(8,\xi) &= (-4 - 12\xi + 12\xi^2 + 20\xi^3)/16 \\
M_2(9,\xi) &= 0 \\
M_2(10,\xi) &= 0
\end{aligned} \tag{I.11}$$

$$\begin{aligned}
N_0(1, \xi) &= 0 \\
N_0(2, \xi) &= 0 \\
N_0(3, \xi) &= 0 \\
N_0(4, \xi) &= (2 - 3\xi + \xi^3)/4 \\
N_0(5, \xi) &= (1 - \xi - \xi^2 + \xi^3)(\Delta/8) \\
N_0(6, \xi) &= 0 \\
N_0(7, \xi) &= 0 \\
N_0(8, \xi) &= 0 \\
N_0(9, \xi) &= (2 + 3\xi - \xi^3)/4 \\
N_0(10, \xi) &= (-1 - \xi + \xi^2 + \xi^3)(\Delta/8)
\end{aligned} \tag{I.12}$$

$$\begin{aligned}
N_1(1, \xi) &= 0 \\
N_1(2, \xi) &= 0 \\
N_1(3, \xi) &= 0 \\
N_1(4, \xi) &= (-3 + 3\xi^2)/(2\Delta) \\
N_1(5, \xi) &= (-1 - 2\xi + 3\xi^2)/4 \\
N_1(6, \xi) &= 0 \\
N_1(7, \xi) &= 0 \\
N_1(8, \xi) &= 0 \\
N_1(9, \xi) &= (3 - 3\xi^2)/2\Delta \\
N_1(10, \xi) &= (-1 + 2\xi + 3\xi^2)/4
\end{aligned} \tag{I.13}$$

Appendix II - Computer Program CYCPILE

CYCPILE

Version 1.0

A COMPLETE PROGRAM FOR CALCULATING MONOTONIC AND CYCLIC LATERAL
LOADS ON SINGLE PILES INCLUDING FREE-FIELD MOVEMENTS

by

Saman Vazinkhoo

Dr. Peter M. Byrne

Dr. Ricardo O. Foschi

DEPARTMENT OF CIVIL ENGINEERING
UNIVERSITY OF BRITISH COLUMBIA
CANADA

1996

© Saman Vazinkhoo, 1996

Abstract

This document is the user's manual for the computer program CYCPILE. This program analyzes the response of single piles to cyclic and static lateral loads caused by earthquakes and lateral ground movements. In this program, a finite element beam model is used for representing the pile which, at the present, assumes a linear-elastic-perfectly-plastic stress-strain relationship. The soil is represented by non-linear springs in the form of p-y curves. Pile gapping is taken into account by either enforcing zero tensile pressures on the soil, or, by using the cyclic P-y curves presented in Vazinkhoo (1996). Input loads may be given in terms of displacements or forces which can be specified at either one or more nodes, or, as free field displacements along the pile length. P-delta effects are taken into account in the formulation of the finite element model. A varying axial load may be input at the top, although settlement of the pile due to an axial load is not considered.

At this time, the model and the program are not capable of analyzing a fully dynamic problem where inertia forces may have considerable effect on the results. Such capabilities are being developed and will be available in a later version of the program.

This report contains detailed description of the structure and flow of the program CYCPILE. A number of example problems are also presented for guidance.

Table of Contents

Abstract	139
Table of Contents	140
List of Figures	141
Chapter 1. Introduction	142
1.1 Introduction	142
1.2 Purpose and Scope	143
1.3 Applications	144
Chapter 2. Analytical Model	145
2.1 Pile Model	145
2.2 Soil Model	148
Chapter 3. Program Setup	150
3.1 Program Flow	151
3.2 Program Structure	153
3.3 Current Program Capacities	154
3.4 Description of the Input File	154
3.5 Program Output	161
3.6 Problems That May Be Encountered While Running CYCPILE	161
Chapter 4. Example Problems	163
4.1 Example No. 1 Three Point Bending Test on a Timber Pile	163
4.2 Example No. 2 Lateral Load Test on a Model Pile in The HGS Testing Device	173
List of References	178

List of Figures

Figure 2.1 Pile model used in program CYCPILE	146
Figure 2.2 Comparison of lab test data and CYCPILE prediction for a timber pile	147
Figure 2.3 A typical cyclic p-y curve used in CYCPILE based on Yan & Byrne's method	149
Figure 3.1 General flow chart for program CYCPILE	152
Figure 4.1 Schematic of pile in example problem no. 1	164
Figure 4.2 Variables and other information about pile in example No. 1	165
Figure 4.3 Input load history and results for example problem No. 1	166
Figure 4.4 Schematic of the problem solved in example No. 2	174
Figure 4.5 Comparison between lab test results, LATPILE and CYCPILE predictions	175

Chapter 1. Introduction

1.1 Introduction

In seismically active areas, it is important to consider lateral loads in design and analysis of new and existing structures founded on piles. Historically, piles have been mostly designed for carrying vertical loads. The computer program CYCPILE has been developed to accurately analyze the behaviour of piles under different lateral loading conditions. This program constitutes part of a Master of Applied Science requirements for the author at the University of British Columbia. Details of the method used in this program are presented in the thesis and a technical paper.

In short, the method is composed of a finite element beam model for the pile and non-linear springs, or P-y curves, for the soil. The user can input varying materials for the pile and the soil along the length of the pile. Axial loads can be input at the top of the pile although pile settlements and axial capacities are not calculated. Input axial loads are incorporated in the model to account for determining P-delta effects only. The Gaussian integration scheme (for a discussion of this integration technique the user is referred to Nakamura, 1993) is used in solving equations leading to the stiffness matrix of the Finite Element system. Non-linear soil properties are determined using a tangent stiffness approach.

By using the gaussian integration technique, the model is capable of calculating the deformed shape and the moments along the length of the pile very accurately. The model is capable of analyzing the non-linear behaviour of the soil-pile interaction. The pile is assumed to have a linear-elastic-perfectly-plastic stress-strain relationship. Pile gapping is modelled either by assuming that soil cannot undergo tension, or, by using the cyclic P-y curves presented in Vazinkhoo (1996).

The soil properties are given through the input of P-y curves at certain depths and for each of the

Chapter 1. Introduction

soil layers. Alternatively, the user can select the type of a P-y curve for a soil layer using the Yan-Byrne (1992) or the API (1987) methods and the curves are calculated by the program.

The program has been checked and verified with the results of laboratory and field experiments to ensure that the model and methodology used in the program will give accurate results to practical problems. However, since in an actual situation other factors such as dynamic effects of the super-structure supported by the pile will be important, it is desirable to include these problems in the model. Such capability is not available at this time, but is presently in the development stage at the University of British Columbia. The dynamic effects can be approximated by using a pseudo-static approach.

1.2 Purpose and Scope

The purpose of this documentation is to aid the user in the actual use of the computer program. The algorithms and the structure used in the program are also discussed.

The analytical model used in program CYCPILE is briefly discussed in Chapter 2 of Vazinkhoo (1996). The derivation of the model is presented in Vazinkhoo (1996). Chapter 3 is devoted to the discussion of the use of the computer program and contains the following: 1) A detailed description of the program and its capabilities including program flow and structure ; 2) the input file format and all input variables ; 3) all output information; and, 4) problems that may be encountered while running CYCPILE.

Some example problems are solved in chapter 4 to assist users in understanding the different input and output options and variables. Since most of the examples are using actual test data, it will give the user an idea of the accuracy of the program.

Chapter 1. Introduction

1.3 Applications

The program is presently capable of analyzing any combination of the following:

- a. Non-linear soil stress-strain and yielding through input of P-y curves
- b. Automatic calculation of P-y curves based on either Yan-Byrne or the API method.
- c. Soil-pile gapping
- d. Cyclic or monotonic loading
- e. Varying pile cross sections along the pile length
- f. Different pile materials along the pile length
- g. Pile yielding
- h. Free-field loading
- i. Direct loading at any node along the pile
- j. Specified displacements at any node along the pile
- k. P-Delta effects from applied axial load

Chapter 2. Analytical Model

2.1 Pile Model

The pile is represented by a one-dimensional finite element model as shown in Figure 2.1. As can be seen, the pile may have varying cross-section dimensions and applied loadings.

As shown in Figure 2.1 the pile is divided into separate elements which may have varying lengths. The elements are connected to each other at the nodes. Although the nodes are used as reference points, almost all calculations and outputs are done at the Gaussian integration points (see Nakamura (1993) for a discussion of the Gaussian integration technique). Both node and element numbering start from the bottom up. Coordinates can be increasing or decreasing with depth. Negative coordinates are allowed. The finite element formulation is discussed in Vazinkhoo (1996).

The user generally divides the pile into a number of elements the length of which may vary with depth. Since the finite element formulation used is fairly accurate, the number of elements needed can be limited to a few elements for each layer or pile cross-section. However, if the pile cross-section dimensions change with depth, the element lengths should be small enough to obtain good results. Experience and judgement should be used in determining the element lengths for a specific problem.

The axial deformations in the pile due to axial and lateral loads are calculated but care must be taken in their interpretation because soil resistance in the axial direction is not taken into account. The effect of axial loads on lateral bending and buckling (P-delta effect) is approximately considered. Figure 2.2 shows a comparison of results between an actual three point bending test on a timber pile and the predicted behaviour using CYCPILE. As can be seen, the model compares very well with the lab tests. This analysis is presented as an example problem in section 4.1 of Chapter 4.

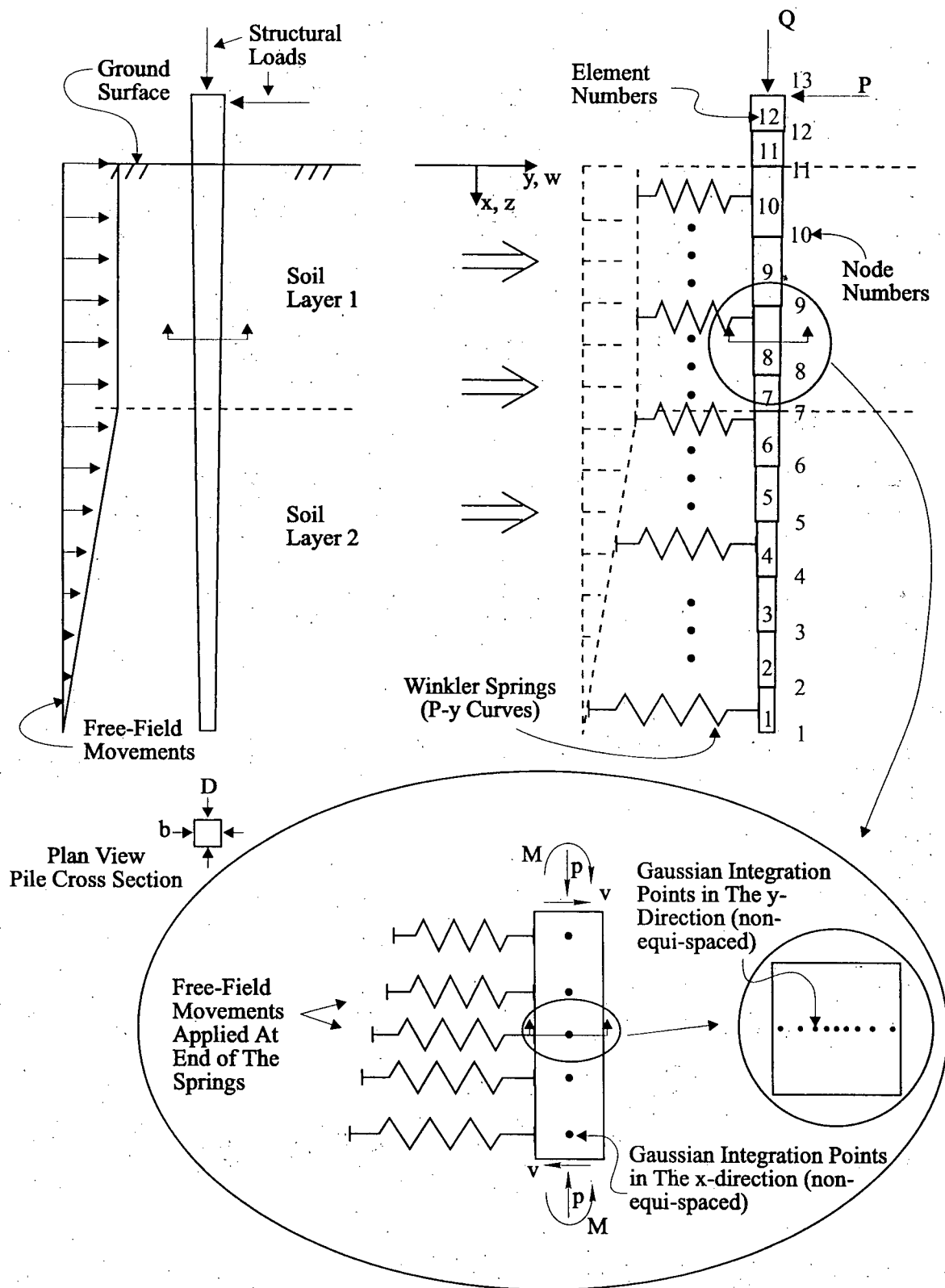


Figure 2.1 Pile model used in program CYCPILE

Chapter 2. Analytical Model

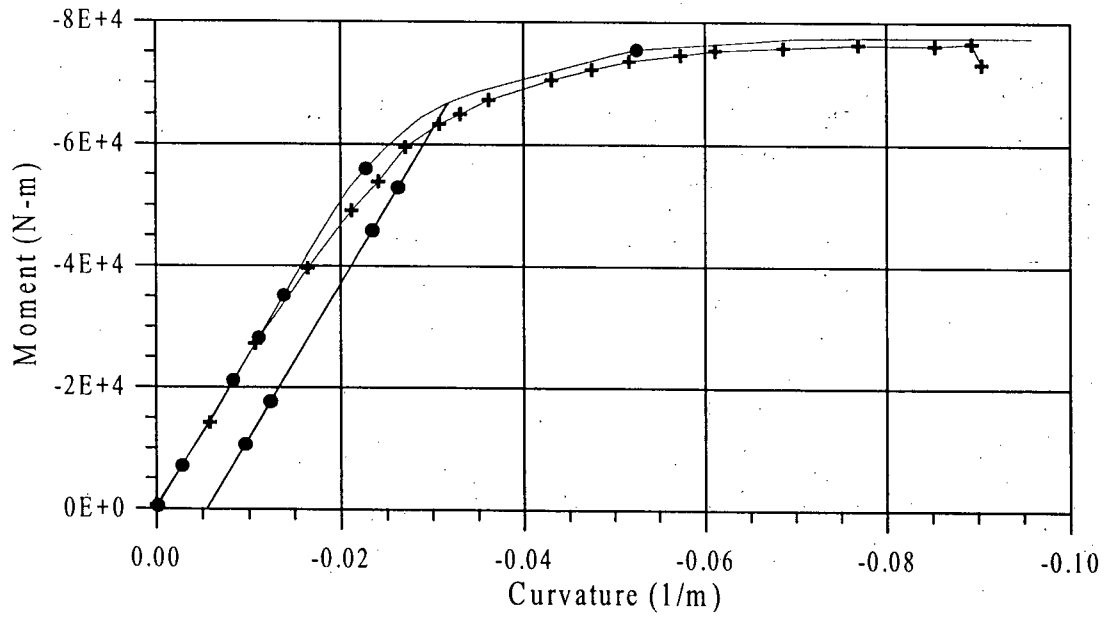
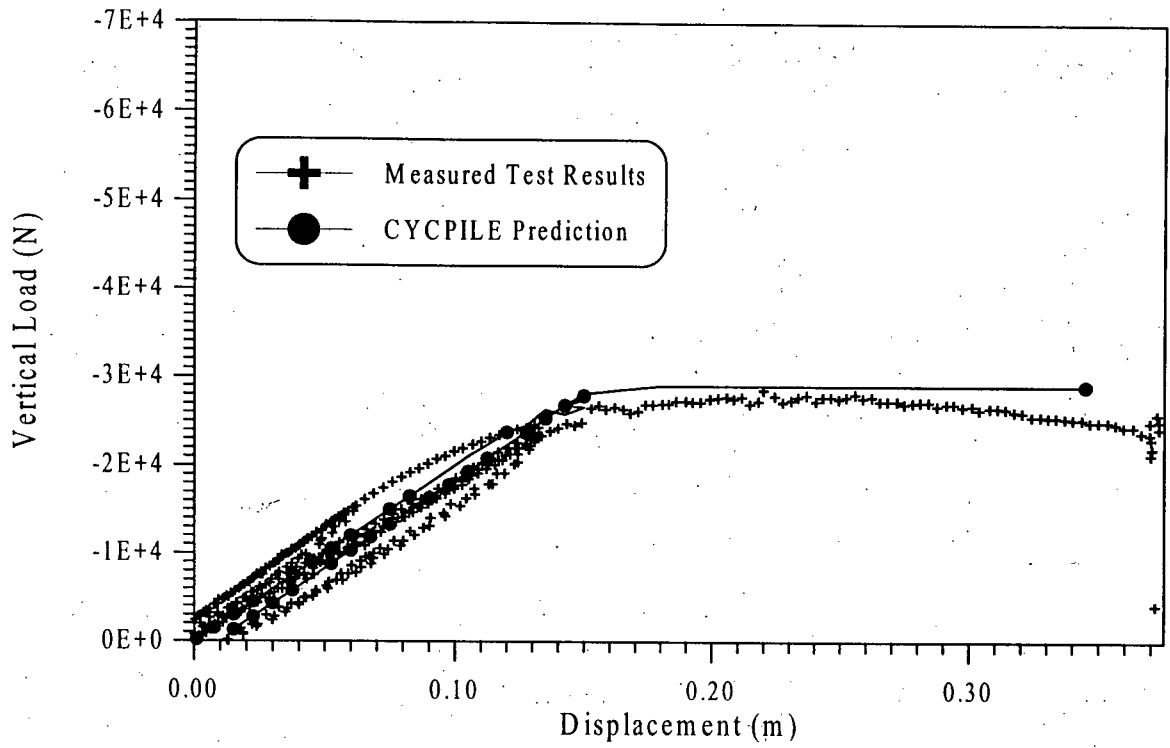


Figure 2.2 Comparison of lab test data and CYCPILE prediction for a timber pile

Chapter 2. Analytical Model

2.2 Soil Model

The soil in the computer program CYCPILE is modelled as non-linear springs with the use of P-y curves as shown in Figure 2.1. P-y curves may be obtained in a number of different ways, e.g., the American Petroleum Institute (API) code for both clays and sands. However, Yan and Byrne (1992), based on extensive laboratory model tests, have proposed a more fundamental and representative method for obtaining P-y curves for sands. This method is quite different from the API code and gives better results than the API method. Given the appropriate parameters, the program CYCPILE is capable of automatically calculating the P-y curves for either of the above methods. Of course, P-y curves may also be input simply as a set of points on the curve in which case linear interpolation is used between points. The user also specifies the initial modulus, E_{init} or E_{max} , which is used as the unloading portion.

Soil-pile gapping is either modelled by assuming that the soil is not capable of carrying any tensile forces or by using the cyclic P-y curves presented in Vazinkhoo (1996). Comparison with field tests show that the results are sufficiently accurate. A typical cyclic P-y curve based on the Yan & Byrne (1992) P-y curve and the assumption of zero tension in the soil is shown on Figure 2.3. Also shown on this Figure is a typical cyclic P-y curve constructed using the method presented in Vazinkhoo (1996).

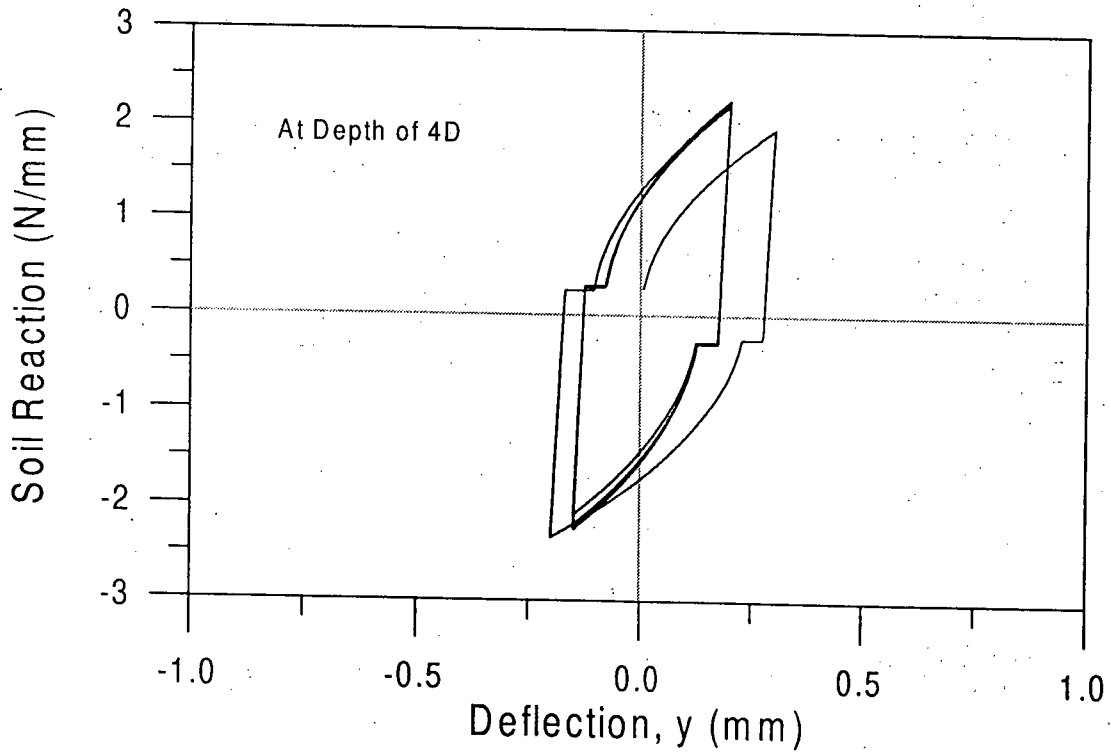
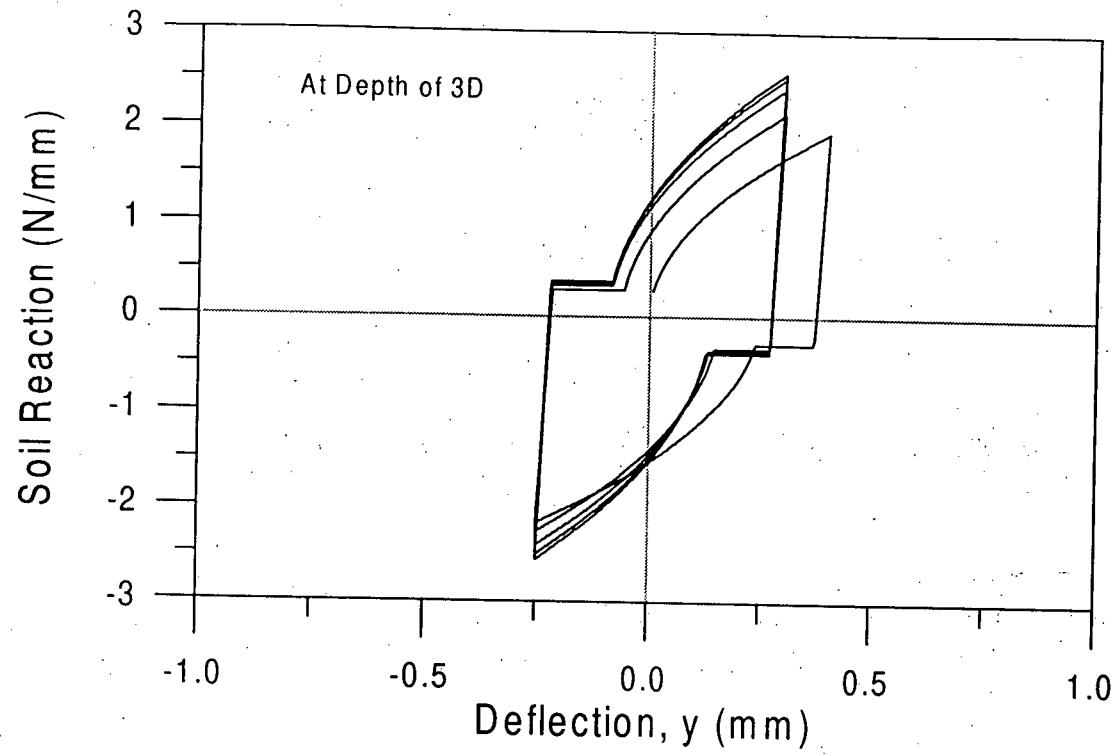


Figure 2.3 A typical cyclic p-y curve used in CYCPILE based on Yan & Byrne's method

Chapter 3. Program Setup

The computer code for CYCPILE has been written in FORTRAN 77 and compiled with Microsoft® Fortran Powerstation version 1.0 with Microsoft Visual Work Bench® version 3.2¹. The machine used for developing the program CYCPILE was an IBM®² compatible PC with an Intel®³ 486DX33 micro processor. The minimum hardware requirements to run CYCPILE are:

- a. a 386-based or higher CPU,
- b. a math co-processor,
- c. at least 8.0 Mb of free Hard Disk space (varies depending on the size of problem),
- d. 2 Mb of RAM (Extended).

Due to the large number of arrays used and defined in this program, most FORTRAN compilers will give an executable file that is much larger than the allowed 640K for DOS-based computers. The compiler used for compiling CYCPILE (mentioned above), is capable of making the executable file such that memory allocation for all arrays is done at run time rather than including the required memory in the executable file.

CYCPILE has been tested with a variety of problems and is believed to be free from serious defects. Troubles are usually found to be caused by user-oriented errors in input files or misrepresentation of the physical system which results in unexpected response of the real structure.

The program CYCPILE has been designed to work with any consistent system of units by specifying the appropriate value for atmospheric pressure. Because of the integration technique

¹ Microsoft and Microsoft Visual Work Bench are trade marks of Microsoft Corporation.

² IBM is a trade mark of International Business Machines Corporation.

³ Intel is a trade mark of Intel Corporation.

Chapter 3. Program Setup

used in this program, relatively few elements may be used to represent the pile accurately. It must be cautioned, however, that under certain instances such as when modelling a tapered pile, many more elements may be needed. Experience and judgement should be used in determining the number of elements needed for a certain problem. It should be mentioned that processing time increases rapidly with increased number of elements. A trial and error process can be used to find a suitable number for a particular problem.

3.1 Program Flow

The general flow of the program is shown in Figure 3.1. All program control, problem specifications, and all other information are input through two input files. One contains the input load history and the other contains all other data. All interpolations needed to obtain information along the pile are performed at the start of the program.

The program uses the tangent modulus in stiffness calculations. This allows for a marching solution scheme. At each load step, the stiffness matrix for the pile is constructed and the problem is solved to obtain moments, shear and shape of the deformed pile which are printed to the output files. This information is also saved in the memory and used as the starting condition for the next load step at which time all parameters are adjusted and the stiffness matrix for this load step is constructed. This process continues until processing terminates. Convergence is checked for each load step and the solution loop is executed until the convergence criteria has been satisfied.

Often, especially when applying cyclic loads, the specified tolerance may not be reached due to small errors in some portions of the pile where relatively very small displacements take place. In calculating the tolerance, these small errors are divided by a very small number and appear to be large inaccuracies. Such large inaccuracies in the tolerance calculations are misleading and have little effect on the overall accuracy of the actual problem. For this reason, the program prompts the user after every NITER iterations (set by the user in the input file) and the user can choose to either continue with another NITER iterations, assume that the tolerance has been reached and

Chapter 3. Program Setup

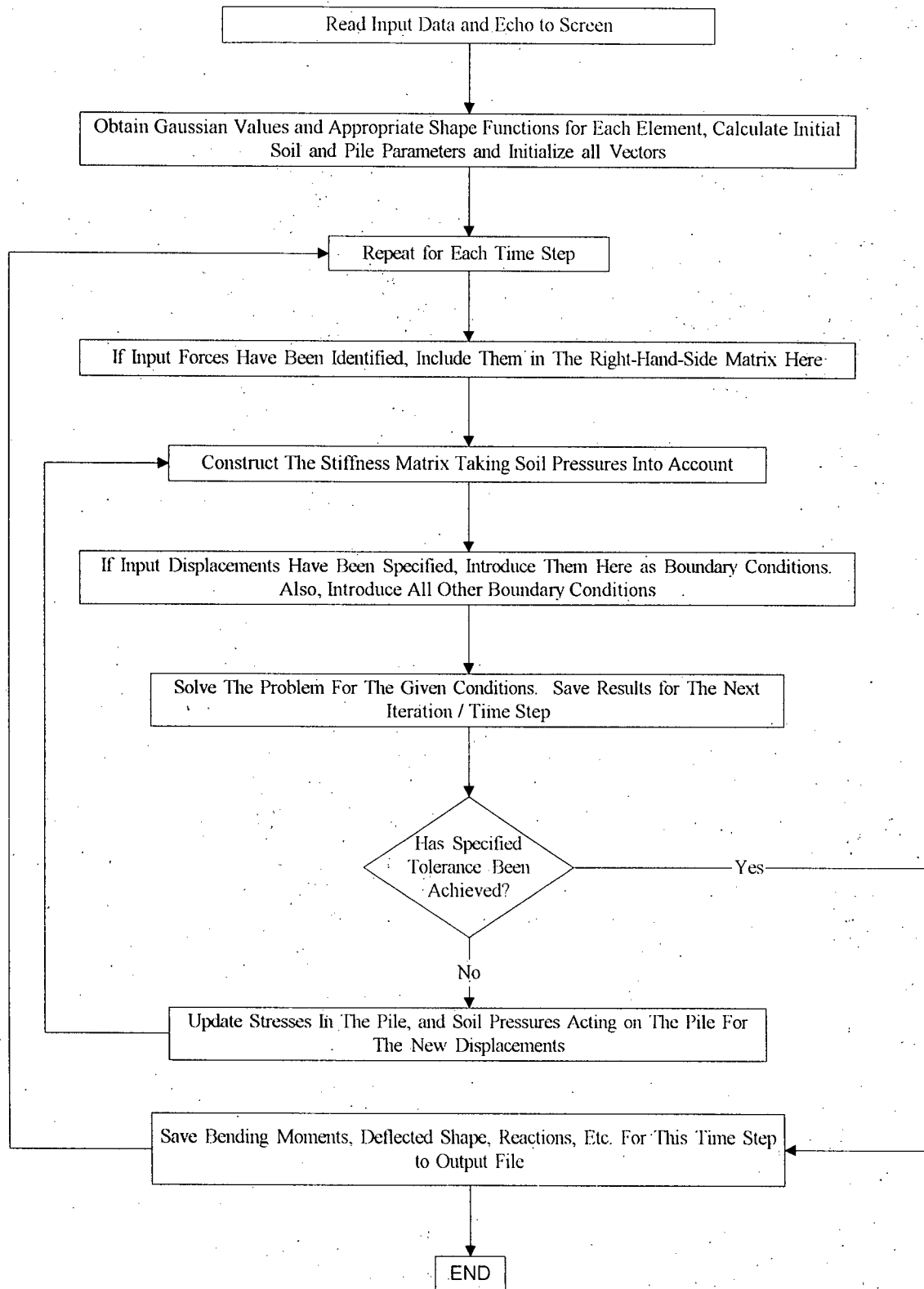


Figure 3.1 General flow chart for program CYCPILE

Chapter 3. Program Setup

move on to the next time step, or, stop the execution of the program.

3.2 Program Structure

The computer program CYCPILE consists of a main routine and the following six subroutines: SHAPES, STRESS, PSUP, GAUSS, DECOMP and SOLV.

The main routine is responsible for all input and output, initialization of all arrays, construction of the stiffness matrix and inclusion of boundary and end conditions.

Subroutine SHAPES obtains the values of the shape functions at each Gaussian integration point for each element. These values are used in the formulation of the stiffness matrix.

Subroutine STRESS looks up the appropriate stress for a given strain level at a point in the pile.

Subroutine PSUP looks up the appropriate P-y curve. Soil-pile gapping is taken into account here.

Subroutine GAUSS returns the appropriate Gaussian coordinates and integration factors given the number of desired Gaussian points.

Subroutine DECOMP decomposes the one-dimensionalized stiffness matrix so that it can be solved with the SOLV subroutine.

Subroutine SOLV solves the decomposed one-dimensionalized stiffness matrix and stores the solution in the right-hand-side matrix.

The one-dimensional stiffness matrix is setup so that it only stores the lower half of the matrix that have non-zero values since the stiffness matrix is symmetrical as is often done in finite element programs.

Chapter 3. Program Setup

3.3 Current Program Capacities

All arrays in program CYCPILE are individually defined for purposes of clarity. As mentioned above, the compiler which we used allows for the memory allocation to take place at run time. This makes the size of the program smaller. The compiler makes use of an extended memory manager (DOSXMSF.EXE) which should be present in the same sub-directory or in a sub-directory specified in the path statement in the AUTOEXEC.BAT file. This memory manager enables the use of extended memory and makes use of scratch files if it needs them.

The program CYCPILE is capable of analyzing any combination of the following:

- a. Non-linear soil stress-strain and yielding through input of P-y curves
- b. Automatic calculation of P-y curves based on either Yan-Byrne or the API method.
- c. Soil-pile gapping
- d. Cyclic or monotonic loading
- e. Varying pile cross sections along the pile length
- f. Different pile materials along the pile length
- g. Pile yielding
- h. Free-field loading
- i. Direct loading at any node along the pile
- j. Specified Displacements at any node
- k. P-Delta effects from applied axial load

The solution of the dynamic problem is currently being developed and will be available in the near future.

3.4 Description of the Input File

The input data can be given in free format. The example files contain the data using comma separated fields. As mentioned earlier, any consistent system of units may be employed by

Chapter 3. Program Setup

specifying the atmospheric pressure in the units of choice. All numbering for nodes, elements, layers, etc. are from the bottom to the top. However, the coordinates can increase or decrease with depth. Negative coordinates are also allowed. The following describes the input file:

Line #	Variable Name	Format	Description
1	TITLE	A80	TITLE OF THE PROBLEM

THE FOLLOWING LINE CONTROLS THE PROBLEM:

2	ELEMENTS	I4	NUMBERS OF ELEMENTS ALONG THE PILE
2	SOIL LAYERS	I4	NUMBER OF DIFFERENT SOIL LAYERS
2	PILE MATS	I4	NUMBER OF DIFFERENT PILE MATERIALS
2	BC NODES	I4	NUMBER OF DIFFERENT NODES WITH BOUNDARY CONDITIONS
2	INPUT PTS	I4	NUMBER OF POINTS IN THE INPUT HISTORY
2	CYC LOAD NODES	I4	NUMBER OF NODES WITH INPUT LOAD HISTORY
2	IS CYC	A1	= 'Y' IF LOADING TYPE IS TRUELY CYCLIC, = 'N' OTHERWISE THIS IS USED FOR CALCULATION OF API P-y CURVES, IF DEFINED
2	FREE FLD NODES	I4	NUMBER OF NODES ASSOCIATED WITH FREE FIELD INPUT
2	PA	F15.6	ATMOSPHERIC PRESSURE IN DESIRED UNITS
2	STATIC VER LOAD	F15.6	THE STATIC VERTICAL LOAD ON THE PILE
2	TOLERANCE	F15.6	DESIRED TOLERANCE FOR THE PROBLEM
2	NITER	I4	NUMBER OF ITERATIONS TO PROMPT

REPEAT THE FOLLOWING LINE FOR EACH NODE:

3	NODE	I4	NODE NUMBER. NODES ARE NUMBERED FROM BOTTOM TO TOP. THE TOTAL NUMBER OF NODES IS ALWAYS ONE PLUS TOTAL NUMBER OF ELEMENTS.

Chapter 3. Program Setup

3	X COORD(NODE)	F15.6	COORDINATE OF THE NODE IN THE VERTICAL DIRECTION
3	IS FF(NODE)	I4	= 1 IF FREE-FIELD DISPLACEMENTS WILL BE APPLIED AT THIS NODE = 0 OTHERWISE

REPEAT THE FOLLOWING LINE FOR EACH ELEMENT:

4	ELEM	I4	ELEMENT NUMBER
4	XSEC TYPE(ELEM)	I2	THE SHAPE OF THE PILE CROSS SECTION, THE CHOICES ARE: = 1 -SOLID CIRCLE = 2 -HOLLOW CIRCLE = 3 -RECTANGLE
4	OUT DIA(ELEM)	F15.6	IF XSEC TYPE() = 1: = DIAMETER OF PILE IF XSEC TYPE() = 2: = OUTSIDE DIAMETER OF PILE IF XSEC TYPE() = 3: = DEPTH OF PILE (IN DIRECTION OF BENDING)
4	IN DIA(ELEM)	F15.6	IF XSEC TYPE() = 1: = 0.0 IF XSEC TYPE() = 2: = INSIDE DIAMETER OF PILE IF XSEC TYPE() = 3: = WIDTH OF PILE
4	MAT NUM(ELEM)	I4	PILE MATERIAL FOR THIS ELEMENT
4	IN LAYER(ELEM)	I4	SOIL LAYER ASSOCIATED WITH THIS ELEMENT

REPEAT THE FOLLOWING LINES FOR EACH SOIL LAYER:

5	LAYER	I4	SOIL LAYER NUMBER
5	SOIL TYPE(LAYER)	A4	SOIL TYPE FOR THE LAYER: = CLAY, = SAND, = USER; THIS OPTION DEFINES HOW TO CALCULATE P-y CURVES FOR THE SOIL LAYER.

Chapter 3. Program Setup

5	PY TYPE(LAYER)	A4	METHOD OF CALCULATING P-y CURVES: = YANB, FOR YAN & BYRNE APPROACH, = APIC, FOR APPROACH USED IN THE API CODE, = USER, FOR USER SPECIFIED P-y CURVES; NOTE: THE YAN & BYRNE METHOD CAN ONLY BE SPECIFIED IF SOIL TYPE() = SAND. THE API CODE METHOD CAN ONLY BE SPECIFIED IF SOIL TYPE() = SAND OR = CLAY.

IF PY TYPE() = YANB, ENTER THE FOLLOWING LINE:

6	GAMMA(LAYER)	F15.6	THE UNIT WEIGHT OF SOIL FOR THIS SOIL LAYER
6	DR(LAYER)	F15.6	THE RELATIVE DENSITY OF SOIL FOR THIS SOIL LAYER (%) (USED TO CALC. EMAX)
6	EMAX(LAYER)	F15.6	THE MAXIMUM ELASTIC MODULUS OF SOIL FOR THIS SOIL LAYER (NOT USED)

IF PY TYPE() = APIC AND SOIL TYPE() = SAND, ENTER THE FOLLOWING LINE:

6	GAMMA(LAYER)	F15.6	THE UNIT WEIGHT OF SOIL FOR THIS SOIL LAYER
6	DR(LAYER)	F15.6	THE RELATIVE DENSITY OF SOIL FOR THIS SOIL LAYER (%)
6	ETA(LAYER)	F15.6	THE FACTOR ETA FROM API CODE FOR THIS SOIL LAYER
6	N HI(LAYER)	F15.6	THE FACTOR n hi FROM API CODE FOR THIS SOIL LAYER (COEFFICIENT OF SUBGRADE MODULUS)
6	C1(LAYER)	F15.6	FACTOR C1 FROM THE API CODE
6	C2(LAYER)	F15.6	FACTOR C2 FROM THE API CODE
6	C3(LAYER)	F15.6	FACTOR C3 FROM THE API CODE

Chapter 3. Program Setup

FOR OTHER PY TYPE() AND SOIL TYPE() NOT COVERED ABOVE, ENTER THE FOLLOWING LINES (TYPE "USER" IS ALSO INCLUDED HERE):

6	GAMMA(LAYER)	F15.6	THE UNIT WEIGHT OF SOIL FOR THIS SOIL LAYER
6	NUM PY(LAYER)	I4	NUMBER OF P-y CURVES IN THIS LAYER
6	NUM PY PTS(LAYER)	I4	NUMBER OF POINTS TO BE ENTERED FOR EACH P-y CURVE (50 MAXIMUM)
6a	NODE PY(LAYER, NUM PY)	I4	NODE NUMBER OF THE FOLLOWING P-y CURVE
6a	EMAX U(NODE PY, NUM PY)	F15.6	EMAX AT THIS NODE
6b	Y PY IN(NODE PY, J)	F10.4	THE Y-POINTS OF THE P-y CURVE AT THIS NODE
6b	P PY(NODE PY, J)	F10.4	THE P-POINTS OF THE P-y CURVE AT THIS NODE NOTE: REPEAT LINES 6a AND 6b NUM PY TIMES. FREE-FIELD DEFLECTIONS WILL BE INTERPOLATED, IF NECESSARY, FOR ALL NODES REQUIRING FREE-FIELD INPUT.

REPEAT THE FOLLOWING LINES FOR EACH PILE MATERIAL:

7	PILE MAT	I4	PILE MATERIAL NUMBER
7	MAT TYPE(PILE MAT)	A4	DEFINES THE MATERIAL TYPE FOR SOME PILE SEGMENT: = ELPL, FOR AN ELASTO-PLASTIC MATERIAL LIKE STEEL, = WOOD, FOR WOOD, = USER, THE STRESS-STRAIN CURVE IS USER DEFINED BY THE USER.

IF MAT TYPE() = ELPL, ENTER THE FOLLOWING LINE:

8	E(PILE MAT)	F15.6	YOUNG'S ELASTIC MODULUS OF THE MATERIAL
8	YIELD STRS(PILE MAT)	F15.6	YIELD STRESS OF THE MATERIAL

Chapter 3. Program Setup

IF MAT TYPE() = WOOD, ENTER THE FOLLOWING LINE:

8	E(PILE MAT)	F15.6	YOUNG'S ELASTIC MODULUS OF THE MATERIAL
8	YIELD STRS(PILE MAT)	F15.6	YIELD STRESS OF THE MATERIAL IN COMPRESSION

IF MAT TYPE() = USER, ENTER THE FOLLOWING LINE (NOT AVAILABLE AT THIS TIME):

8	NUM SE PTS(PILE MAT)	I4	NUMBER OF POINTS ON THE SIGMA vs EPSILON CURVE (STRESS STRAIN CURVE) NOTE: INCLUDE THE NEGATIVE PORTION OF THE CURVE HERE
8	E INIT(PILE MAT)	F15.6	INITIAL YOUNG'S ELASTIC MODULUS
8a	EPSILON(PILE MAT, (I, I=1, NUM SE PTS(PILE MAT)))	8F10.4	THE EPSILON-POINTS OF THE STRESS STRAIN CURVE
8b	SIGMA(PILE MAT, (I, I=1, NUM SE PTS(PILE MAT)))	8F10.4	THE SIGMA-POINTS OF THE STRESS STRAIN CURVE

IF BC NODES IS NOT ZERO, FOR EACH BC NODES ENTER THE FOLLOWING LINE OTHERWISE SKIP THIS LINE:

9	BC NODE(I)	I4	NODE NUMBER WITH BOUNDARY CONDITION, I=1 TO BC NODES
9	NUM BCS(BC NODE(I))	I4	NUMBER OF DIFFERENT BOUNDARY CONDITIONS TO BE SPECIFIED
9	BC(BC NODE(I), J, J=1, NUM BCS (BC NODE(I)))	I4	= 1, IF W = 0 = 2, IF W' = 0 = 3, IF W'' = 0 = 4, IF U = 0 = 5, IF U' = 0

IF CYC LOAD NODES IS NOT ZERO, FOR EACH CYC LOAD NODES ENTER THE FOLLOWING LINE OTHER WISE SKIP THIS LINE:

10	CYC NODE	I4	THE NODE NUMBER WITH SPECIFIED LOAD HISTORY

Chapter 3. Program Setup

10	CYC LOAD TYPE(CYC NODE)	A5	= DISPL, FOR DISPLACEMENT LOADING CONDITION = FORCE, FOR FORCE LOADING CONDITION

SPECIFY THE STEP NUMBERS FOR WHICH OUTPUT IS DESIRED IN THE NEXT TWO LINES:

12	CYC NODE OUT	15	NODE NUMBER FOR PRINTED OUTPUT AT EVERY STEP
12	NUM OUTPUT STEPS	15	NUMBER OF DIFFERENT STEPS AT WHICH OUTPUT IS REQUIRED
13	OUTPUT STEP((I, I=1, NUM OUTPUT STEPS))	8I5	STEP NUMBERS AT WHICH OUTPUT IS REQUIRED

The input load history (CYC NODE) is given in a second file the format of which is:

Line #	Variable Name	Format	Description
1	TITLE1	A80	TITLE OF THE INPUT LOAD HISTORY
2a	CYC NODE	I5	NODE NUMBER FOR THIS LOAD HISTORY
2b	(CYC HOR x(CYC NODE, I), I= 1, NUM CYC PTS))	8F15.6	INPUT LOAD HISTORY. IF CYC LOAD TYPE(CYC NODE) = DISPL, x = DISP IF IT = FORCE, x = LOAD REPEAT LINES 2a AND 2b FOR ALL CYC NODE NUMBERS GIVEN IN INPUT FILE

NOTE: THE NODE NUMBERS GIVEN HERE MUST CORRESPOND EXACTLY TO THE ONES
GIVEN IN THE INPUT FILE.

IF FREE FLD NODES IS NOT ZERO, FOR EACH CYC LOAD NODES ENTER THE FOLLOWING LINE
OTHER WISE SKIP THIS LINE:

4	FF NODE	I4	THE NODE NUMBER WITH SPECIFIED FREE FIELD INPUT
4a	FF DISP IN(FF NODE, (I, I= 1, INPUT PTS))	8F10.4	THE HORIZONTAL DISPLACEMENTS AT NODE "FF NODE"

Chapter 3. Program Setup

3.5. Program Output

The input file is echoed to the screen before the start of program. The step number, iteration number and tolerance for that iteration is also echoed to the screen as the program works its way through the problem.

There are four output files. One contains output at each load step at a specified node. This output consists of load step number, deflection, calculated force and input force (if exists) at the node, curvature and moment at the Gaussian points just above and just below the node, and shear forces calculated by numerically differentiating the moments. The second output file contains output at desired load steps for all points along the length of the pile. This output consists of depth, curvature, moment, deflection, shear forces and calculated force at all gaussian points along the pile length. This information is repeatedly given at all load steps. The third output file contains the stresses at all gaussian integration points for desired load steps. The fourth file contains the axial strains and displacements along the pile length for the desired load steps.

3.6 Problems That May Be Encountered While Running CYCPILE

Although this program has been thoroughly checked and is believed to be free of errors, it is possible that something may have been overlooked. Most problems occur due to mistakes in the input file. Some numerical inconsistencies may occur at times if the step size in the input load history file is too large. The magnitude of these inconsistencies depends on relatively how large the step size is. In general one should avoid having large changes between successive load increments especially when load reversal occurs.

Often, especially when applying cyclic loads, the specified tolerance may not be reached due to small errors in some portions of the pile where relatively very small displacements take place. In calculating the tolerance, these small errors are divided by a very small number and appear to be large inaccuracies. These large inaccuracies in the tolerance calculations are misleading and

Chapter 3. Program Setup

have little effect on the overall accuracy of the actual problem. For this reason, the program prompts the user after every NITER iterations (set by the user in the input file) and the user can choose to either continue with another NITER iterations, assume that the tolerance has been reached and move on to the next time step, or, stop the execution of the program.

Chapter 4. Example Problems

The validity of the current method of analysis of cyclic and static lateral loads for linear and non-linear problems has been demonstrated under a separate cover (Vazinkhoo, 1996). The following examples are selected problems from the above validation process.

4.1 Example No. 1 Three Point Bending Test on a Timber Pile

In this example problem there are no soil layers. It is a laboratory test on a full size pile in a three-point-bending test. This test was performed for BC Hydro at the University of British Columbia as part of a study on seismic withstand of timber piles (Lee et al, 1992). The objective of this laboratory test was to understand the lateral bending behaviour of a pile under known and controlled conditions. Figure 4.1 shows a schematic of this problem. Figure 4.2 shows the various measured variables and quantities along with a picture of the setup. Figure 4.3 shows the loading condition and comparison of results of the laboratory test and the prediction of the program. Note that it appears that the pile material undergoes slight modulus degradation as it yields. At present, the program does not have the capability of taking the pile modulus degradation into account. The input file, TIMB-N.IPT, is given on page 26 followed by the output files, TIMB-N.DOT and TIMB-N.MNT.

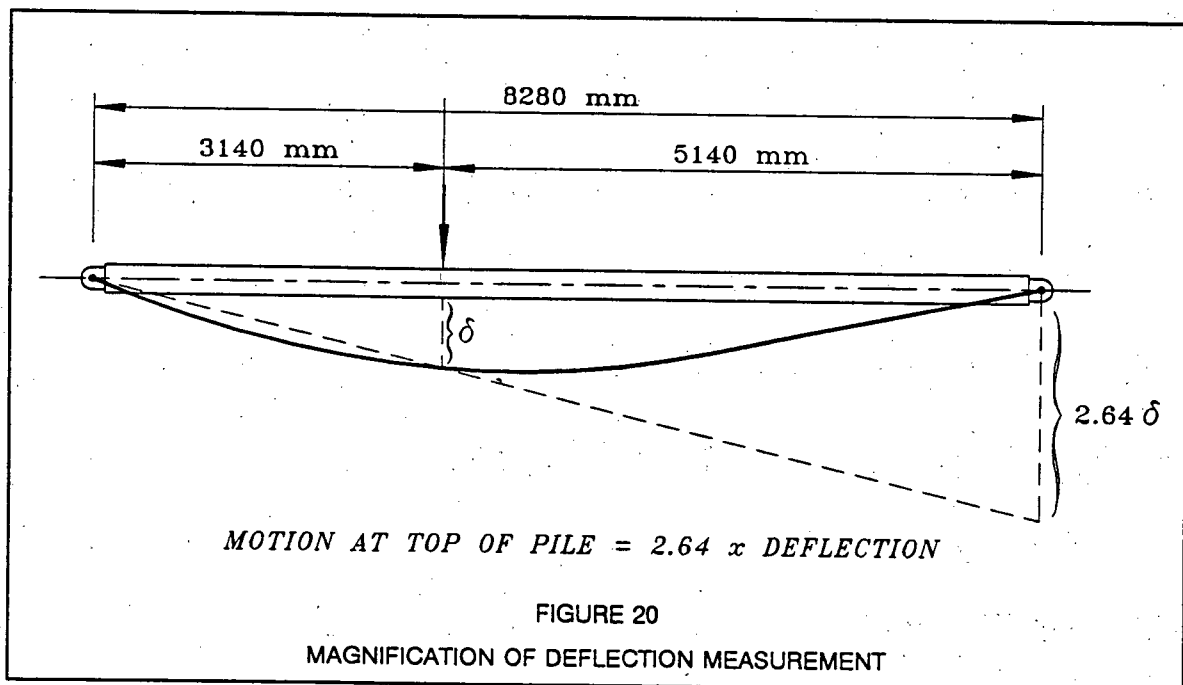


Figure 4.1 Schematic of pile in example problem no. 1. After Lee et al (1992).

Chapter 4. Example Problems

	At Max Vertical Load	At Failure
Transverse Load	27.7 kN	24.4 kN
Moment	70.7 kN-m	76.9 kN-m
Deflection	206.0 mm	378.0 mm
Bending Stress	33.7 MPa	36.7 MPa
Axial Stress	1.3 MPa	1.3 MPa
Curvature	0.043 1/m	0.089 1/m

Axial Load 75.8 kN
M.O.E. 9.7 GPa

Physical Dimensions

	POSITION								
	1	2	3	4	5	6	7	8	9
Location mm	160	1140	2140	3140	4140	5140	6140	7140	8280
Circ. mm	805	820	850	870	880	905	925	940	965
Top mm	18	27	43	43	54	52	52	34	18
Side mm	18	31	31	29	29	39	37	32	18
Vert Offset mm	0	9	25	25	36	34	34	16	0
Hor. Offset mm	0	13	13	11	11	21	19	14	0
Radius mm	128	131	135	138	140	144	147	150	154
Area mm ² x E-3	51.6	53.5	57.5	60.2	61.6	65.2	68.1	70.3	74.1
I mm ⁴ x E-6	212	228	263	289	302	338	369	393	437

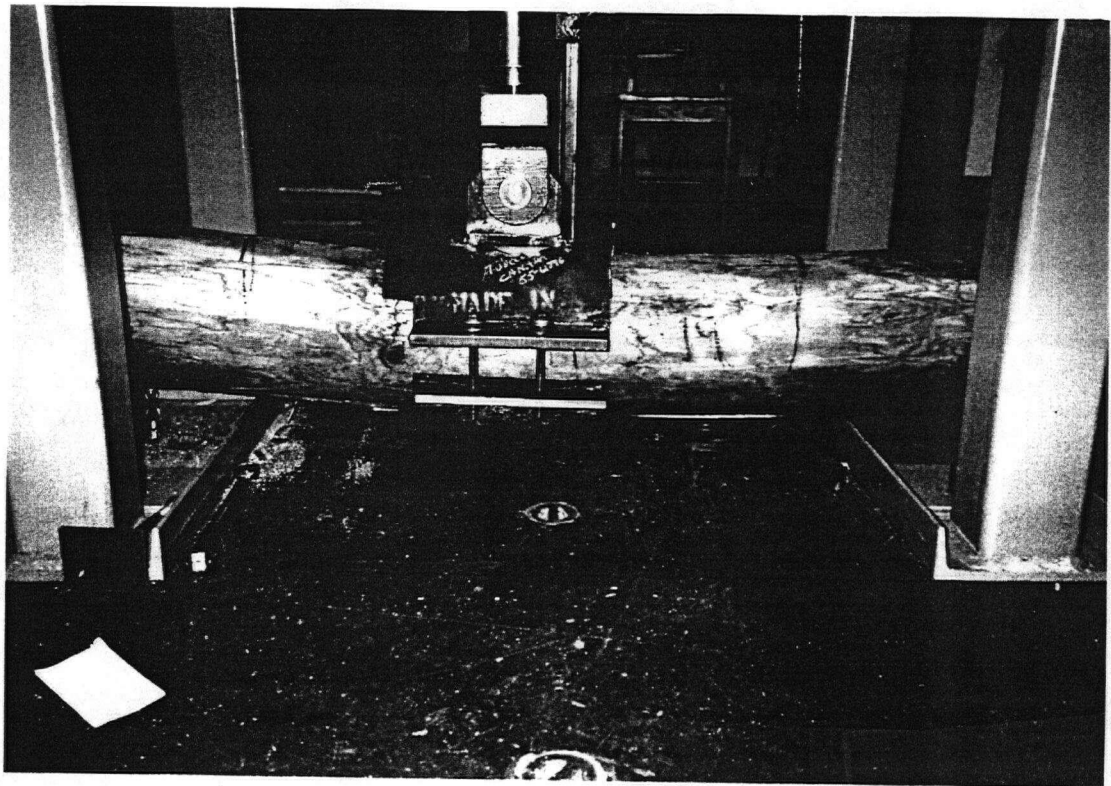


Figure 4.2 Variables and other information about pile in example No. 1. After Lee et al (1992).

Chapter 4. Example Problems

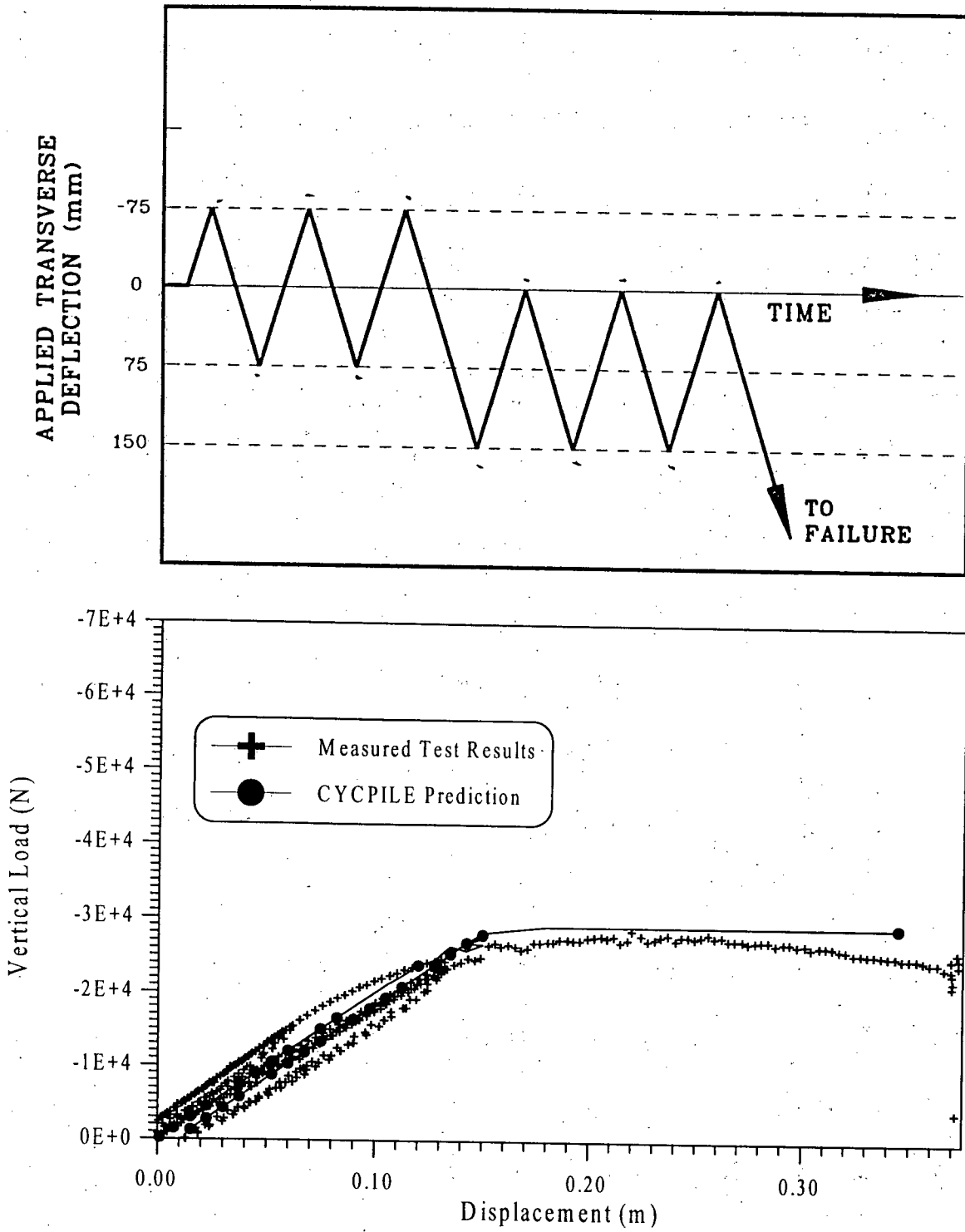


Figure 4.3 Input load history and results for example problem No. 1

Chapter 4. Example Problems

TIMB-N.IPT:

TIMBER PILE LAB TEST CHECK

50,0,1,2,300,1,'Y',0,101.325E+03,75.8E+03,0.0001,100

1,0.0000,0

2,0.1656,0

3,0.3312,0

4,0.4968,0

5,0.6624,0

6,0.8280,0

7,0.9936,0

8,1.1592,0

9,1.3248,0

10,1.4904,0

11,1.6560,0

12,1.8216,0

13,1.9872,0

14,2.1528,0

15,2.3184,0

16,2.4840,0

17,2.6496,0

18,2.8152,0

19,2.9808,0

20,3.1464,0

21,3.3120,0

22,3.4776,0

23,3.6432,0

24,3.8088,0

25,3.9744,0

26,4.1400,0

27,4.3056,0

28,4.4712,0

29,4.6368,0

30,4.8024,0

31,4.9680,0

32,5.1336,0

33,5.2992,0

34,5.4648,0

35,5.6304,0

36,5.7960,0

37,5.9616,0

38,6.1272,0

39,6.2928,0

40,6.4584,0

41,6.6240,0

42,6.7896,0

43,6.9552,0

44,7.1208,0

45,7.2864,0

46,7.4520,0

47,7.6176,0

Chapter 4. Example Problems

48,7.7832,0
49,7.9488,0
50,8.1144,0
51,8.2800,0
1,1,0.256000,0.0,1,0
2,1,0.257000,0.0,1,0
3,1,0.258000,0.0,1,0
4,1,0.259000,0.0,1,0
5,1,0.260000,0.0,1,0
6,1,0.261000,0.0,1,0
7,1,0.262000,0.0,1,0
8,1,0.263333,0.0,1,0
9,1,0.264667,0.0,1,0
10,1,0.266000,0.0,1,0
11,1,0.267333,0.0,1,0
12,1,0.268667,0.0,1,0
13,1,0.270000,0.0,1,0
14,1,0.271000,0.0,1,0
15,1,0.272000,0.0,1,0
16,1,0.273000,0.0,1,0
17,1,0.274000,0.0,1,0
18,1,0.275000,0.0,1,0
19,1,0.276000,0.0,1,0
20,1,0.276667,0.0,1,0
21,1,0.277333,0.0,1,0
22,1,0.278000,0.0,1,0
23,1,0.278667,0.0,1,0
24,1,0.279333,0.0,1,0
25,1,0.280000,0.0,1,0
26,1,0.281333,0.0,1,0
27,1,0.282667,0.0,1,0
28,1,0.284000,0.0,1,0
29,1,0.285333,0.0,1,0
30,1,0.286667,0.0,1,0
31,1,0.288000,0.0,1,0
32,1,0.289000,0.0,1,0
33,1,0.290000,0.0,1,0
34,1,0.291000,0.0,1,0
35,1,0.292000,0.0,1,0
36,1,0.293000,0.0,1,0
37,1,0.294000,0.0,1,0
38,1,0.295000,0.0,1,0
39,1,0.296000,0.0,1,0
40,1,0.297000,0.0,1,0
41,1,0.298000,0.0,1,0
42,1,0.299000,0.0,1,0
43,1,0.300000,0.0,1,0
44,1,0.301143,0.0,1,0
45,1,0.302286,0.0,1,0
46,1,0.303429,0.0,1,0
47,1,0.304571,0.0,1,0

Chapter 4. Example Problems

48,1,0.305714,0.0,1,0
49,1,0.306857,0.0,1,0
50,1,0.308000,0.0,1,0
1, 'ELPL'
8.9E+09,22.7E+06
1,2,1,3
50,3,1,3,4
19, 'DISPL'
10
10,30,120,240,260,270,271,275,280,300

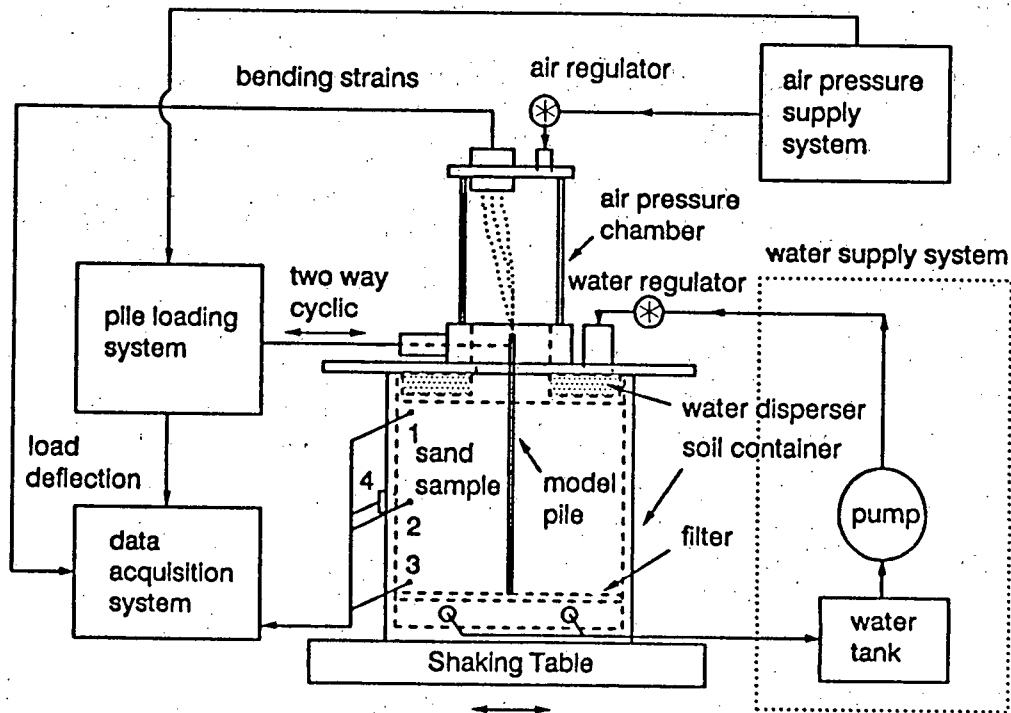
Chapter 4. Example Problems

.12739E+00	-.17724E-02	.33341E+04	.28288E-01	.00000E+00
.79566E+01	-.18118E-03	.70359E+03	.22027E-01	.00000E+00
.79870E+01	-.11417E-03	.44338E+03	.17777E-01	.00000E+00
.80316E+01	-.17370E-03	-.67457E+03	.11555E-01	.00000E+00
.80762E+01	.31384E-03	-.12188E+04	.53327E-02	.00000E+00
.81066E+01	.11016E-03	-.42781E+03	.10840E-02	.00000E+00
.81222E+01	.12280E-03	-.48404E+03	-.10840E-02	.00000E+00
.81526E+01	.36434E-03	-.14361E+04	-.53325E-02	.00000E+00
.81972E+01	.26768E-03	-.10551E+04	-.11553E-01	.00000E+00
.82418E+01	.46210E-04	-.18214E+03	-.17774E-01	.00000E+00
.82722E+01	.59071E-04	-.23284E+03	-.22021E-01	.00000E+00

Chapter 4. Example Problems

4.2 Example No. 2 Lateral Load Test on a Model Pile in The HGS Testing Device

This example problem is based on a laboratory test on an instrumented aluminum model pile embedded in dense sand. In this case, the loading was applied monotonically. The stresses were increased to field stress levels using the Hydraulic Gradient Similitude technique (Yan and Byrne, 1992). Comparison is made between CYCPILE and test results as well as between CYCPILE and LATPILE predictions. Figure 4.4 shows a schematic along with the different variables for the problem. Figure 4.5 shows the lab test results, LATPILE and CYCPILE predictions. As can be seen, the comparison between LATPILE and CYCPILE is excellent while both predict the lab test results fairly well. The input file, FIXED-N.IPT is shown on page 35 followed by the two output files, FIXED-N.DOT and FIXED-N.MNT.

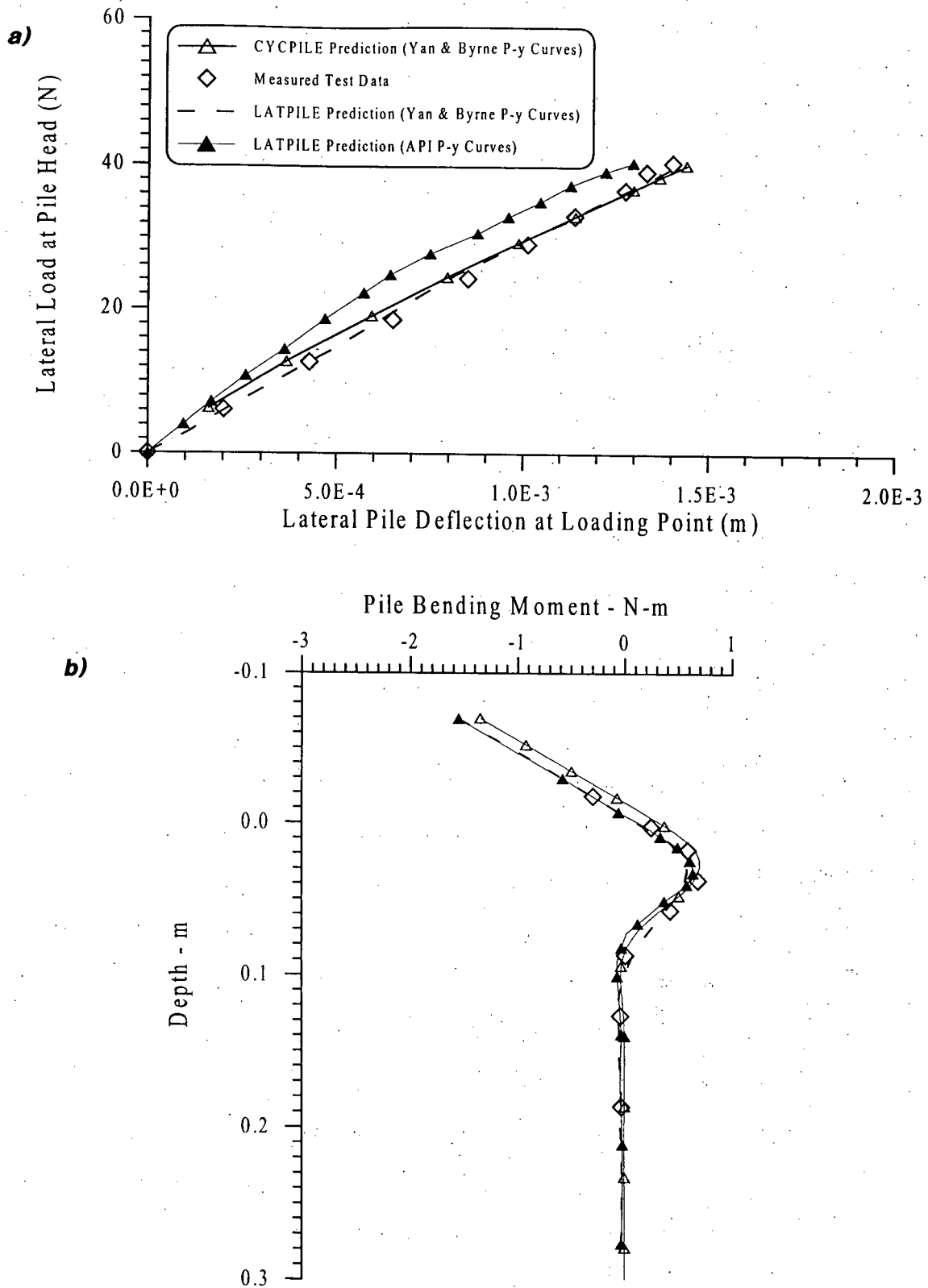


Note: 1,2,3 - pore water pressure transducer #PWP1,#PWP2,#PWP3
4 - lateral soil stress transducer LATP

Soil Container Dimension: 445x230x420mm

Figure 4.4 Schematic of the problem solved in example No. 2

Chapter 4. Example Problems



Chapter 4. Example Problems

FIXED-N.IPT:

CYCPILE CHECK

20,1,1,2,9,1,'Y',0,101.325E+3,0.0,0.05,100

1,0.0,0

21,0.392,0

1,2,0.00635,0.00473,1,1

20,2,0.00635,0.00473,1,0

1,'SAND','YANB'

0.432E+06,75.0,0.0

1,ELPL

0.70E+11,0.300E+09

1,1,4

21,1,2

21,'FORCE'

9

1,2,3,4,5,6,7,8,9

List of References

- [1] API-RP2 (1987), *Recommended Practice for Planning, Designing and Constructing Fixed Offshore Platforms*. American Petroleum Institute, Washington, D.C. 17th Edition, April 1, 1987.
- [2] Lee, M.K., Stewart, R.A., Imrie, A.S., "Timber Pile Lateral Test Program, Seismic Withstand of Timber Piles, Volume 1 of 2, Evaluation of Practice versus Theory", BC Hydro, Hydroelectric Engineering Division, Report No. H2607, April, 1992.
- [3] Nakamura, S., *Applied Numerical Methods in C*, PTR Prentice Hall, Englewood Cliffs, New Jersey, 1993.
- [4] Vazinkhoo, S. (1996) "Modelling of Single Vertical Piles Subjected to Monotonic and Cyclic Lateral Loads and Free-Field Movements", M.A.Sc. Thesis, Department of Civil Engineering, University of British Columbia.
- [5] Yan, L. and Byrne, P.M. (1992), "Lateral Pile Response to Monotonic Pile Head Loading", *Canadian Geotechnical Journal*, Vol. 29, pp. 955-970.